Addis Ababa University

Addis Ababa Institute of Technology

School of Electrical and Computer Engineering

Design and Simulation of Speed Control of PMSM with Fuzzy Logic Self-Tuning PID Controller using MATLAB

By:

Henok Teshager

Thesis Submitted To Addis Ababa Institute of Technology in Partial Fulfillment of the Requirements for the Degree of Master of Science in Electrical and Computer Engineering (Control)

Advisor:

Dr. Dereje Shiferaw

October, 2017

Addis Ababa, Ethiopia

Addis Ababa University

Addis Ababa Institute of Technology

School of Electrical and Computer Engineering

Thesis Submitted To Addis Ababa Institute of Technology in Partial Fulfillment of the Requirement for the Degree of Master of Science in Electrical and Computer Engineering (Control Engineering)

By:

Henok Teshager

Dr: _____	_____	_____
Chairman Department of Graduate Committee	Signature	Date
Dr.Dereje Shiferaw	_____	_____
Advisor	Signature	Date
_____	_____	_____
Internal Examiner	Signature	Date
_____	_____	_____
External Examiner	Signature	Date

Declaration

I, the undersigned, declared that this MSc thesis is my original work, has not been presented for fulfillment of a degree in this or any other University and all sources and materials used for the thesis is acknowledged.

Henok Teshager _____

Name Signature

Addis Ababa _____

Place Date of Submission

This thesis work has been submitted for examination with my approval as a University Advisor.

Dr. Dereje Shiferaw _____

Advisor's Name Signature

Acknowledgement

Beside to God, this work would not be possible without the guidance and support of many people. First of all, I would like to thank my advisor Dr. Dereje Shiferaw, for his intellectual guidance and continuous encouragement. His patience and the time he invested in the whole process of this thesis work as well as his willingness to support me at any time helped me to bring this thesis in to fruition.

Secondly, I must express my very deep gratitude to my families for providing me with consistent support and encouragements throughout my life and to finalize this work. I am also thankful for my friends in AAiT, for all the unforgettable moments we shared together. Finally I would like to acknowledge Gondar University, for granting and sponsoring me for this scholarship program.

Abstract

This thesis focuses on the speed control of Permanent Magnet Synchronous Motor (PMSM) drive system with Fuzzy logic self-tuning PID controller using MATLAB/ Simulink 2015a. The performance of the proposed controller of PMSM was analyzed in terms of speed tracking capability, torque response quickness, high and low speed behavior, parameter sensitivity and speed reversal conditions. Comparison is also made between FPID with the conventional PI and PID controller mechanisms. The result shows that the FPID has more significant advantage in overshoot reduction by (11.7% and 21%) than PID and PI controllers and with very good steady state error of 0.035% without load test. While with load test the FPID controller have good performance with 0.043% steady state error percentage.

Key words: *PMSM, Vector control, PID controller, Fuzzy logic, self-tuning FPID controller*

You have to also include the fact that FPID is slow compared to the PID

Table of Contents **Page**

List of Figures

List of Tables

List of Acronyms

AC	Alternating current
DC	Direct Current
EMF	Electro motive force
FLC	Fuzzy logic controller
FOC	Filed oriented control
mmf	magneto motive force
PI	Proportional integral
PID	Proportional integral derivative
PM	Permanent magnet
PMSM	Permanent Magnet Synchronous motor
PWM	Pulse width modulation
SPMSM	Surface mount permanent magnet synchronous motor
SVMPWM	Space vector pulse width modulation
VSI	Voltage source inverter
i_{qs_ref}	Reference q axis synchronous current
i_{ds_ref}	Reference d axis synchronous current
i_{qs}	q -axis synchronous current
i_{qs}	d -axis synchronous

1. Chapter One

Introduction

1.1 Background of the Study

The evolution of alternating current (AC) electrical motor drives has been always conditioned by the application and the design of the several types of AC electrical machines. Drive systems have seen through the years a continuous evolution of methods and techniques in order to achieve same or better performances, by using more economically convenient or robust types of machines. The development of high-quality permanent magnet materials into commercial production has encouraged several manufacturers to launch various permanent magnet synchronous machines (PMSM) into the market.

Synchronous motors are most widely used in industrial applications as both high efficiency and accurate performances are required in industrial applications. The PMSM is increasingly playing an important role in advanced motor drives. A PMSM or permanent-magnet motor (PMM) is a synchronous motor that uses permanent magnets rather than windings in the rotor that create constant magnetic field. There are two types of PMSM depending on the mounting of permanent magnets. One is surface mounted and another is interior PMSM. Interior permanent magnet (IPM) is the most widely used type in PMSM. PMSM has gained a wide acceptance in motion control applications in the low-to-medium power ratings such as robotics, house appliances, water pump, adjustable speed drives and electric vehicles due to its high performance, compact structure, high air-gap flux density, high power density, and high torque to inertia ratio, and high efficiency [1], [2].

This popularity is justified by numerous advantages over commonly used motors. The absence of the external rotor excitation eliminates losses on the rotor, makes PMSM highly efficient and high torque to inertia ratio so that it gives fast response. In addition, the absence of the rotor winding renders slip rings on the rotor and brushes obsolete, and thus reduces the maintenance cost. The replacement of the rotor winding with permanent magnet (PM) in PMSM makes it compact structure or smaller in size that results a high power density [2].

Recent research has reported that the PMSM is being increasingly using in high-performance applications which require speed controllers that provide not only accuracy and high performance, but also flexibility and efficiency in the design process and implementation. However, in industrial applications, there are many uncertainties, such as system parameter uncertainty, external load disturbance, friction force and un-modeled uncertainty always diminish the performance quality of the pre-design of the motor driving system. To cope with this problem, in recent years, many intelligent control techniques and other control methods have been developed and applied. Various control strategies and methodologies are available for speed control of PMSM ranging from fuzzy logic to classical proportional-integral-derivative (PID) based control (like Model Predictive control, Sliding mode control and Variable Structure Control etc.) algorithms. These approaches improve the control performance of the motor from different aspects [3], [4].

Nevertheless, all of the above controller techniques depend on the exact mathematical model of the drive system, which is difficult to achieve practically. Application of computational intelligence techniques like Fuzzy Logic Control (FLC) can yield interesting solution in the field of speed control of drives. FLC does not depend on the mathematical model of the drive system. In this thesis self-tuning scheme using fuzzy logic PID controller is proposed to improve the performance of synchronous motor drive. Hence, the tuning must be made on-line and automatic in order to avoid tedious task in manual control. But, the well-known *Ziegler-Nichols* m*ethod* to tune the coefficients of a PID controller is very simple, but cannot guarantee to be always effective [5]. The establishment of the simulation model of PMSM and its control system is of great significance to the verification of a variety of control algorithms and the optimization of entire control system. To achieve high performance, the vector control of the PMSM drive is adopted.

1.2 Motivation

Even though, PMSM motors are becoming an attractive alternative for applications in high performance variable speed drives or motion control application areas, the control mechanism is complex. Due to this complexity the control performance of PMSM drives are highly sensitive to variations of external load and system parameters [1], [5]. These parameter variations are the dominant factors which affects the performance of the system. To overcome this problem for the past few decades the conventional PID controller were used by tuning their parameter gains using manually (i.e. Nicolas Ziegler method).

However, it is too tedious work, so tuning the PID components in on-line method is becoming the mandatory task in some application areas to cope parameter uncertainties, external load disturbance and speed reversal. Many modern control techniques have been developed to solve the problem such as Variable Structure Control (VSC), Model Reference Adaptive Control (MRAC) and Sliding Mode Controller (SMC). All of these controller mechanisms need the exact mathematical model of the drive system on the other hand; it is not always feasible to obtain an accurate mathematical model of the controlled system.

However, FLC offers a way of dealing with modeling problems by implementing linguistic, non-formally expressed control laws derived from expert knowledge without the exact mathematical model of the drive system. Hence, by combining the conventional PID controller mechanism with artificial intelligent methods, we can optimize performance of the system without changing its PID structure. So, in this thesis, a fuzzy logic based self-tuning of PID controller method is employed.

1.3 Objective of the Study

1.3.1 General Objective

This thesis intended to study and design speed control of PMSM based on fuzzy logic self-tuning PID controller, which is artificial intelligent technique for PMSM drive system. It is being expected that this control scheme can track the reference speed well under some parameter uncertainties and load disturbance.

1.3.2 Specific Objectives

The specific objectives of the research have been outlined as follows:

- Developing speed control of PMSM with PI controller
- Developing speed control of PMSM with PID controller
- Designing speed control of PMSM with fuzzy PID controller
- Comparing the FPID controller results with conventional controllers by simulation using MATLAB/SIMULINK

1.4 Statement of the Problem

Since, PMSM has being increasingly used in high-performance applications, such as robots and industrial machines, which require speed controllers that provide not only accuracy and high performance, but also flexibility and efficiency in the design process and implementation. However, there are many uncertainties in industrial applications, such as system parameter uncertainty, external load disturbance, friction force and un-modeled uncertainty always diminish the performance quality of the pre-design of the motor driving system. Therefore, it is important to that applying an intelligent control techniques to enhance the performance of PMSM.

1.5 Methodology

This thesis proceeds through different phases starting from the beginning of the work up to the final report of the designing and simulation of speed control of PMSM drive. Maintaining the whole process is quite important to minimize the probability of the problem happening during the work.

- The first task is organizing the literature reviews where all the theoretical information regarding the PMSM drive to be gathered from and a comparison of previous similar research papers have been discussed.
- The characteristics and mathematical modeling of PMSM drive theory have been studied
- Based on mathematical model of the PMSM drive, a Fuzzy Logic self- tuning PID control law has been developed.
- Then, speed control of PMSM using a Fuzzy Logic self- tuning PID controller has been simulated by MATLAB/Simulink**.**
- Finally, the paper discussed the results based on the simulation result gained from MATLAB/Simulink and recommends the future works that have already been done.

1.6 Literature Review

PM motor drives have been an area of interest for the past thirty years. Different researchers have carried out modeling, analysis and simulation of PMSM drives. This content offers a brief review of some of the published work on the PMSM drive system. So many researchers are proposed different control scheme to control speed of synchronous motors to improve their performance.

~~Simulation based~~ The mathematical model of PMSM motor has been ~~applied~~ simulated using MATLAB in [6]. The simulation results in this paper showed the performance characteristics of permanent magnet synchronous motor, i.e. speed of motor remain constant even with variation of load torque. In addition, the stator currents and electromagnetic torque magnitudes also have been found in the simulation.

In [7], the field-oriented control (FOC) systems with PID replacing proportional integral (PI) from standard model has been presented. The system has been ~~experimented~~ on MATLAB/SIMULINK 2010a and the results with proposed structure outperformed the standard model. This work presented the comprehensive performance analysis on the principle of operation, design considerations and control algorithms of the FOC for a PMSM drive system and PID for speed control in closed loop operation. To perform speed control of typical PMSM drives, PID controllers and FOC method have been classically used.

The detailed modeling of FLC for PMSM derive system has been presented using Simulink in [8]. The simulation in this paper included all realistic components of the system, which enables the calculation of current and voltages in different parts of the invertors and motor under transients and steady state condition. The FLC has been used for speed control of this type of motor. The dynamic response of PMSM with the proposed controller has been studied under different load disturbances. The effectiveness of the proposed FLC was compared with that of the conventional PI & PID controllers. The proposed controller has been used in order to overcome the nonlinearity problem of PMSM and to achieve faster settling response.

The modeling and simulation of a permanent magnet synchronous motor speed controller by effective use vector control method with space vector pulse width modulation has been presented in [9]. In this paper the transient and steady state values of current, speed and duty cycles are

analyzed in detail. And the result showed that the designed system is capable of to maintain the constant speed within different inputs by achieving minimum overshoot and quick response.

A fuzzy proportional derivative (PD) speed control scheme for robust speed tracking of a PMSM has been presented in [10]. The researcher was being motivated by the common control engineering knowledge that transient performance can be improved, if the P gain is higher and the D gain is smaller in the beginning, a linearizing control scheme with a fuzzy PD controller has been proposed.

1.7 Thesis Outline

This thesis is organized into six chapters including the first Chapter which describes the introduction part of the paper.

Chapter two describes the theory and operation principle of PMSM. Different PMSM construction details, difference with synchronous motors, starting characteristics of PMSM, and its different applications are presented. Chapter three discusses on a dynamic modeling of the PMSM drive with Field oriented control based on co-ordinate transformation is described.

Chapter four describes controller deign for PMSM drive system, which has two main parts; the first one deal with PID controller designing section and the second part discusses on the designing of self-tuning fuzzy PID controller of the system.

Chapter five discusses on simulation results of the drive system on MATLAB/Simulink. Included in this chapter, simulation results based on load torque disturbance and motor parameter variation has been depicted. Lastly, chapter six draws the conclusions from the work done in this thesis and recommends further research possible in the future.

1.8 Scope of the Study

As it was being mentioned on the objectives of the study, the scope of this thesis is simulating and comparing the results of the conventional PI and PID controller mechanisms with the unified artificial intelligence and conventional PID controller using MATLAB 2015a. And also the vector (field oriented) control of PMSM drive system doesn't include the field weakening region.

2. Chapter Two

Introduction to Synchronous Motor

Electric Motors are electromagnet devices used to convert electrical energy into useful mechanical work. The Serbian-American engineer Nikolai Tesla invented the first alternating-current induction motor. Tesla's motor is generally considered to be the prototype of the modern electric motor. This was the first brushless motor. The synchronous motor, which is also a brushless motor, was invented by Tesla as well [11]. AC motors have no commutators, and their speed is only limited by the physical constraints of the motor. These two advantages led to the wide spread utilization of ac motors in motion control applications in the following decades. There are ~~two~~ three major classifications of ac motors shown in Figure 2.1.

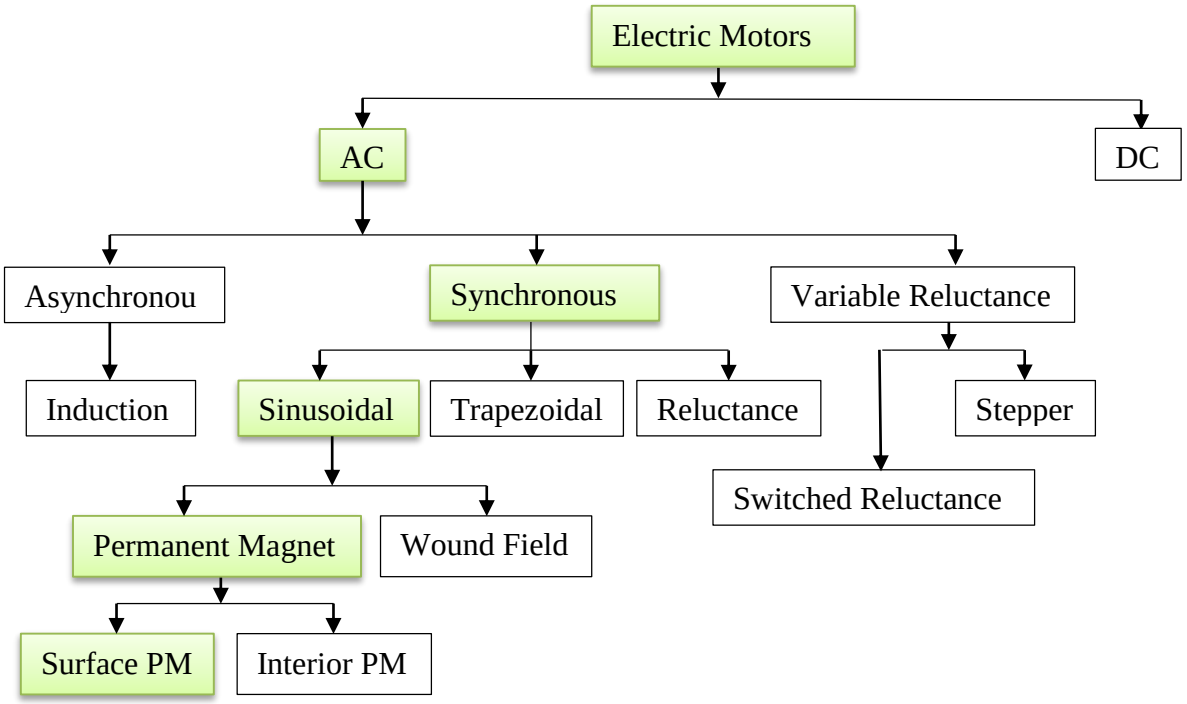

Figure 2:1 Electric motor type classification

The first is induction motors that are electrically connected to power source. Through electromagnetic coupling, the rotor and the stator fields interact, creating rotation without any other power source.

The second one is, synchronous motor which is an AC two-winding machine in which the fixed stator winding is connected to a supply line operating at a constant frequency and the other winding is excited by direct current. It owes its name, "synchronous", to the fact that the rotor must rotate at synchronous speed, that is, the speed corresponding to the frequency of the AC supply.

Synchronous motors are like induction motor in that they both have stator windings to produce a rotating magnetic field. Unlike an induction motor, the synchronous motor is excited by an external DC source and therefore requires slip rings and brushes to provide current to the rotor and produce magnetic field. An AC synchronous motor rotates at a fixed speed, despite any increase or decrease in load [12].

Synchronous motors are those which rotate at the speed of the stator revolving field, which is called the synchronous speed. The synchronous speed, Ns, is determined by the frequency of the stator supply, *fs*, and the number of stator pole pairs, *p*. Unlike the induction motor, the rotor also has *p*-pole pairs; excited by a separate DC source .The stator of a three-phase synchronous motor normally has a sine distributed three-phase winding. When excited with a three-phase balanced supply, a rotating magnetic field develops. The speed of this field (the *Synchronous Speed*) is given by Equation 2.1. We will assume that this field is sinusoidal distributed in space in the air gap [13].

$$Ns = \frac{120 * fs}{P} \tag{2.1}$$

Where, Ns - synchronous speed in rpm, fs - frequency of ac supply in HZ, *P* - number of poles per phase.

Generally, some characteristic features of synchronous motor are as follow [12]:

- Speed is independent of the load, provided an adequate field current is applied.
- Accurate control in speed and position using open loop controls such as stepper motors.
- They will hold their position when a DC current is applied to both the stator and the rotor windings.
- Their power factor can be adjusted to unity by using a proper field current relative to the load. Also, a "capacitive" power factor, (current phase leads voltage phase), can be obtained by increasing this current slightly, which can help achieve a better power factor

correction for the whole installation. So, it can be operated under wide range of power factors both lagging and leading.

- Their construction allows for increased electrical efficiency when a low speed is required (as in ball mills and similar apparatus).
- It is not inherently self-starting. It has to be run at synchronous speed by some means before it can be synchronized to supply.

The major classification of synchronous motor is based on the rotor structure, and it is grouped as the rotor with DC excitation winding and permanent magnet (as shown in Figure 2.2). DC-excited motors are usually made in larger sizes (larger than about 1 horsepower or 1 kilowatt) these motors require DC supplied to the rotor for excitation. The DC may be supplied from a separate DC source or from a DC generator directly connected to the motor shaft. In non-excited motors, the rotor is made of permanent magnets instead of field windings. At synchronous speed it rotates in step with the rotating magnetic field of the stator, so it has an almost-constant magnetic field through it [4].

Among these synchronous motor types, this thesis work focuses on permanent magnet PMSM. The stator of a PMSM has conventional three phase windings. In the rotor, PM materials have the same function as that of the field winding in a conventional synchronous machine. The use of a PM to generate substantial air gap magnetic flux makes it possible to design highly efficient PM motors [1], [2].

2.1 Permanent Magnet Synchronous Motor

The availability of modern PM with considerable energy density led to the development of DC machines with PM field excitation in 1950s. Introduction of PMs to replace the electromagnetic poles with windings requiring an electric energy supply source resulted in compact dc machines. Likewise, in synchronous machines, the conventional electromagnetic field poles in the rotor are replaced by the PM poles and by doing so the slip rings and brush assembly are dispensed with. These two developments contributed to the development of PMSMs and brushless DC machines. In PMSM, the required field flux is produced by permanent magnets mounted on the rotor. In these motors, the excitation electro-magnetic force (EMF) cannot be varied.

All the equation governing the performance of salient-pole synchronous motors are also applicable to PMSM with excitation EMF taken as constant. The absence of field winding, DC supply to field

winding and two slip rings leads to reduction in motor losses. For the same frame size, PMSM has higher pull-out torque and more efficiency as compared to salient-pole motor [14].

The stator portion of PMSM has an uneven distribution of magnetic poles and the solid steel rotor has permanent magnets embedded in it, the purpose of this is to give the rotor a preferred starting point while providing an apparent shift in field during starting due to the uneven reluctance of the stator. They are not self-starting. Because of the constant magnetic field in the rotor these cannot use induction windings for starting, and must have electronically controlled variable frequency stator drive. A typical PMSM stator and rotor is shown in Figure 2.2.

Figure 2:2 Conventional Synchronous DC excited and PMSMs

(i) Permanent magnet materials

The most common materials in modern high performance PM machines constructions are Samarium Cobalt (SmCo) and Neodymium Iron Boron (NdFeB), because they can have very high energy product, which leads to a high remanence flux density and a high coercive field strength. These two desirable properties are base for PM machines. NdFeB magnets are more preferable than Samarium Cobalt due to; their high remanence flux density up to 1.5 T, low cost, requires less space, strongest rare earth magnet and with proper design there is no danger of accidental demagnetization through short circuit [15], [16].

Disadvantages of NdFeB magnets are the sensitivity of the magnets to corrosion and the fact that they are very brittle and can therefore crack easily if exposed to mechanical shocks or to tensile

stress. In addition to the strong dependence of the PMSM characteristics on temperature, usually the biggest drawback of a PMSM drive system in general is the lack of proper field weakening. Because of the constant flux set by the magnets, and the very weak armature reaction of surface magnet permanent magnet synchronous motors (SMPMSM), the field weakening is very difficult and also impractical [16].

2.1.1 Classification of Permanent Magnet Motors

PM motors are classified based on the flux density distribution and the shape of current excitation. They are PMSM and PM brushless DC motors (BLDC).

The PMSM has a sinusoidal-shaped back EMF (it is an induced voltage in the stator by the motion of the rotor) and is designed to develop sinusoidal back EMF waveforms. They have the following characteristics [1]:

- Sinusoidal distribution of magnet flux in the air gap
- Sinusoidal current waveforms
- Sinusoidal distribution of stator conductors.

BLDC has a trapezoidal-shaped back EMF and is designed to develop trapezoidal back EMF waveforms. They have the following characteristics:

- Rectangular distribution of magnet flux in the air gap
- Rectangular current waveform
- Concentrated stator windings.

Further PMSMs can be classified into different types based different ways of arrangement of magnets on the rotor. Depending on the placement they are called either as surface permanent magnet motor (SPM) or interior permanent magnet (IPM) synchronous motor. Surface mounted PM motors have a surface mounted permanent magnet rotor. Each of the PM is mounted on the surface of the rotor, making it easy to build, and specially skewed poles are easily magnetized on this surface mounted type to reduce the magnitude of torque harmonics (ripple) due to the harmonic content of the magneto-motive force (MMF)-waves.

They are not preferred for high-speed applications, generally greater than 3000 rpm but machines with very small rotor diameter can be found to have speeds in the range of 50,000 rpm also. These motors are considered to have small saliency, thus having practically equal inductances in both axes, Lq = Ld [1], [17].

One of the main desirable features of the surface-mount permanent magnet machine is its high torque density. Furthermore, when designed to operate at specific speeds, these machines also possess high efficiency. These two features are accomplished in part because the permanent magnets do not generate the resistive losses of electromagnets. Not only does this reduce overall losses and hence improve efficiency, the lack of heat generation in the rotor means that the rotor does not require cooling, which would otherwise increase the overall size of the machine. Another feature of the surface-mount permanent magnet machine is the relatively large air gap between the stator and rotor irons, due to the presence of the magnets on the rotor. This results in a relatively small self-inductance of the stator windings. In many applications this small self-inductance is an advantage, as it allows high levels of stator current, and hence high torque levels, without saturating the stator and rotor irons of the machine [1].

Thin PMs are mounted on the surface of rotor core using adhesives. Alternating magnets of the opposite magnetization direction produce radially directed flux density across the air gap. This flux density then reacts with currents in windings placed in slots on the inner surface of the stator to produce torque. Figure 2.3 (a) shows the placement of the magnet.

IPM Motors have interior mounted permanent magnet rotor as shown in Figure 2.3 (b). Each PM is mounted inside the rotor. It is not as common as the surface mounted type but it is a good candidate for high-speed operation.

By designing a rotor magnetic circuit such that the inductance varies as a function of rotor angle, the reluctance torque can be produced in addition to the mutual reaction torque of synchronous motors. These motors are considered to have saliency with q axis inductance greater than the d axis inductance (Lq > Ld).

In this thesis SPM radial flux machine chosen due to the SPM drive with a saliency ratio ξ=1(i.e. Lq = Ld) and thus without reluctance torque is simpler to analyze and design than an IPM drive.

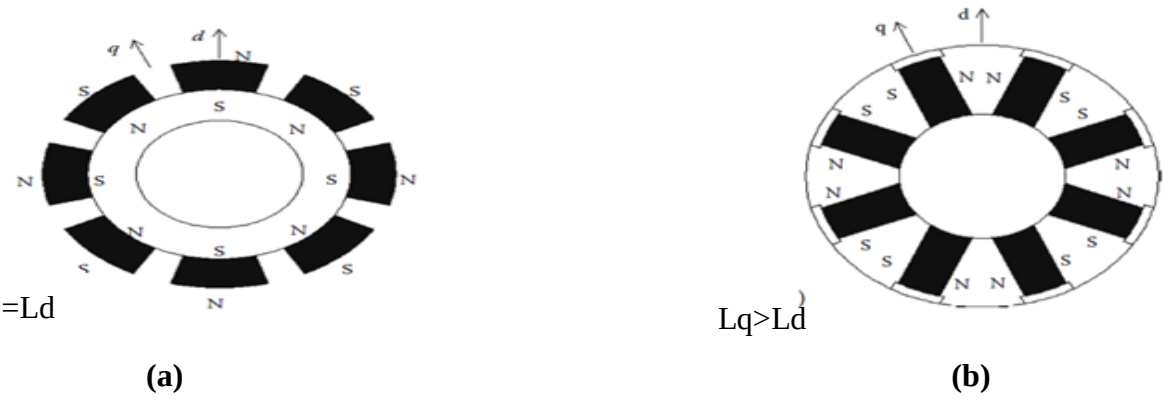

Figure 2:3 Rotor configurations: a) Surface Mounted PM (SPM); b) Interior PM (IPM) [1]

2.2 Characteristics and Principle Operation of PMSM

PMSM is one of the SM types that have the stator phase windings and rotor permanent magnets. The air gap magnetic field is provided by these PMs and hence it remains constant. The conventional DC motor commutates itself with the use of a mechanical commutator whereas PMSM needs electronic commutation for the direction control of current through the windings. As the PMSM motors have the armature coils at the stator, they need to be commutated externally with the help of an external switching circuit and a three phase inverter.

The PMSM and the driving inverter bridge topology are shown in Figure 2.4.

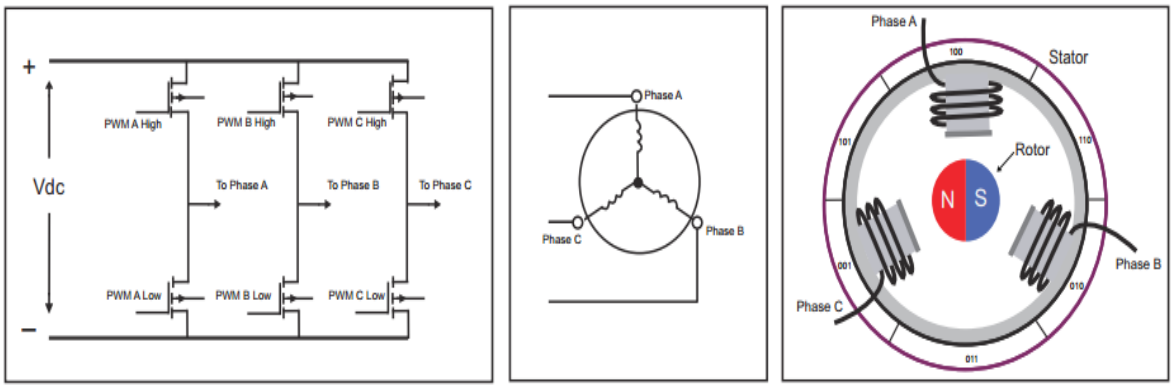

Figure 2:4 PMSM motor and driving inverter topology

The three phase balanced currents which are supplied to the stator windings results a stator magnetic field that spatially rotates around the stator at a constant angular speed. Unlike induction

machines, synchronous machines have zero slip, and the rotor maintains the same angular speed as the stator generated field.

In PM motors, one of the magnetic fields is created by PMs and the other is created by the stator coils. The torque is produced because the interaction of the two magnetic fields causes the motors to rotate. The maximum torque is produced when the magnetic vector of the rotor is at 90 degrees to the magnetic vector of the stator.

The general characteristics of PMSM motors are compact in shape, high efficiency (no excitation current), smooth torque, low acoustic noise and fast dynamic response (both torque and speed), but they are expensive than induction motors. Despite the fact that, the transition from single speed to variable speed systems is in progress in recent years, another transition is in effect within the field of variable speed motor drives. DC and induction motor drives, which have dominated the field until now, are being replaced by PMSM. Because PMSM motors have a lot of advantages over these motors in terms of performance and efficiency in variable speed drive systems, while they have their own demerits also [18].

2.2.1 Advantages of PMSM

The following are the reason why PMSM motors are more attractive in variable speed control system in many application areas than other motors.

Advantages of PMSM over DC motors are [1], [16]:

- less audible noise
- longer life
- sparkles (no fire hazard)
- higher speed
- higher power density and smaller size
- better heat transfer

Advantages of PMSM over IM motors are [1], [16]:

- **Higher Efficiency**: The PM machines have a very high efficiency due to the use of PMs for excitation which consume no power. Moreover, the absence of mechanical commutator and brushes results in low mechanical friction losses.
- **Higher power density:** The use of high energy density magnets has allowed achieving very high flux densities in the PM machines. As a result of high flux densities, high torque can be produced from a given volume of motor compared to other motors of same volume especially for lower than 10 kW applications.
- **Ease of Control:** The PM motors can be controlled compared to IM motors because the control variables are easily accessible and constant throughout the operation of the motor.
- **Higher power factor:** due to the absence of magnetizing current in PMSM motor because they have the excitation in the form of the rotor magnet**.**
- **Higher torque to inertia ratio**: The rare earth and neodymium boron PM machine has a lower inertia when compared with an IM because of the absence of a rotor cage; this makes for a faster response for a given electric torque. In other words, the torque to inertia ratio of these PM machines is higher.
- **Better heat transfer:** The rotor losses in a PM machine are negligible compared with those in the induction motor. A problem that has been encountered in the machine tools industry is the transferal of these rotor losses in the form of heat to the machine tools and work pieces, thus affecting the machining operation. This problem is avoided in permanent magnet machines.

2.2.2 Disadvantages of PMSMs

However, the PM machines also suffer from some disadvantages such as [1], [16]

- **Cost:** Rare-earth magnets commonly used in PM machines are very expensive.
- **Magnet demagnetization:** The magnets can be demagnetized by large opposing magneto-motive force and high temperatures.
- **Inverter Failure:** Due to magnets on the rotor, PM motors present major risks in the case of short circuit failures of the inverters. The rotor is always energized and constantly induces EMF in the short circuited windings. A very large current circulates in those windings and an accordingly large torque tends to block the rotor.

- They have complex control strategies and there is a problem of maintenance of rotor magnet.

2.2.3 Application Area of PMSM

Due to their valuable advantages, PMSMs have different applications in different areas. Among those many application areas [16]:

- In industry
  - Industrial drives, e.g., pumps, servo drives, automation processes, robots etc.
- Public life:
  - Heating, ventilating and air conditioning (HVAC) systems, catering equipment, coin laundry machines, environmental control systems etc.
- Domestic life :
  - Kitchen equipment
  - Bathroom equipment
  - Washing machines and clothes dryers
- Transportation e.g. elevators and escalators, people movers light railways and streetcars
- Aerospace e.g. rockets, and satellites
- Defense e.g. tanks, missiles, radar systems
- Medical and health equipment e.g. dental hand pieces (dentist's drills), electric wheelchairs

3 Chapter Three

PMSM Drive System Overview

3.1 Introduction to Electric Drives

Basically the concept of AC motor control is obtained from the terminology of electric drive system. A drive operates and controls the speed, torque and direction of moving objects. Drives are generally employed for speed or motion control applications. The drives used for controlling electric motors are known as electrical drives. The drives can be constant or variable type. The constant speed drives are inefficient for variable speed operations; in such cases variable speed drives are used to operate the loads at any one of a wide range of speeds [15].

The adjustable speed drives are necessary for precise and continuous control of speed, position, or torque of different loads. Along with this major function, there are many reasons to use adjustable speed drives. Some of these include [15]:

- To achieve high efficiency: Electrical drives enable to use wide range of power, from mill-watts to megawatts for various speeds and hence the overall cost of operating the system is reduced
- To increase the speed of accuracy of stopping or reversing operations of motor
- To control the starting current
- To provide the protection
- To establish advanced control with variation of parameters like temperature, pressure, level, etc.

The components of a modern AC electric drive system are illustrated in Figure 3.1.

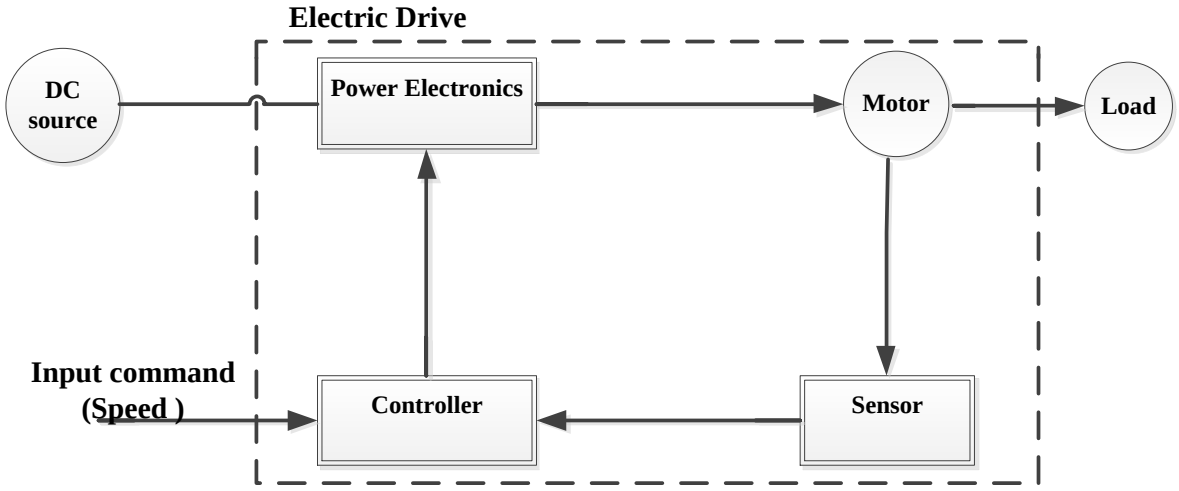

Figure 3:1 AC electric drive block diagram

Figure 3.1 shows that an electric drive system: electric motor, power electronic converter, controller, sensors and the actual load or apparatus are the major components included in the drive. The electric motor is the core component of an electrical drive that converts electrical energy (directed by power processor) into mechanical energy (that drives the load). ~~The motor can be DC motor or AC motor depends on the type of load.~~

AC drives are used to drive the AC motor especially three phase induction and synchronous motors because these are predominant over other motors in most of the industries. In industrial terms, AC drive is also called as variable frequency drive (VFD), variable speed drive (VSD), or adjustable speed drive (ASD)**.** Though there are different types of AC drives, all of them work on same principle of converting fixed incoming voltage and frequency into variable voltage and frequency output. The frequency of the drive determines how fast the motor should run while the combination of voltage and frequency decides the amount of torque that the motor generates [15].

3.2 AC Motor Control Strategies

The speed of AC motors generally depends on the frequency of the supply voltage and the number of magnetic poles per phase in the stator. Early speed controllers were influenced by switching in

different numbers of poles and the control mechanisms were only available manually in rough steps. However, modern electronic inverters make continuously variable frequency supplies possible permitting closed loop speed control.

There are different speed control techniques implemented for variable frequency drives of AC motor control strategies. In detail the basic classifications of AC motor control system is shown in Figure 3.2. The control techniques used in modern AC drive systems are mainly classified as scalar and vector control systems. Those techniques are described as follows [15].

Scalar control: controls magnitude variation of the control variables only, and disregards the coupling effects of the machine.

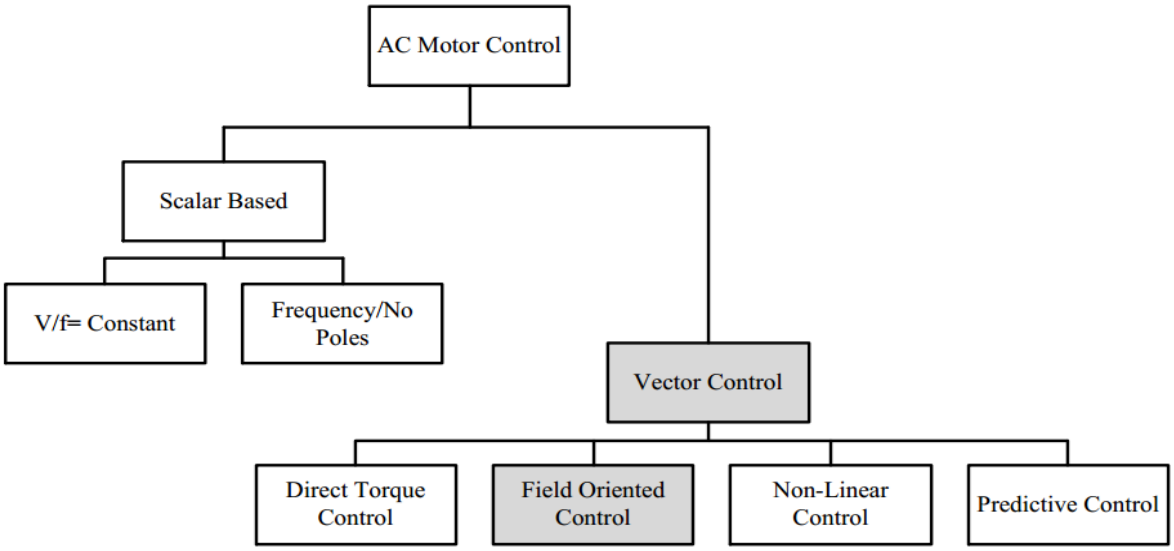

Figure 3:2 AC motor control classifications

Vector control: To solve the problems associated with scalar control methods, the vector methods were invented in the beginning of 1970s [15].

Moreover, the demonstration that synchronous motor can be controlled like separately exited DC motor brought a renaissance in the high-performance control of AC drives.

Apart from controlling the amplitude and frequency of the supplied voltages, the angle can also be controlled in this control method. It means that the magnitude and the angle of the space vectors

are controllable. Because the machine performances like separately exited DC motor, vector control is also known as decoupling, orthogonal, or Trans vector control. Vector control is applicable to both synchronous and induction motor drives [19], [20], and [21].

There are different classifications of vector control methods [15]:

- Direct torque control
- Field oriented control
- Non-linear control
- Predictive control

Among those different types of vector control methods this thesis is employed with Filed oriented control mechanism. Therefore, the next section discusses the FOC control algorithm and mathematical model of the PMSMs. It also shows how FOC reassembles the behavior of the separately excited DC motor in order to control the torque and flux independently, through certain mathematical transformations including Park and Clarke with their inverse transformations, which can be represented with space vector theory. Finally, it explains the dynamics involved in the PMSM drive [15].

3.3 Fundamental Principle of PMSM using FOC

Electrical drive control becomes more accurate in the sense that vector control or FOC manages not only are the ~~DC~~ dq current and voltage but also the three phase currents and voltages. High-performance motor control is characterized by smooth rotation over the entire speed range of the motor, full torque control at low speed and fast accelerations and decelerations. To achieve such control, FOC is an efficient method to control a synchronous motor in adjustable speed drive applications with quickly changing load in a wide range of speeds. It is based on three major points: the machine current and voltage space vectors, the transformation of a three-phase speed and time dependent system into a two co-ordinate time invariant systems and effective Pulse Width Modulation pattern generation. Based on these, the control of AC machine acquires every advantage of DC machine control and frees itself from the mechanical commutation drawbacks [22].

3.3.1 Basic Principles of FOC and Space Vector Transformations

FOC controls the stator currents represented by a vector. This control is based on projections, which transform a three-phase time and speed dependent system into a two co-ordinate (d and q) time invariant system. These projections lead to a structure similar with that of a DC machine control. In order to the motor behave like DC motor, the control needs knowledge of the position of the instantaneous rotor flux or rotor position of PMSM. This needs a resolver or an absolute optical encoder.

The idea of FOC method is to control the current of the machine in space quadrature with the magnetic flux created by the PMs based on the behavior of the separately excited DC motor. ~~This type of DC motor like other DC motors consists of a stator and a rotor.~~ The stator is stationary and it has permanent magnets and/or windings called field winding, while the rotor has a rotating armature, which has a winding called armature winding. This motor is known as separately excited DC motor because the field winding is physically and electrically separate from the armature winding as shown in Figure 3.3. Having independent control of field and armature current allows controlling the torque and the flux independently [17], [23].

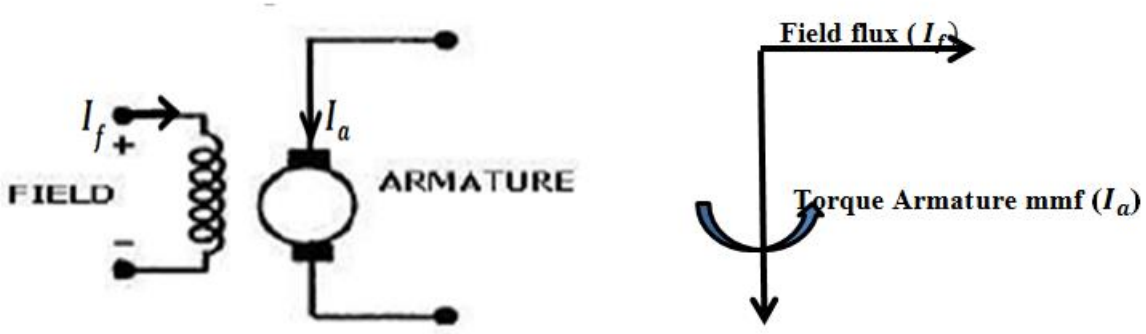

Figure 3:3 Separately excited DC motor

The armature current is supplied via brushes and a commutator, which are mechanically arranged in order to keep the flux from the rotor and the stator field orthogonal in order to have optimal torque over all speed range.

The action of the commutator is to reverse the direction of the armature winding currents as the coils pass the brush position that the armature current distribution is fixed in space no matter what rotor speed exists. As shown in the Figure 3.3, the field flux and armature MMF are maintained in a mutually perpendicular orientation independent of rotor speed. The result of this orthogonally is that the field flux is unaffected by the armature current so the field flux and the armature MMF are decoupled.

Like separately excited DC motor Field Oriented Control seeks to recreate these orthogonal components in AC machines in order to control the torque producing current separately from the magnetic flux producing current so as to achieve the responsiveness of a DC motor. FOC structure handles instantaneous electrical quantities. This makes the control accurate in every working operation (steady state & transient) and independent of the limited bandwidth mathematical model. FOC controlled machines need two constants as input references: the torque component (aligned with the q-coordinate) and the flux component (aligned with d- coordinate) [22].

The FOC thus solves the classic scheme problems, in the following ways [22]:

- The ease of reaching constant reference (torque component and flux component of the stator current)
- The ease of applying direct electromagnetic torque, T_{em} control in the (d, q) reference frame.

$$T_{em} = \frac{3}{2} P \Psi_m i_q \tag{3.1}$$

Where T_{em} is generated electromagnetic torque, P is pole pair, Ψ_m is permanent magnet flux linkage and i_q is quadrature axis current (torque producing current component)

Section 3.6 discusses about these two components in detail.

3.3.1.1 FOC Overview

FOC consists of representing the 3-phase currents (I_a,I_b I_c) into a complex space vector I_s , and then projecting it into a two orthogonal stationary reference frame. This transformation is called Clark Transformation, and it provides two stationary variables ($I_{s\alpha}$ and $I_{s\beta}$) which are time-varying quadrature currents. Then, the Park transformation converts the two orthogonal stationary

reference frames into two orthogonal rotating frames based on rotor flux position. The Park transformation has the unique property of eliminating all time varying inductances due to rotor spinning from the voltage equations of the AC machine. For steady state conditions I_{sd} and I_{sq} are constant and can be controlled with two PI controllers. I_{sq} is related to torque where as I_{sd} is related to flux. I_{sdref} is set to zero in order to have a direct proportionality between torque and current [15], [24].

Having controlled these components, the inverse Park transformation converts the rotating reference frame back into stationary reference. This transformation provides two variables $V_{s\alpha ref}$ and $V_{s\beta ref}$, which are the components of a reference voltage vector.

The Space Vector Modulation (SVM) determines the switching sequence of the upper three power transistors of an inverter, in this case a voltage source inverter (VSI). The idea of this technique is to approximate the reference voltage vector by a combination of eight switching patterns. The term approximate means that it makes the average output voltage of the inverter (in small period T) to be the same as the average of reference vector in the same period [25]. Figure 3.4 shows the description of each block which is involved in FOC in more detail, but it is necessary to review the concept of space vector.

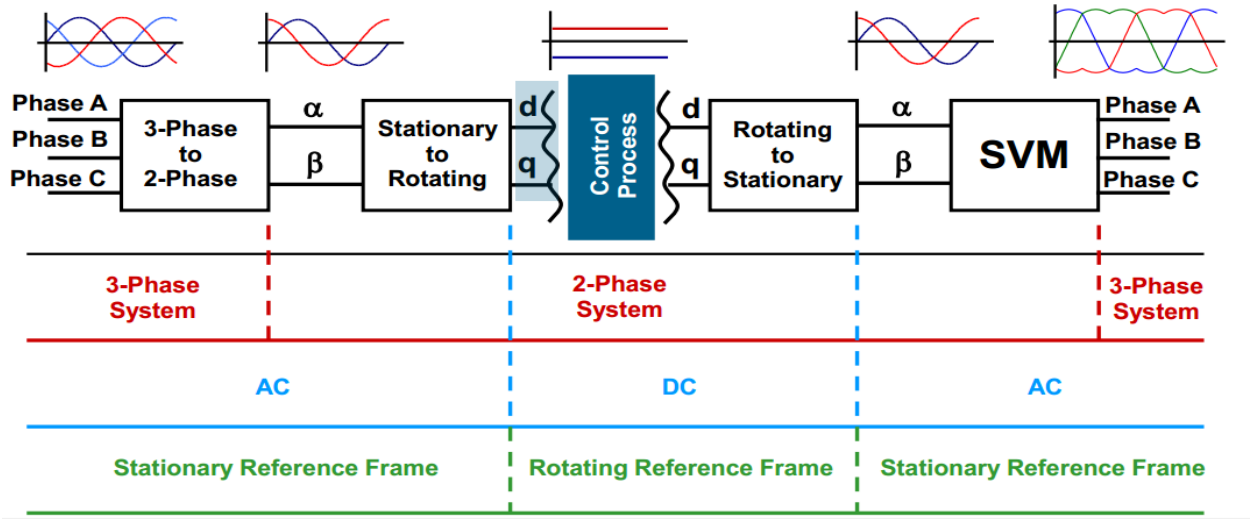

Figure 3:4 FOC overviews [19]

In general the FOC has the following producers [19]**:**

- Measure the motor quantities (phase voltages and currents).
- Transform them to the 2-phase system (α, β) using a Clarke transformation.
- Calculate the rotor flux space vector magnitude and position angle.
- Transform stator currents to the d-q coordinate system using a Park transformation.
- The stator current torque- (i_{sq}) and flux- (i_{sd}) producing components are separately controlled.
- The output stator voltage space vector is calculated using the decoupling block.
- An inverse Park transformation transforms the stator voltage space vector back from the d-q coordinate system to the 2-phase system fixed with the stator.
- Using the space vector modulation, the output 3-phase voltage is generated.

To perform these controls, the electrical equations will project from a three-phase non-rotating frame to a two coordinate rotating frame. This mathematical projection (Clarke and Park transformation) greatly simplifies the expression of the electrical equations and removes their time and position dependencies.

Filed Oriented Control Advantages

One of the main advantages of using FOC is that to generate the most optimal torque in the motor by aligning rotor and stator flux. It improves dynamic response by adjusting both amplitude and phase of the control signals fed back to the motor. Applications such as direct drive washing machines benefit with this advantage [16].

In FOC, stator field is continuously updated based on the position of the rotor field. By continuously pulling the rotor to a new position, the rotor is always magnetized with a new vector, thus reducing torque ripple. Applications where low speeds are required take advantage of this property of FOC. Sinusoidal commutation accomplished with FOC, also reduces audible noise produced by other types of control [2].

Another advantage of FOC is enabling speeds above motor's rated speed. This is accomplished by energizing the stator windings at an angle where the rotor's magnetic field is weakened, and the

resulting magnetic field vector composed by stator's field and rotor's field is increased. Speed range can be increased considerably by using field weakening or phase advance control, while in this thesis field weakening region is not deliberated [2].

3.3.1.2 Space Vector transformation

Since, the FOC consists of controlling the stator currents represented by a vector. This control is based on projections, which transform a three-phase time and speed dependent system into a two co-ordinate (d and q co-ordinates) time invariant system. Assume that we have the three phase supply voltage is balanced SPMSM model and the transformations will be takes place usually based on following assumptions [22]:

- Space harmonics of the flux linkage distribution are neglected.
- Slot harmonics and deep bar effects are not considered.
- Saturation is neglected.
- Permanent magnets behave linearly.
- Neutral point is isolated.
- Rotor flux is assumed to be concentrated across d-axis and zero flux along q-axis
- Rotor flux is assumed to be fixed at a given operating point
- Machine core losses are negligible
- Rotor temperature alters the flux, but the variation with time is assumed to be negligible
- There are no field current dynamics

Rotor reference frame is chosen because rotor position determines independently the stator voltages & currents, induced EMF, and torque. The d-q coordinate system rotates at the same speed of rotor; there is zero speed difference between rotor speed and revolving stator field. The stator d-q axis has a fixed phase relationship with rotor magnetic axis, which is d-axis in modeling.

The three-phase voltages, currents and fluxes of AC-motors can be analyzed in terms of complex space vectors. With regard to the currents, the space vector can be defined as follows. Assuming that i_a, i_b, i_c are the instantaneous currents in the stator phases as shown in Figure 3.5, and then the complex stator current vector $\vec{i_s}$ is defined by:

$$\vec{i_s} = i_a + \alpha i_b + \alpha^2 i_c \qquad (3.2)$$

Where $\alpha = e^{j\frac{2}{3}\pi}$ and $\alpha^2 = e^{j\frac{4}{3}\pi}$ represent the spatial operators. The following figure shows the stator current complex space vector:

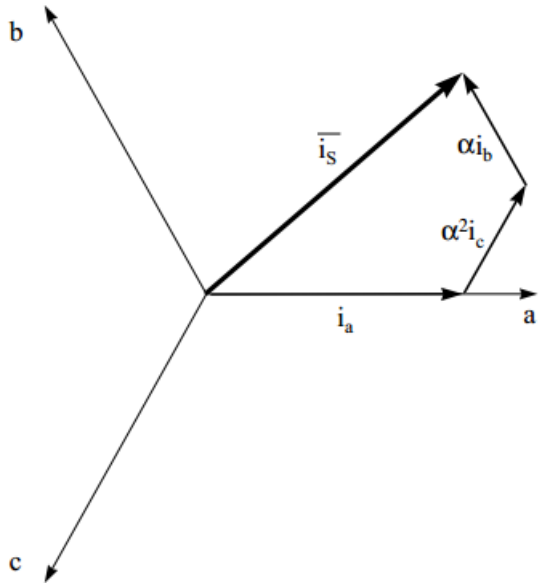

Figure 3:5 Stator current space vector and its component in (a, b, c) axes

This current space vector depicts the three-phase sinusoidal system. It still needs to be transformed into two time-invariant co-ordinate systems. This transformation has two basic steps:

Clark Transformation (a, b, c) to (α, β) coordinates

The space vector can be reported in another reference frame with only two orthogonal axis called (α, β). Assuming that the axis "a" and the axis "α" are in the same direction we have the following vector diagram in Figure 3.6 [22]:

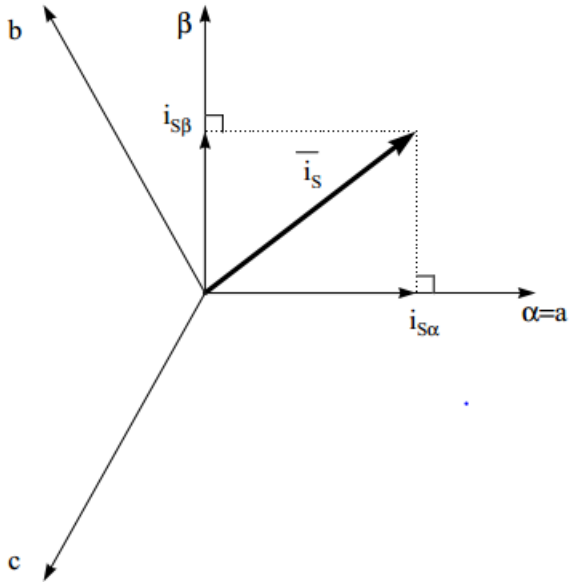

Figure 3:6 Stator current space vector and its components in the stationary reference frame

The projection that modifies the three phase system into the (α, β) two dimension orthogonal systems are defined as below [22]:

$$\begin{bmatrix} i_{s\alpha} \\ i_{s\beta} \end{bmatrix} = \begin{bmatrix} \frac{2}{3} & \frac{-1}{3} & \frac{-1}{3} \\ 0 & \frac{\sqrt{3}}{3} & -\frac{\sqrt{3}}{3} \end{bmatrix} \begin{bmatrix} i_a \\ i_b \\ i_c \end{bmatrix} \quad \text{wrong} \tag{3.3}$$

Or

$$i_{s\alpha} = i_a$$

$$i_{s\beta} = \frac{1}{\sqrt{3}} i_a + \frac{2}{\sqrt{3}} i_b \tag{3.4}$$

Since, $i_a + i_b + i_c = 0$

However, the two phase currents still depend on time and speed. So another transformation needs to be proceeding.

Park Transformation (α β) to (d, q) coordinates

This is the most important transformation in the FOC. In fact, this projection modifies a two-phase orthogonal system (α, β) in the d, q rotating reference frame. If we consider the d axis aligned with the rotor flux, Figure 3.7 below shows the current vector relationship with the two-reference frame [22]: Where– θ_{re} is the electrical rotor flux position.

$$\theta_{re} = p\,\theta_r \tag{3.5}$$

Where p is number of pole pairs and θ_r - is rotor position which is defined as the angle between the direction of the field generated by the permanent magnets and the direction of the field generated by the phase 'a' winding.

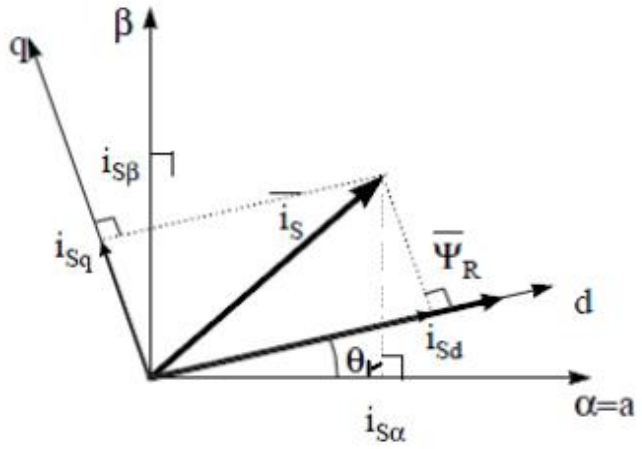

Figure 3:7 Stator current space vector and its component in (α, β) and in the (d, q) rotating reference frame

The flux and torque components of the current vector are determined by the following equations [22]:

$$\begin{aligned} i_{sd} &= i_{s\alpha}\cos\theta_{re} + i_{s\beta}\sin\theta_{re} \\ i_{sq} &= -i_{s\alpha}\sin\theta_{re} + i_{s\beta}\cos\theta_{re} \end{aligned} \tag{3.6}$$

These components depend on the current vector (α, β) components and on the rotor flux position; if we know the right rotor flux position then, by this projection, the d, q component becomes a constant. Two- phase currents now turn into dc quantity (time-invariant). At this point, the torque control becomes easier where constant i_{sd} (flux component) and i_{sq} (torque component) current components controlled independently.

Inverse Park transformation is also used to transform v_{sd} and v_{sq}voltages to $v_{s\alpha}$ and $v_{s\beta}$ voltages system [22]:

$$v_{s\alpha} = v_{sd} \cos \theta_{re} - v_{sq} \sin \theta_{re}$$
$$v_{s\beta} = v_{sd} \sin \theta_{re} + v_{sq} \cos \theta_{re} \quad (3.7)$$

At this point you were asked to include inverse park transformation and rotor position detection,Still you have to

3.4 Mathematical Modeling of PMSM

In order to understand and analyze vector control (FOC) of a PMSM drive system the mathematical model have to define in a fixed reference frame.

The dynamic model of the PMSM is derived using a two-phase motor in direct and quadrature (hereafter referred to as d-q) axes. This approach is desirable because of the conceptual simplicity obtained with only one set of two windings on the stator. The rotor has no windings, only magnets. The magnets are modeled as a current source or a flux linkage source, concentrating all its flux linkages along only one axis.

PMSM is very similar to the standard wound rotor synchronous machine except that the PMSM has no damper windings and excitation is provided by a PM instead of a field winding. Hence, the *d*, *q* model of the PMSM can be derived from the well-known model of the synchronous machine with the equations of the damper windings and field current dynamics removed.

For the control and simulation of the electrical machine a mathematical model is required. In a PMSM where inductances vary as a function of rotor angle, the 2 phase (d-q) equivalent circuit model is commonly used for simplicity and intuition. In this section, a two phase model for a PMSM is presented. The dynamical model of PMSM is modeled based on the following assumptions [1], [2]:

1) Saturation is neglected.

2) Stator windings produce sinusoidal MMF distribution.

3) Eddy currents and hysteresis losses are negligible.

4) Balanced three-phase supply voltage is considered.

5) Number of turns on the stator windings is equal.

Voltage Equation

The derivations of the electrical equations are simplified due to the concept of rotating transformation. The two axis voltage equations for the stator winding which are of an IPMSM (but is the same for SPMSM where *Ld* and *Lq* have the same value).

The d- and q-axes stator voltages are derived as the sum of the resistive voltage drops and the derivative of the flux linkages in the respective windings is given by [1];

$$V_q = R_s i_q + \frac{d}{dt}\left(\Psi_q\right) + \omega_{re}\Psi_d \tag{3.8}$$

$$V_d = R_s i_d + \frac{d}{dt}\left(\Psi_d\right) - \omega_{re}\Psi_q \tag{3.9}$$

And, $\Psi_d = L_d \mathrm{i}_d + \Psi_m$ And $\Psi_q = L_q \mathrm{i}_q$ (3.10)

Where, V_d and V_q are the (d, q) axis stator voltages,

i_d and i_q are the (d, q) axis stator currents

L_d and L_q are the d, q axis inductances

ω_{re} is rotor electrical angular velocity

Ψ_m is flux linkage due to the rotor magnets linking the stator

Ψ_d and Ψ_q are the (d, q) axis stator flux linkages

R_s is the stator winding resistance

NB: The stator winding numbers of turns are equal, $R_s = R_d = R_q$

We can obtain a more convenient equation by substituting Equation (3.10) into Equations (3.8) and (3.9) respectively [1]:

$$V_q = R_s i_q + \frac{d}{dt}\left(L_q \mathrm{i}_q\right) + \omega_{re}(L_d \mathrm{i}_d + \Psi_m)$$

$$V_q = (R_s + L_q \frac{d}{dt})\mathrm{i}_q + \omega_{re} L_d \mathrm{i}_d + \omega_r \Psi_m \tag{3.10}$$

$$V_d = R_s i_d + \frac{d}{dt}(L_d \mathrm{i}_d + \Psi_m) - \omega_{re} L_q \mathrm{i}_q$$

$$V_d = (R_s + L_d \frac{d}{dt}) i_d - \omega_{re} L_q \mathrm{i}_q \tag{3.12}$$

From the dynamic Equation (3.8) and (3.9) the equivalent circuit of the PMSM can be derived for the stator q-axis and d-axis coordinates shows in Figure 3.8.

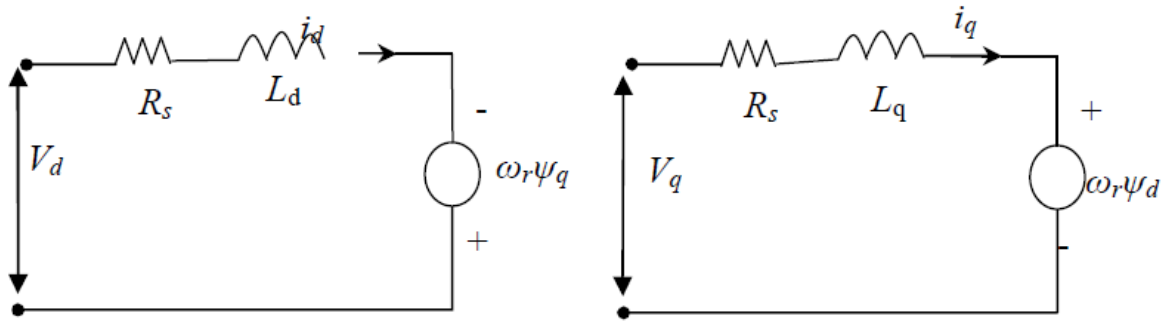

(a) d-axis circuit (b) q-axis circuit

Figure 3:8 Equivalent circuit of PMSM dynamic model

Electromagnetic Torque Equation

The electromagnetic torque is the most important output variable that determines the mechanical dynamics of the machine such as the rotor position and speed. The derivation of electromagnetic torque is made as follows [2]. The mechanical power is the product of the mechanical rotor speed and air gap or electromagnetic torque. Hence, the air gap torque, T_{em} is derived from the terms involving the rotor speed ω_r, in mechanical rad/s, as [2]

$$P_m = \omega_m T_{em} = \frac{3}{2}\omega_r(\Psi_d i_q - \Psi_q i_d) \quad (3.13)$$

Rotor or electrical speed is related to mechanical speed as

$$\omega_r = \omega_{re} = \omega_m P \quad (3.14)$$

Where, P_m is output mechanical power

ω_m is mechanical angular velocity of the rotor shaft

ω_{re} is electrical angular rotor velocity

T_{em} is generated electromagnetic torque

P is number of pole pairs

By substituting Equations (3.10) and (3.14) into Equation (3.13) we will obtain [13]

$$T_{em} = \frac{3}{2}P[\Psi_m i_q + (L_d - L_q) i_q i_d] \quad (3.15)$$

In Equation (3.15), the first term is called "mutual reaction torque" occurring between i_q and the permanent magnet, while the second term corresponds to "reluctance torque" due to the saliency.

The motor used in this thesis is surface mounted PMSM which means that $L_d = L_d = L_S$ therefore the "reluctance torque" is equal to zero, so the torque expression for SPMSM is [2]:

$$T_{em} = \frac{3}{2} P \Psi_m \mathrm{i}_q = \mathrm{K}_t \mathrm{i}_q \tag{3.16}$$

Where $\mathrm{K}_t = \frac{3}{2} P \Psi_m$, is torque constant

The rotation of motor could be described by the following dynamic equation which is expressed as in terms of electromagnetic torque [1] [2]:

$$T_{em} = T_l + J \frac{d}{dt} \omega_{\mathrm{m}} + B \omega_{\mathrm{m}} \tag{3.17}$$

Where T_l is load torque, J is inertia and B is viscous friction coefficient

Constant torque operation

By considering three phase balanced current as input we can analyze the constant torque operation. As these constants, they are similar to the armature and field currents in the separately excited DC machine. The q axis current is distinctly equivalent to the armature current of the dc machine; the d axis current is field current, but not in its entirety. It is only a partial field current; the other part is contributed by the equivalent current source representing the permanent magnet field.

For this reason the q axis current is called the torque producing component of the stator current and the d axis current is called the flux producing component of the stator current i_d and i_q in terms of $\mathrm{I_S}$ as follows [1]:

$$i_d = I_s \cos \alpha$$
$$i_q = I_s \sin \alpha \tag{3.18}$$

Where α is the angle between the rotor field and stator current phasor or torque angle.

Constant torque control strategy is derived from field oriented control theory, where the maximum possible torque is desired at all times like the DC motor. This is performed by making the torque producing current i_q equal to the supply current I_S. That results in selecting the angle α to be 90° shown in Figure 3.9. Then electromagnetic torque Equation (3.16) can be.

$$T_{em} = K_t i_q = K_t I_S \sin\alpha \quad (3.19)$$

Where, α is the angle between the rotor field and stator current phasor.

Like the DC motor, the torque is dependent of the motor current.

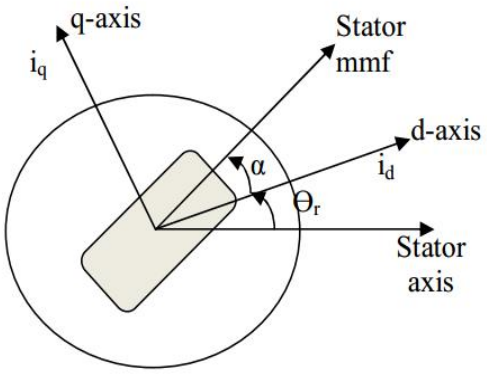

Figure 3:9 PMSM motor axes

To control independently the direct-axis stator current i_d (field producing component) and the quadrature-axis stator current i_q (torque-producing component) it is necessary to cancel the effect of these coupling terms at the output of the current PI controller.

Therefore, the stator voltage components given by Equation (3.11) and (3.12) have to be decoupled. The stator currents i_d and i_q can only be independently controlled (decoupled control) if the stator voltage equations are decoupled, so these stator current components are indirectly controlled by controlling the terminal voltages of the synchronous motor [1]. This is only to show that the non-linear component of the system, the FOC controlling mechanism overcomes this non-linarites, so its effect is not included in the simulation design part. So as this stand the decoupling voltage components for d and q axis respectively is given by:

$$V_{q\,D} = \omega_{re} L_d i_d + \omega_{re} \Psi_m \quad (3.20)$$

$$V_{d\,D} = \omega_r L_q i_q \quad (3.21)$$

3.5 General Control Scheme of PMSM Drive System

In this section descriptions of the different components of the drive system has been explained. The overall block schematic of FOC of PMSM is shown as in the Figure 3.10.

The FOC is based on current controlled VSI structure. The function of an inverter is to change a dc input voltage to a symmetrical ac output voltage of desired magnitude and frequency. The output voltage could be fixed or variable at a fixed or variable frequency. A variable output voltage can be obtained by varying the input dc voltage and maintaining the gain of the inverter constant.

On the other hand, if the DC input voltage is fixed and is not controllable, this is normally accomplished by PWM control within the inverter**.** The detail control scheme for the FOC of PMSM drives is shown in the Figure 3.10.

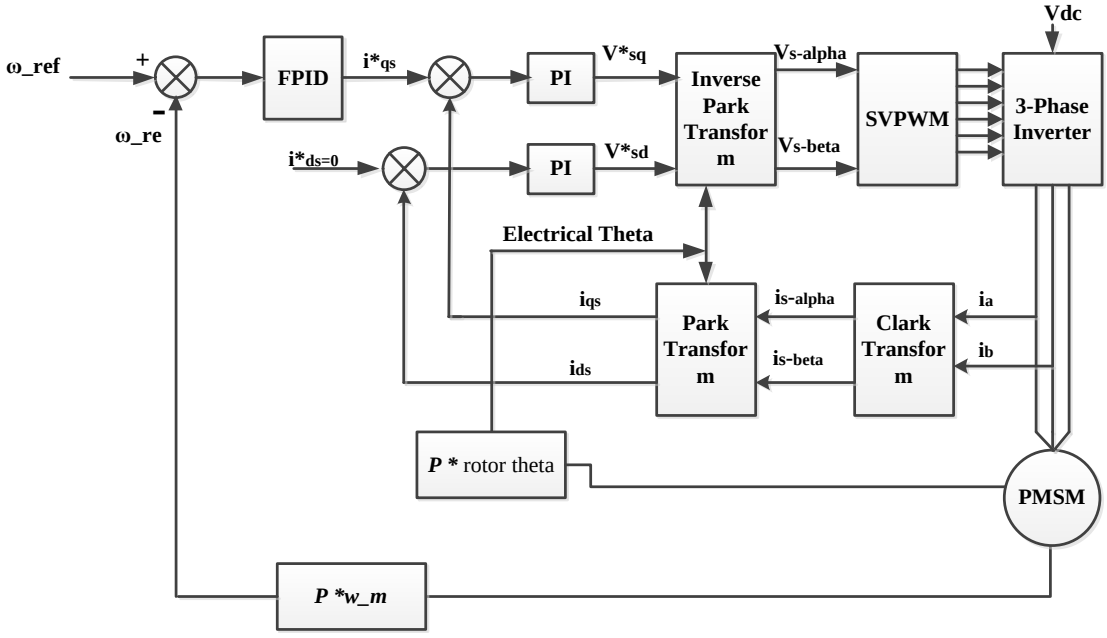

Figure 3:10 FOC for PMSM drive system

3.5.1 Voltage Source Inverter

A variable frequency drive has two stages of power conversion, a rectifier and an inverter. ~~Sometimes inverter is also used to refer to the entire drive~~. The rectifier part is used when the supply is obtained from AC sources, whereas the inverter is used when the sources is DC supply. The inverter is composed of electronic switches (thyristors or transistors) that switch the DC power

on and off to produce a controllable AC power output at the desired frequency and voltage. The inverters can be broadly classified into two types [2]:

- Voltage source inverter (VSI)
- Current source inverter (CSI)

The VSI is more common and it produces well defined switched voltage waveforms at the terminal of the motor. The voltage control of these inverters is usually obtained using PWM. The current source inverter or CSI provides switched current waveforms at the motor terminals. The output current of a CSI drive contains high harmonics, which necessitates that CSI drives include filters on the input and output sides. So this addition of components increases the cost of the design and complexity [28].

VSI inverters are typically more efficient for high dynamic applications with fast changes in motor speed or toque than CSI inverters. Because the IGBT switching devices used in VSI inverter are inherently more efficient and fast in switching times than GTO or SGCT used in CSI versions.

Three-phase PWM Voltage Source Inverter

The power circuit topology of a three-phase voltage source inverter is shown in Figure 3.11. Each power switch is a transistor or insulated gate bipolar transistor (IGBT) with anti-parallel diodes. The pole or the leg voltages are denoted by a capital suffix letter V_A, V_B, V_C and can attain the value + 0.5 V_{dc} when the upper switch is operating and - 0.5 V_{dc} when the lower switch is operating. The phase voltage applied to the load is denoted by the letters v_{an}, v_{bn}, v_{cn}. The operation of the upper and the lower switches are complimentary (a small dead band is provided in real time implementation) [1] [15].

The relationship between the leg voltage and switching signals are [15];

$$V_k = S_k * V_{dc} \; ; \quad k = A, B, C \tag{3.22}$$

Where $S_k = 1$ when the upper power switch is 'ON' and $S_k = 0$ when the lower switch is 'ON.' If the load is assumed to be a star connected three-phase, then the relation between the phase-to-neutral load voltage and the leg voltages can be written as [15]:

$$V_A(t) = v_a(t) + v_{nN}(t)$$

$$V_B(t) = v_b(t) + v_{nN}(t)$$
$$V_C(t) = v_c(t) + v_{nN}(t) \quad (3.23)$$

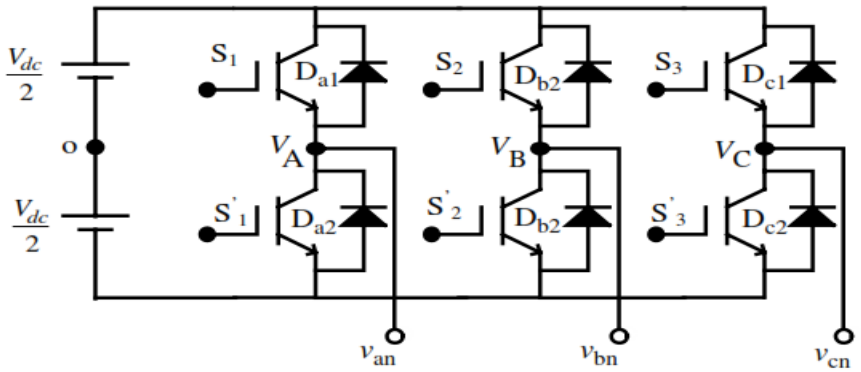

Figure 3:11 Power circuit topology of a three-phase VSI [15]

By adding each term of the Equation (3.23), and setting the sum of phase to neutral voltage to zero (assuming a balanced three-phase voltage whose instantaneous sum is always zero), the following is obtained [15]:

$$v_{nN}(t) = \frac{1}{3}[V_A(t) + V_B(t) + V_C(t)] \quad (3.24)$$

Substituting Equation (3.24) back into (3.23), the following expressions for the phase-to-neutral voltage are obtained [15]:

$$v_a(t) = \frac{2}{3}V_A(t) - \frac{1}{3}[V_B(t) + V_C(t)]$$
$$v_b(t) = \frac{2}{3}V_B(t) - \frac{1}{3}[V_A(t) + V_C(t)]$$
$$v_c(t) = \frac{2}{3}V_C(t) - \frac{1}{3}[V_B(t) + V_A(t)] \quad (3.25)$$

Equation (3.25) can also be written using the switching function definition of Equation (3.22):

$$v_a(t) = \frac{1}{3}V_{dc}[2S_A - S_B - S_C]$$
$$v_b(t) = \frac{1}{3}V_{dc}[2S_B - S_A - S_C]$$
$$v_c(t) = \frac{1}{3}V_{dc}[4S_C - S_B - S_A] \quad (3.26)$$

I checked it from [9] and equation wrong,I could not get [15],you have to either bring me [15] to check it or you have to clearly settle the difference.

And the associated waveforms for six-step modes are shown in Figure 3.12.

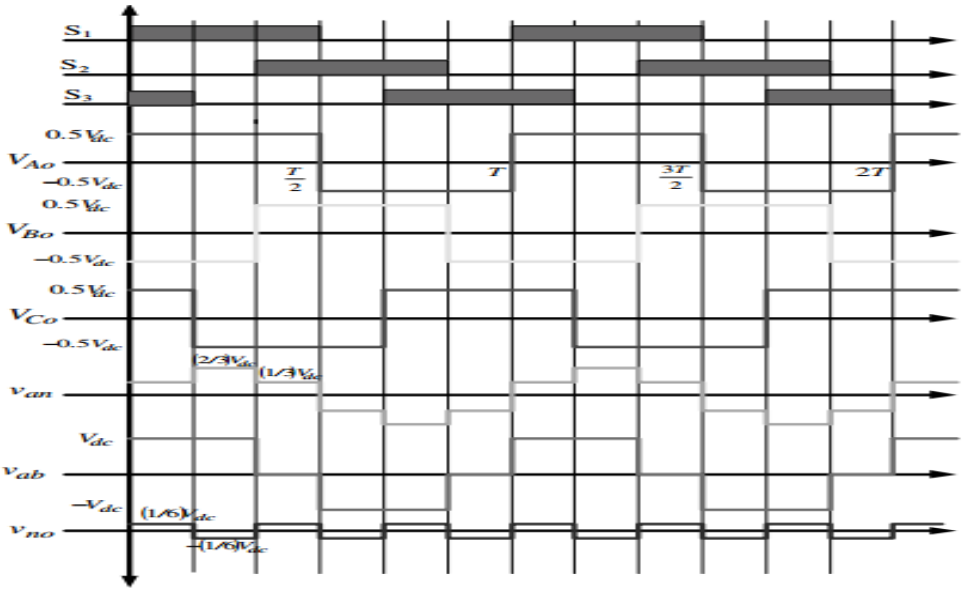

Figure 3:12 Waveforms for square wave mode of operation of a three-phase inverter [15]

From Figure 3.12 we understand that the leg voltage takes on the values +0.5 Vdc and -0.5 Vdc and the phase voltage has six steps in one fundamental cycle. The steps in the phase voltages have amplitudes of ±1/3 Vdc and ± 2/3 Vdc and the line voltage varies between +Vdc and -Vdc, while the common mode voltage varies between +1/6 Vdc and -1/6 Vdc. During the six-step operation of the inverter, the values of the leg voltages are shown in Table 3.1.To determine the phase-to-neutral voltages for the six-step mode, the leg voltages from Table 3.1 is substituted into Equation (3.26), and the corresponding values are listed in Table 3.2 for a star-connected load. The line voltages are obtained by using Equation (3.27) and are listed in Table 3.3

$$vab = van - vbn$$
$$vbc = vbn - vcn$$
$$vca = vcn - van \quad (3.27)$$

Table 3.1 Leg/Pole voltages of a three-phase VSI during six-step mode of operation

Switching Mode	Switches ON	Leg voltage VA	Leg voltage VB	Leg voltage VC
1	S1, S'2, S3	0.5Vdc	-0.5Vdc	0.5Vdc
2	S1, S'2, S'3	0.5Vdc	-0.5Vdc	-0.5Vdc
3	S1, S2, S'3	0.5Vdc	0.5Vdc	-0.5Vdc

4	S'1, S2, S'3	-0.5Vdc	0.5Vdc	-0.5Vdc
5	S'1, S2, S3	-0.5Vdc	0.5Vdc	0.5Vdc
6	S'1, S'2, S3	-0.5Vdc	-0.5Vdc	0.5Vdc

Table 3.2 Phase-to-neutral voltages for six-step mode of operation

Switching mode	Switches ON	Phase Voltage van	Phase voltage vbn	Phase voltage vcn
1	S1, S'2, S3	1/3 Vdc	-2/3 Vdc	1/3 Vdc
2	S1, S'2, S'3	2/3 Vdc	-2/3 Vdc	-1/3 Vdc
3	S1, S2, S'3	1/3 Vdc	1/3 Vdc	-2/3 Vdc
4	S'1, S2, S'3	-1/3 Vdc	2/3 Vdc	-1/3 Vdc
5	S'1, S2, S3	-2/3 Vdc	1/3 Vdc	1/3 Vdc
6	S'1, S'2, S3	-1/3 Vdc	-1/3 Vdc	2/3 Vdc

The maximum output peak phase-to-neutral voltage in the six-step mode is 0.6367Vdc or $(2/\pi)$ Vdc and that of the line-to-line voltage is 1.1Vdc.

Table 3.3 Line voltages for six-step mode of operation

Switching mode	Switches ON	Line Voltage vab	Phase voltage vbc	Phase voltage vca
1	S1, S'2, S3	Vdc	Vdc	0
2	S1, S'2, S'3	Vdc	0	Vdc
3	S1, S2, S'3	0	Vdc	Vdc
4	S'1, S2, S'3	Vdc	Vdc	0
5	S'1, S2, S3	Vdc	0	Vdc
6	S'1, S'2, S3	0	Vdc	Vdc

3.5 PWM Techniques

With advances in solid-state power electronic devices and microprocessors, various in- vector control techniques employing PWM techniques are becoming increasingly popular in AC motor drive applications. These PWM-based drives are used to control both the frequency and the magnitude of the voltages applied to motors. PWM strategy plays an important role in the minimization of harmonics and switching losses in converters, especially in three-phase

applications. The main aim of any modulation technique is to obtain a variable output with a maximum fundamental component and minimum harmonics. These PWM techniques; SPWM (Sinusoidal PWM) or carrier-based PWM, Third-harmonic-PWM (THIPWM) and SVPWM (Space Vector PWM) are well known techniques. The Space Vector modulation technique is an advanced, computation intensive PWM technique and is possibly the best among all the PWM techniques for drives applications [1], [2], [15].

3.5.1 Space Vectors Pulse Width Modulation (SVPWM)

The SVPWM technique is one of the most popular PWM techniques due to a higher DC bus voltage use (higher output voltage when compared with the SPWM). The concept of the SVPWM relies on the representation of the inverter output as space vectors or space phasors. Space vector representation of the output voltages of the inverter is realized for the implementation of SVPWM. Space vector simultaneously represents three-phase quantities as one rotating vector, hence each phase is not considered separately. The three phases are assumed as only one quantity. The space vector representation is valid for both transient and steady state conditions in contrast to phasor representation, which is valid only for steady state conditions.

Using PWM VSI possible to control both frequency and magnitude of the voltage and current applied to the PMS motor drive. As a result, SVPWM inverter-fed PMSM drives are more variable, reliable and offer a wide range speed [26], [27]. SVPWM is accomplished by rotating a reference vector around the state diagram, which is composed of six basic none zero vectors forming a hexagon shown in Figure 3.13.

A circle can be inscribed inside the state map and corresponds to sinusoidal operation. The area inside the inscribed circle is called the linear modulation region or Under-modulation region. As shown below in Figure 3.13, the area between the inside circle and outside circle of the hexagon is called the nonlinear modulation region or over-modulation region.

The concepts in the operation of linear and nonlinear modulation regions depend on the modulation index, which indirectly reflects on the inverter utilization capability.

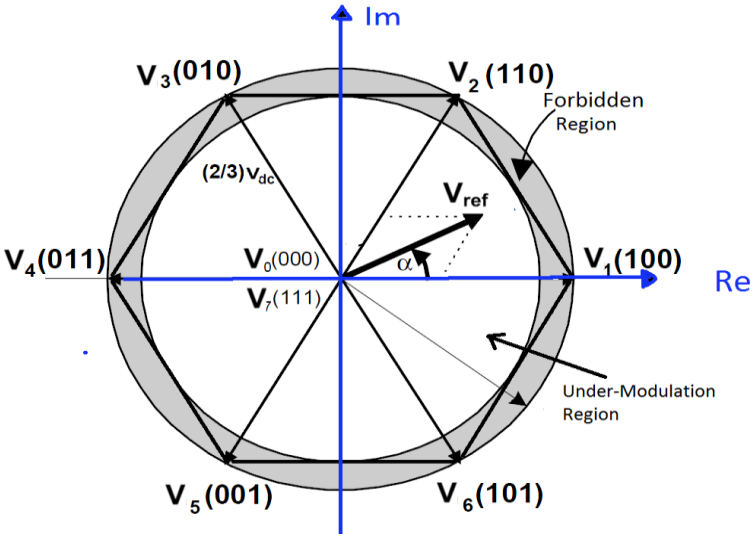

Figure 3:13 Under-modulation and over-modulation region in space vector representation [26]

In order to minimize the switching loss that is caused by the pure SVPWM, Max-Min offset is added to inject third harmonics and reduce the requirement of filter design. In this respect max-min offset technique is used in order to overcome this problem.

Based on [15] the design of the offset is as follows: the MATLAB Simulink design is show in Appendix A.

Offset = $-(\frac{V_{\max}+V_{\min}}{2})$; $V_{\max}= max\{V_{An}, V_{Bn}, V_{cn}\}$; $V_{\min} = min\{V_{An}, V_{Bn}, V_{cn}\}$

The output voltage magnitude reaches the same value as that of the third harmonics injection PWM.

3.6.1 Principle and Implementation of Space Vector PWM

As it has been discussed on the previous pages, the three-phase inverter is therefore controlled by six switches and with eight inverter configurations. The eight inverter states can be transformed into eight corresponding space vectors. In summery the relationship between the space vector and the corresponding switching states is given in Figure 3.14.

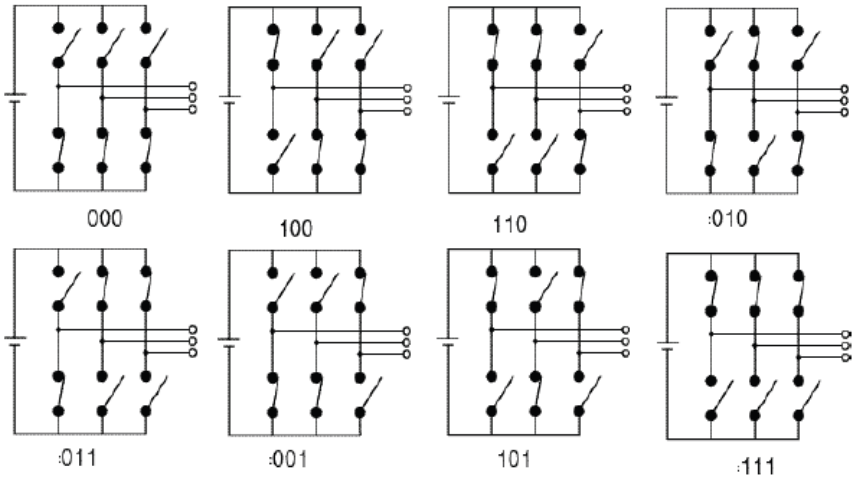

Figure 3:14 Eight switching state of a three-phase inverter [27]

We use orthogonal coordinates to represent the three-phase two-level inverter in the phase diagram. There are eight possible inverter states that can generate eight space vectors. These are given by the complex vector expressions [26]:

$$\vec{v}_k = \frac{2}{3} v_{dc} e^{j(k-1)\frac{\pi}{3}} \quad \text{if } k = 1; 2; 3; 4; 5; 6$$
$$0 \quad \text{if } k = 0; 7: \tag{3.28}$$

Which means each sector is bounded by two active vectors. Both $\vec{v}_0$ and $\vec{v}_7$ voltage vectors are with zero amplitude located at the origin of the hexagon. The eight active and non-active state vectors are geometrically.

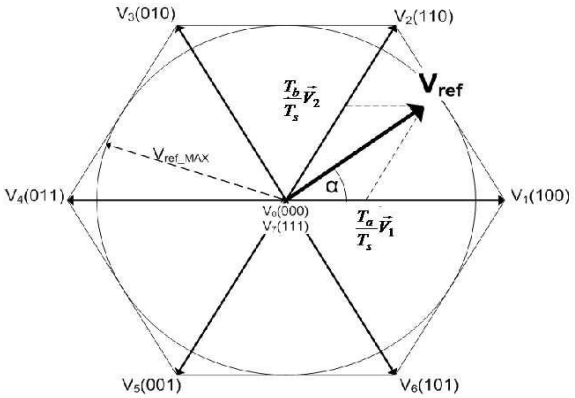

Figure 3:15 Space vectors of three-phase bridge inverter [26].

The reference voltage vector $\vec{v}_{ref}$ rotates in space at an angular velocity. When the reference voltage vector passes through each sector, different sets of switches will be turned on or off. As a result, when the reference voltage vector rotates through one revolution in space, the inverter output varies one electrical cycle over time. The inverter output frequency coincides with the rotating speed of the reference voltage vector. The zero vectors ($\vec{v}_0$ and $\vec{v}_7$) and active vectors ($\vec{v}_1$ to $\vec{v}_6$) do not move in space. Figure 3.15 shows the reference vector $\vec{v}_{ref}$ in the first sector. The six active voltage space vectors are shown on the same graph with an equal magnitude of $2V_{dc}/3$ and a phase displacement of 60^o.

The principle of SVPWM requires the determination of a sector, calculation of vector segments, and it involves region identification based on the modulation index and calculation of switching time durations. The procedure for implementing a two-level space vector PWM can be summarized as follows based on [28] [29].

- ✓ First, calculate the angle θ and reference voltage vector $\vec{v}_{ref}$ based on the input voltage components.
- ✓ Second, calculate the modulation index and determine if it is in the over-modulation region.
- ✓ Third, determine the sector in which $\vec{v}_{ref}$ lies, and the adjacent space vectors of $\vec{v}_k$ and $\vec{v}_{k+1}$ based on the sector angle θ.
- ✓ Fourth, determine the time intervals T_a and T_b and T_0 based on sampling time, and the angle.
- ✓ Finally, determine the modulation times for the different switching states.

Calculate Angle and Reference Voltage Vector: in this stage, the three phase output voltage vector is represented by a reference vector that rotates at an angular speed of $\omega = 2\pi f$. The SVPWM uses the combinations of switching states to approximate the reference vector. A reference voltage vector ($\vec{v}_{ref}$) that rotates with angular speed ω in the α, β plane represents three sinusoidal waveforms with angular frequency w in the abc coordinate system.

The space vector with magnitude ($\vec{v}_{ref}$) rotates in a circular direction at an angular velocity of ω where the direction of rotation depends on the phase sequence of the voltages. If it has a positive

phase sequence, then it rotates in the counter clockwise direction. Otherwise, it rotates in the clockwise direction with a negative phase sequence.

The three phase voltages could be described with only two components, α and β, in a two dimensional plane. The magnitude of each active vector is $2vdc/3$. The active vectors are 60^0 apart and describe a hexagon boundary. The locus of the circle projected by the space reference vector $\vec{v}_{ref}$ depends on $\vec{v}_0$, $\vec{v}_1$, $\vec{v}_2$, $\vec{v}_3$, $\vec{v}_4$, $\vec{v}_5$, $\vec{v}_6$, $\vec{v}_7$ [26]

$$\vec{v}_{ref} = \frac{2}{3}[v_a + \propto v_b + \propto^2 v_c] \tag{3.29}$$

Where, $\propto = e^{j2\pi/3}$. The magnitude of the reference vector is given by:

$$\left|\vec{v}_{ref}\right| = \sqrt{{v_\alpha}^2 + {v_\beta}^2} \quad [26] \tag{3.30}$$

The phase angle is also express as $\theta = \tan^{-1}\left(\frac{v_\beta}{v_\alpha}\right)$. Where $\theta \in [0,2\pi]$

Calculate Modulation Index of Linear Modulation (under modulation): in the under modulation region, the rotating reference vector always remains within the hexagon. The largest output voltage magnitude is the radius of the largest circle that can be inscribed within the hexagon. This means that the linear region ends when the reference voltage is equal to the radius of the circle inscribed within the hexagon.

The ratio between the reference vector and the fundamental peak value of the square phase voltage wave $2\,V_{dc}/\pi$ is called the modulation index. The mode of operation is determined by the modulation index (MI). From a Fourier analysis, the fundamental voltage magnitude is given by [29];

$$V_{max\_six\ step} = \frac{4}{\pi}\left[\int_0^{\frac{\pi}{3}} \frac{v_{dc}}{3}\sin\theta d_\theta + \int_{\frac{\pi}{3}}^{\frac{\pi}{2}} \frac{2v_{dc}}{3}\sin\theta d_\theta\right]$$

$$V_{max\_six\ step} = \frac{4v_{dc}}{3\pi}\left[\left(-\cos\frac{\pi}{3}+1\right)+\left(-2\cos\frac{\pi}{2}+2\cos\frac{\pi}{3}\right)\right]$$

$$V_{max\_six\ step} = \frac{2v_{dc}}{\pi} \tag{3.31}$$

The ratio between the reference vector $\vec{v}_{ref}$ and the fundamental peak value of the square phase voltage wave ($2V_{dc}/\pi$) is called the modulation index. The mode of operation is determined by the modulation index (MI). In this linear region, the MI can be expressed as [29]

$$\text{MI} = \frac{\vec{v}_{ref}}{V_{\max\_six\ step}} \tag{3.32}$$

From the geometry of Figure 3.13 the maximum modulation index is 0.907 obtained when $\vec{v}_{ref}$ the radius of the inscribed circle equals [29].

This is given by:

$$\overrightarrow{v}_{ref}(max) = \frac{2}{3} Vdc \cos(\pi/6) \tag{3.33}$$

Sector Determination: in order to determine the switching time and sequence it is necessary to know in which sector the reference output $\overrightarrow{v}_{ref}$ lies. The phase voltages correspond to eight switching states, six non-zero vectors and two zero vectors at the origin. Depending on the reference voltage $\overrightarrow{v}_{\alpha}$ and $\vec{v}_{\beta}$ the angle of the reference vector can be used to determine the sector as shown in Table 3.4.

Table 3.4 Sector identification

Sector	Degrees
1	$0 < \theta \leq 60°$
2	$60° < \theta \leq 120°$
3	$120° < \theta \leq 180°$
4	$180° < \theta \leq 240°$
5	$240° < \theta \leq 300°$
6	$300° < \theta \leq 360$

Duty Cycle Calculation: the duty cycle computation is done for each triangular sector formed by two state vectors. The magnitude of each switching state vector is $2v_{dc}/\sqrt{3}$ and the magnitude of a vector to the midpoint of the hexagon line from one vertex to another is $v_{dc}/\sqrt{3}$. The reference space vector rotates and moves through different sectors of the complex plane as time increases. In each PWM cycle, the reference vector $\vec{v}_{ref}$ is sampled at a fixed input sampling frequency (f_s). During this time, the sector is determined and the modulation vector $\vec{v}_{ref}$ is mapped onto two adjacent vectors. The non-zero vectors are written as [26]:

$$\vec{v}_k = \frac{2}{3} v_{dc} e^{j(k-1)\frac{\pi}{3}} \tag{3.34}$$

Where k =1…5

Therefore the non-zero vector for $\vec{v}_k$ and $\vec{v}_{k+1}$ becomes [26]

$$\vec{v}_k = \frac{2}{3} v_{dc} \left[\cos(k-1)\frac{\pi}{3} + j\sin(k-1)\frac{\pi}{3}\right]$$
$$\vec{v}_{k+1} = \frac{2}{3} v_{dc} \left[\cos\left(k\frac{\pi}{3}\right) + j\sin\left(k\frac{\pi}{3}\right)\right] \quad (3.35)$$

Due to symmetry in the patterns in the six sectors, the integration can be carried out only on half pulse width modulation $T_S/2$. Zero voltages are applied during null state times [29].

$$\int_0^{\frac{T_S}{2}} \vec{v}_{ref}\, dt = \int_0^{\frac{T0}{4}} \overrightarrow{v_0}\, dt + \int_{\frac{T_0}{4}}^{\frac{T_0}{2}+Ta} \vec{v}_k\, dt + \int_{\frac{T_0}{4}+Ta}^{\frac{T_0}{2}+Ta+Tb} \vec{v}_{k+1}\, dt + \int_{\frac{T_0}{4}+Ta+Tb}^{\frac{T_S}{2}} \vec{v}_7\, dt$$
$$\int_{\frac{T_0}{4}+Ta+Tb}^{\frac{T_S}{2}} \overrightarrow{v_7}\, dt = 0, \int_0^{\frac{T0}{4}} \overrightarrow{v_0}\, dt = 0 \quad (3.36)$$

Then the Equation (3.36) becomes

$$\int_0^{\frac{T_S}{2}} \vec{v}_{ref}\, dt = \int_{\frac{T0}{4}}^{\frac{T_0}{2}+Ta} \vec{v}_k\, dt + \int_{\frac{T0}{4}+Ta}^{\frac{T_0}{2}+Ta+Tb} \vec{v}_{k+1}\, dt \quad (3.37)$$

Thus the product of the reference voltage vector $\vec{v}_{ref}$ and $T_S/2$ are the sum of the voltage multiplied by the time interval of the chosen space vector. The reference voltage vector $\vec{v}_{ref}$ can be represented as function of $\vec{v}_k$and $\vec{v}_{k+1}$ as follows [29].

$$\vec{v}_{ref}\, \frac{T_s}{2} = \vec{v}_k T_a + \vec{v}_{k+1} T_b$$
$$\vec{v}_{ref} = \vec{v}_\alpha + \mathrm{j}\vec{v}_\beta \quad (3.38)$$

Where T_a and T_b denote the required on time of the active state vectors $\vec{v}_k$ and $\vec{v}_{k+1}$ during each sample period, and k is the sector number denoting the reference location. The calculated times T_a and T_b are applied to the switches to produce space vector PWM switching patterns based on each sector.

The switching time is arranged according to the first half of the switching period while the half is a reflection forming asymmetrical pattern, if $\vec{v}_{ref}$ lies exactly in the middle between two vectors.

Assuming that the reference voltage and the voltage vector $\vec{v}_k$ and $\vec{v}_{k+1}$ are constant during each PWM period T_s and splitting the reference voltage $\vec{v}_{ref}$ into its real and imaginary components gives the following result [29].

$$\begin{bmatrix} v_\alpha \\ v\beta \end{bmatrix} \frac{Ts}{2} = \frac{2v_{dc}}{3} \left(\begin{bmatrix} \cos\frac{(k-1)\pi}{3} & \cos\frac{(k\pi)}{3} \\ \sin\frac{(k-1)\pi}{3} & \sin\frac{(k\pi)}{3} \end{bmatrix} \begin{bmatrix} T_a \\ T_b \end{bmatrix} \right) \tag{3.39}$$

From this equation T_a and T_b can be calculated as follows.

$$\begin{bmatrix} T_a \\ T_b \end{bmatrix} = \frac{\sqrt{3}Ts}{2v_{dc}} \begin{bmatrix} \sin\frac{(k\pi)}{3} & -\cos\frac{(k\pi)}{3} \\ -\sin\frac{(k-1)\pi}{3} & \cos\frac{(k-1)\pi}{3} \end{bmatrix} \begin{bmatrix} v_\alpha \\ v\beta \end{bmatrix} \tag{3.40}$$

Since the sum of $2T_a$ and $2T_b$ should be less than or equal to T_s, the inverter has to stay in a zero state for the rest of the period. The duration of the null vectors is the remaining time in the switching period. Hence, $T_s = T_0 + 2(T_a + T_b)$, then the time interval for the zero voltage vectors is;

$$T_0 = T_s - 2(T_a + T_b) \tag{3.41}$$

The switching times are arranged symmetrically around the center of the switching period .The zero vector v_1(1,1,1) is placed at the center of the switching period, and the zero vector v_0 (0,0,0) at the start and the end, and the total period for a zero vector is divided equally among the two zero vectors. In the under modulation region, the reference voltage vector grows outward in magnitude as the modulation index increases. It reaches the inscribed circle of the hexagon and T_0 will reduce to zero whenever the tip of the reference voltage vector is on the hexagon. If the modulation index increases further T_0 becomes negative and meaningless. reference

The calculated values of the time durations of two adjacent non-zero vectors (T_a and T_b) in terms of T_s/v_{dc} for all six sectors are listed in Table 3.5. Those time Intervals T_a and T_b for each sector are based on the magnitude and phase of the reference voltage. As shown in Figure 3.16, a zero state vector is applied followed with two adjacent active vectors in half of the switching period.

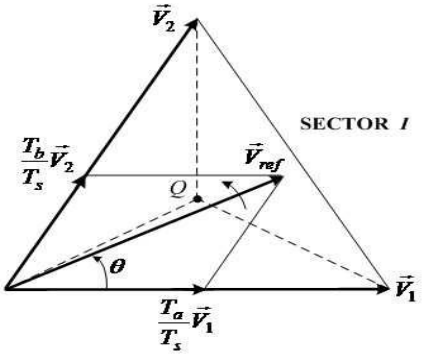

Figure 3:16 Sector identification [30]

The next half of the switching period is symmetrical to the first half. To generate the signals that produce the rotating vector, an equation is required to determine the time intervals for each sector. Table 3.5 shows that the pulse patterns generated by space vector PWM in the given sector [30].

Table 3.5 Duty cycle calculation

Sector	θ	T_a	T_b
1	$0 < \theta \leq 60^0$	$\frac{3v_\alpha}{4} - \sqrt{3}\frac{v_\beta}{4}$	$\sqrt{3}\frac{v_\beta}{2}$
2	$60 < \theta \leq 120^0$	$\frac{3v_\alpha}{4} + \sqrt{3}\frac{v_\beta}{4}$	$\frac{-3v_\alpha}{4} + \sqrt{3}\frac{v_\beta}{4}$
3	$120 < \theta \leq 180^0$	$\sqrt{3}\frac{v_\beta}{2}$	$\frac{-3v_\alpha}{4} - \sqrt{3}\frac{v_\beta}{4}$
4	$180 < \theta \leq 240^0$	$\frac{-3v_\alpha}{4} + \sqrt{3}\frac{v_\beta}{4}$	$-\sqrt{3}\frac{v_\beta}{2}$
5	$240 < \theta \leq 300^0$	$\frac{-3v_\alpha}{4} - \sqrt{3}\frac{v_\beta}{4}$	$\frac{3v_\alpha}{4} - \sqrt{3}\frac{v_\beta}{4}$
6	$300 < \theta \leq 360^0$	$-\sqrt{3}\frac{v_\beta}{2}$	$\frac{3v_\alpha}{4} + \sqrt{3}\frac{v_\beta}{4}$

As shown in Figures 3.16 and 3.17 $\vec{v}_{ref}$ is in sector 1, then $\vec{v}_1$ vector is applied to the inverter during T_a interval, and consequently the vector $\vec{v}_2$ is applied during T_b interval.

The PWM period is shared between $\vec{v}_1$ and $\vec{v}_2$ for durations T_a and T_b, respectively, and the zero vectors $\vec{v}_0$ and $\vec{v}_7$ for duration T_0.

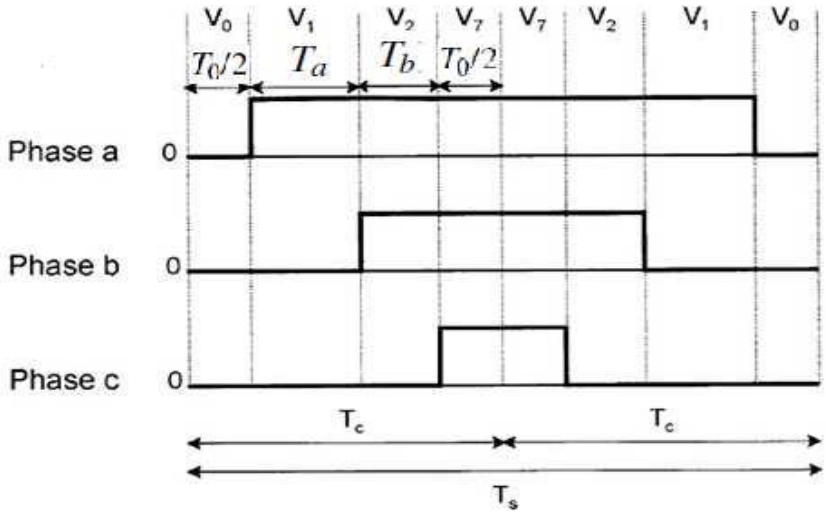

Figure 3:17 Symmetrical pulse pattern wave form for three-phase [20]

The switching sequence is given by $\vec{v}_0$ -$\vec{v}_1$ -$\vec{v}_2$ -$\vec{v}_7$ -$\vec{v}_7$ -$\vec{v}_2$-$\vec{v}_1$-$\vec{v}_0$ during two half-sampling periods. The generated space vector PWM waveforms are symmetrical with respect to the middle of each PWM period. The progress of switching states from the left to the right of that figure proceeds with the following steps [26], [29].

1) When the circuit configuration is in the $\vec{v}_0$ state (time interval is $T_0/2$), all top switches (S_1, S_2, and S_3) opened.
2) When it is in the $\vec{v}_1$ state (with a time interval T_a), switch S_1 is closed.
3) When it is in the $\vec{v}_2$ state (with a time interval T_b), switch S_2 is closed (S_1 is still closed).
4) When it is in the $\vec{v}_7$ state (with a time interval $T_0/2$), switch S_3 is closed. (S_1, and S_2, are still closed).

After the first half of the switching period is done, the switching combination is re-versed. All switches are closed for $T_0/2$ seconds before the circuit configuration is back to $\vec{v}_2$, then $\vec{v}_1$, and $\vec{v}_0$ with corresponding time intervals of T_b, T_a, and $T_0/2$. Following a similar process, the switching cycles are determined for the five remaining vectors.

Determination of the Switching Times for Each Sector: it is necessary to arrange the switching sequence so that the switching frequency of each inverter leg is minimized. To minimize the switching losses, only two adjacent active vectors and two zero vectors are used in a sector. To meet this optimal condition, each switching period starts with one zero vectors and ends with another zero vector during the sampling time.

This rule applies normally to three phase inverters as a switching sequence. Therefore, the switching cycle of the output voltage is double the sampling time and the two output voltage waveforms become symmetrical. Table 3.6 shows a symmetric switching sequence. Referring to this table, the binary representations of two adjacent basic vectors differ in only one bit, so that only one of the upper transistors switches is closed when the switching pattern moves from one vector to an adjacent one [15], [30], [29]. The two vectors are time weighted in a sample period T_s to produce the desired output voltage.

Table 3.6 Seven segment switching sequence

Space vector	Switching state	On state switch	Off state switch	Vector definition
$\vec{v}_0$	000	S_4, S_6, S_2	S_1, S_3, S_5	$\vec{v}_0 = 0$
$\vec{v}_1$	100	S_1, S_6, S_2	S_4, S_3, S_5	$\vec{v}_1 = \frac{2}{3}V_{dc}$
$\vec{v}_2$	110	S_1, S_3, S_2	S_4, S_6, S_5	$\vec{v}_2 = \frac{2}{3}V_{dc}e^{j\frac{\pi}{3}}$
$\vec{v}_3$	010	S_4, S_3, S_2	S_1, S_6, S_5	$\vec{v}_3 = \frac{2}{3}V_{dc}e^{j2\frac{\pi}{3}}$
$\vec{v}_4$	011	S_4, S_3, S_5	S_1, S_6, S_2	$\vec{v}_4 = \frac{2}{3}V_{dc}e^{j\frac{3\pi}{3}}$
$\vec{v}_5$	001	S_4, S_6, S_5	S_1, S_3, S_2	$\vec{v}_5 = \frac{2}{3}V_{dc}e^{j\frac{4\pi}{3}}$
$\vec{v}_6$	101	S_1, S_6, S_5	S_4, S_3, S_2	$\vec{v}_6 = \frac{2}{3}V_{dc}e^{j\frac{5\pi}{3}}$
$\vec{v}_7$	111	S_1, S_3, S_5	S_4, S_6, S_2	$\vec{v}_7 = 0$

4. Chapter Four

Controller Design of PMSM Drive System

4.1 Introduction to Controller Design for PMSM Drive System

PID controller is very popular in the control of motor drive systems. However, the controller parameters are fixed during operation after being chosen through a certain optimal method, the conventional PID controller can't always keep satisfying performances. To handle this problem, the parameters of the controller need to be adjusted dynamically according to the running status of the system. So, in this chapter the development of self-tuning PID controller will be investigated. Fuzzy rules and reasoning are utilized on-line to determine the PID controller parameters based on error and rate of change in error. The rule bases are constructed by examining a typical step response and by observing the effects of the variations of the PID controller parameter gains on the output of the system.

4.1.1 PID Controller

PID controller has been widely used in motor drive systems. More than 90% of industrial controllers are implemented based on PID algorithms. The structure of PID controller is very simple and its control principle is very clear. It is practical and is very easy to be implemented. In addition, because the functionalities of the three factors in PID controller are very clear, they can be tuned efficiently to obtain desired transient and steady-state responses [31].

The proportional part is responsible for following the desired set-point, while the integral and derivative part account for the accumulation of past errors and the rate of change of error in the process respectively.

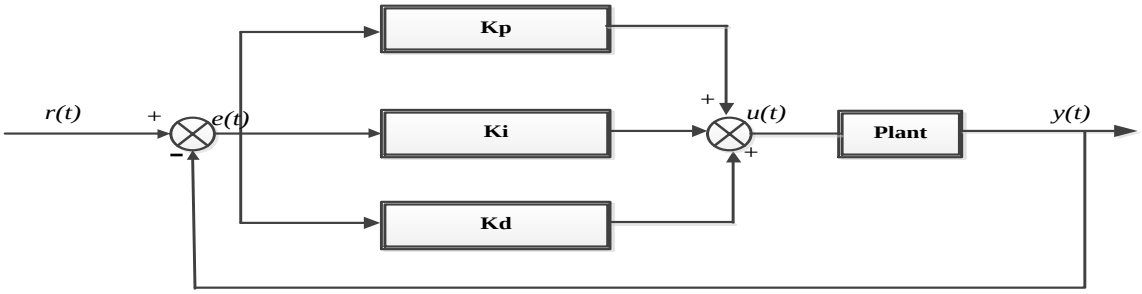

Figure 4:1 Block diagram of the PID controller

The algorithm of PID controller can be given as follows [31]:

$$e(t) = r(t) - y(t) \tag{4.1}$$

$$u(t) = K_p\, e(t) + K_i \int e(t)\, dt + K_i \frac{de(t)}{dt} \tag{4.2}$$

$$u(t) = K_p \{ e(t) + \frac{1}{T_i} \int e(t)\, dt + T_d \frac{de(t)}{dt} \} \tag{4.3}$$

where y(t) is the output of the system, r(t) is the reference input of the system, e(t) is the error signal between y(t) and r(t), u(t) is the output of the PID controller.

The Laplace transformation of Equation (4.3) is given by:

$$U(s) = K_p \left(1 + \frac{1}{T_i s} + T_d s \right) \tag{4.4}$$

Where K_p is proportional gain, K_i is integral gain, K_d is derivative gain T_i is integral time constant and T_d is derivative time constant and, $K_i = K_p / T_i$, $K_d = K_p T_d$.

The relation between PID parameters and the system response specifications is summarized as

follows.

(1) **Proportional term**, if K_p increases the response speed and control accuracy of the system is going to be better. But if K_p is too large, the overshoot will be large and the system will tend to be unstable. Meanwhile, if K_p is too small, the control accuracy will be decreased and the regulating time will be prolonged. The static and dynamic performance will be deteriorated.

(2) **Integration term** is used to eliminate the steady-state error of the system. With bigger K_i, the steady-state error can be eliminated faster. But if K_i is too large, there will be integral saturation at the beginning of the control process and the overshoot will be large. On the other hand, if K_i is too small, the steady-state error will be very difficult to be eliminated and the control accuracy will be bad.

(3) **Differentiation term** can improve the dynamic performance of the system. It can inhibit and predict the change of the error in any direction. But again if K_d is too large, the response process will brake early and the regulating time will be prolonged causing the anti-interference capability of the system to be bad.

4.1.2 Fuzzy Logic Controller

FLC is a control algorithm based on a linguistic control strategy, which is derived from the expert knowledge into an automatic control strategy. The operation of a FLC is based on qualitative knowledge about the system being controlled. The reason why FLC is chosen in this paper is due to [32] [33]:

- Possibility to design without knowing the exact mathematical model of the process
- Simplicity of control and Smooth operation
- High degree of tolerance
- Low cost
- Reduce the effect of Non-linearity
- Inherent approximation capability

4.2.1.1 Basic Terminology in Fuzzy Logic

Degree of membership (μ): is the degree to which a crisp variable belongs to a fuzzy set. It is expressed either as a fractional value ranging from 0 to 1 or percentage ranging from 0 to 100.

Membership Function (MF): is expressed graphically and tends to illustrate how completely a crisp variable belongs to a fuzzy set. To determine the MFs one can use either knowledge of human experts or data collected from various sensors.

In order to define fuzzy MF, designers choose many different shapes based on their preference and experience. There are generally four types of MFs used [33]:

A. Trapezoidal MF
B. Triangular MF
C. Gaussian MF
D. Generalized bell MF

Among those shapes, triangular and trapezoidal shapes are mostly used in FLC designs since they are easy to represent designer's idea and require low computation time. Because of this reason they are also used in this paper.

Crisp variable: is a physical variable that can be measured through instruments and can be assigned a crisp value.

Linguistic variable: if a variable can take words in natural languages as its values, it is called a linguistic variable, where the words are characterized by fuzzy sets defined in universe of discourse in which the variable is defined. Roughly speaking, if a variable can take words in natural languages as its values, it is called a linguistic variable.

General components of FLC

In the designing of FLC have four main components as shown in Figure 4.4 [33].

- ✓ Fuzziffication
- ✓ Inference engine
- ✓ Rule base
- ✓ Defuzzification

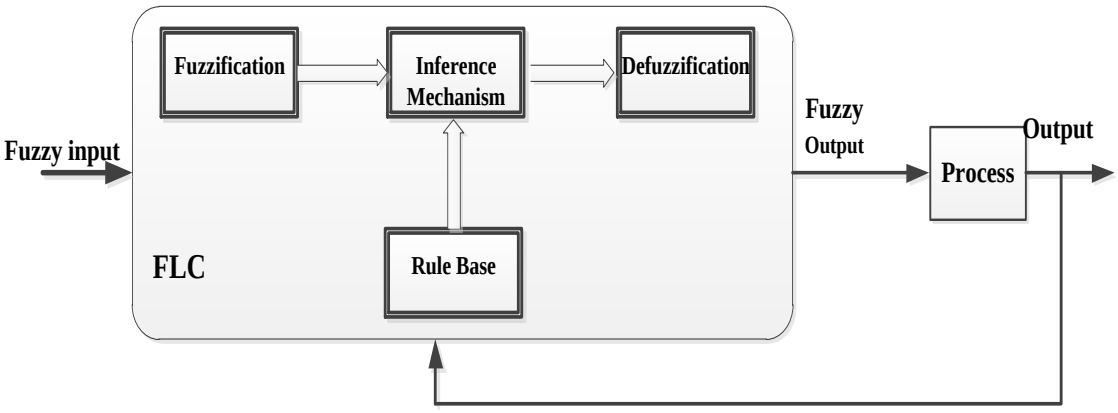

Figure 4:2 General structure of FLC

1. Fuzzification

The first step in designing a fuzzy controller is to decide which state variables represent the system dynamic performance must be taken as the input signal to the controller. Fuzzy logic uses linguistic variables instead of numerical variables. The process of converting a numerical variable (real number or crisp variables) into a linguistic variable (fuzzy number) is called fuzzification. This is achieved with the different types of fuzzifiers. There are generally three types of fuzzifiers, which are used for the fuzzification process [32], [33] [34].

I. Singleton fuzzifier
II. Gaussian fuzzifier
III. Trapezoidal or triangular fuzzifier

2. Rule base

A decision making logic which is, simulating a human decision process, inters fuzzy control action from the knowledge of the control rules and linguistic variable definitions. The rules are in "IF (antecedent)-THEN (consequent)" format and formally the "IF" side is called the antecedent or conditions and the "THEN" side is called the consequent or conclusion. The computer is able to execute the rules and compute a control signal depending on the measured inputs error (e) and change in error (de). In a rule based controller the control strategy is stored in a more or less natural language. A rule base controller is easy to understand and easy to maintain for a non- specialist end user and an

equivalent controller could be implemented using conventional techniques [31], [32]and [33].

3. Inference Mechanism/Inference engine or Fuzzy inference

Inference mechanism is defined as the code which processes the rules, cases, other type of knowledge and expertise based on the facts of a given situation. The inference mechanism evaluates which control rules are relevant at the current time and then decides what the input to the plant should be.

In general there are three main types of fuzzy inference systems such as: Mamdani model, Sugeno model and Tsukamoto model. Out of these three, Mamdani model is the most popular one and is used in this paper. There are two types of Mamdani fuzzy inference system such as, "max and min" and "max and product". The "max and min" Mamdani system is used because it is mostly preferable in Mamdani fuzzy inference system.

Reference

Max- min inference

Max-min is the most common rule of composition. In max-min rule of composition the inferred output of each rule is a fuzzy set chosen from the minimum firing strength. A fuzzy system with two non-interactive inputs x1 and x2 (antecedents) and a single output y (consequent) are described by a collection of n linguistic IF-THEN rules [34];

$$\text{IF } x1 \text{ is } A_1^{(k)} \text{ and } x_2 \text{ is } A_2^{(k)} \text{ THEN } y(k) \text{ is } B^{(k)}, \quad k = 1,2,...n \tag{4.14}$$

Where $A_1^{(k)}$ and $A_2^{(k)}$ are fuzzy sets representing the k^{th} antecedent pairs and $B^{(k)}$ are the fuzzy sets representing the k^{th} consequent.

Based on the Mamdani's max-min composition method of inference, and for a set of n disjunctive rules, the aggregated output for the n rules will be given by:

$$\mu_B{}^{(k)}(y) = \text{Max Min}\left[\mu_{A1}{}^{(k)}(\text{input(i)}), \mu_{A2}{}^{(k)}(\text{input(j)})\right] \tag{4.15}$$

Where i, j are input fuzzy set variables and y is output fuzzy set variable.

The Equation in (4.14) has a simple graphical interpretation, as seen in Figure 4.3.

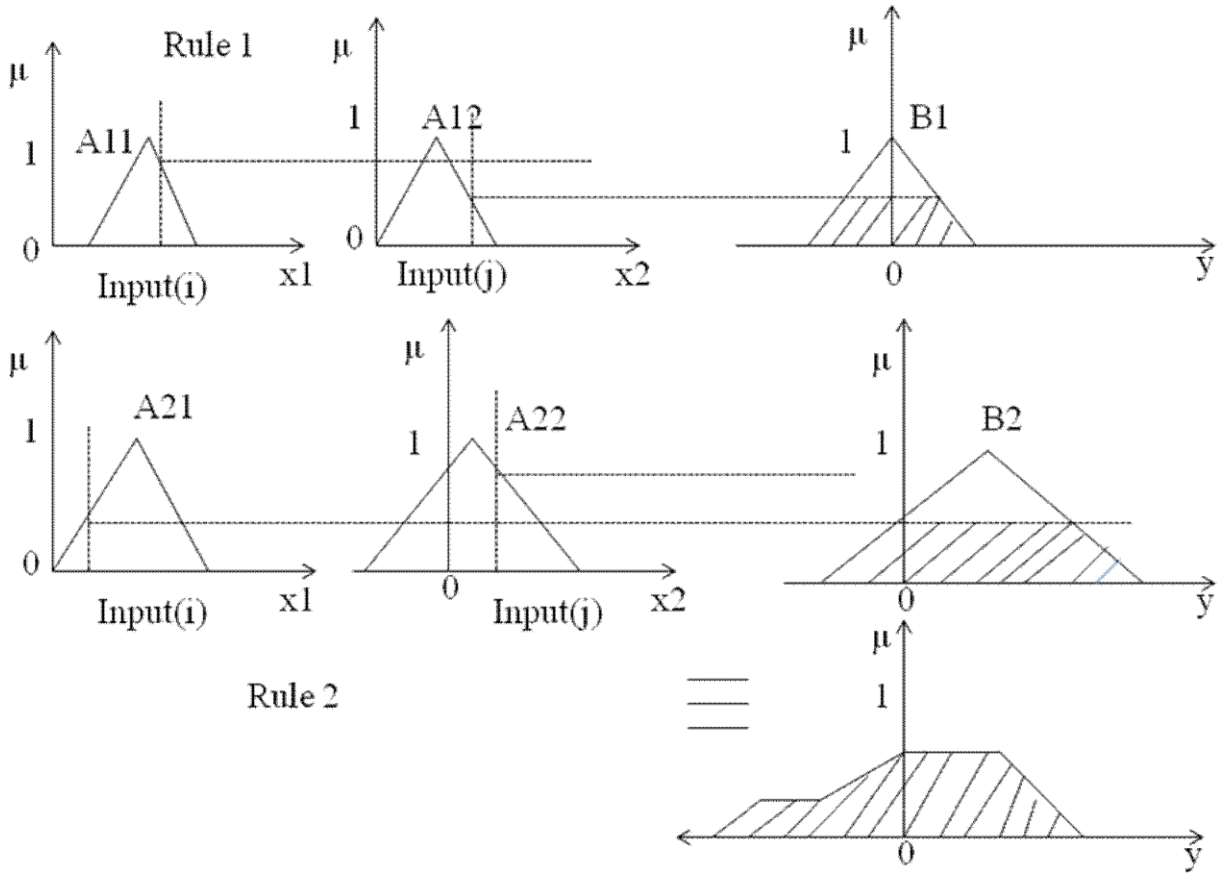

Figure 4:3 Fuzzy inferencing using Mamdani's max-min compositional operator

The fuzzy IF-THEN rule in Figure 4.3 contains two rules. Both rules "IF x_1 is A_{11} and x_2 is A_{12} THEN y is B1" and "IF x_1 is A_{21} and x_2 is A_{22} THEN y is B_2" are intersection fuzzy set operation and take the minimum membership values of the two inputs. Then the outputs of the two rules aggregated using the union fuzzy set operation that takes the maximum membership values of each fuzzy rule outputs.

For this specific example Equation (4.15) can be simplified as $\mu_B(y)$ = Max [Min (μ_{A11}(input(i)), μ_{A12}(input(j)), Min (μ_{A21}(input(i)),μ_{A22} (input (j))].

4. Defuzzification

The reverse of Fuzzification is called Defuzzification. The use of FLC produces required output in a linguistic variable (fuzzy number). According to real world requirements, the linguistic

variables have to be transformed to crisp output. There are many defuzzification methods but the most common methods are as follows [31], [33]:

(a) Center of gravity (COG)

(b) Bisector of area (BOA)

(c) Mean of maximum (MOM)

In this thesis a Center of gravity difuzzification method is adopted, because it is fast and simple operations are used in it, it gives continual change of defuzzification value, hence it is convenient to be used in fuzzy controllers. In center of gravity method the crisp control value is the abscissa of the center of gravity of the fuzzy set is calculated as follows:

$$x^* = \frac{\sum_i \mu_x(x_i).x_i}{\sum_i \mu_x(x_i)} \text{ Or } x^* = \frac{\int \mu_x(x_i).x_i}{\int \mu_x(x_i)} \quad (4.16)$$

Where x_i is a point in the universe of the conclusion (i =1, 2, 3…) and $\mu_x(x_i)$ is the membership value of the resulting conclusion and is shown in Figure 4.4.

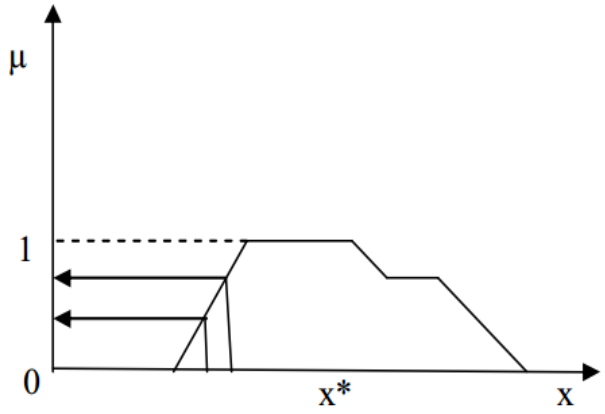

Figure 4:4 Center of gravity defuzzification method

5. Chapter Five

System Design, Results and Discussions

5.1 Fuzzy PID Controller Design for SPMSM

Tuning of a PID controller refers to the tuning of its various parameters (P, I and D) to achieve an optimized value of the desired response. The basic requirement of the output has to be good enough in terms of accuracy and robustness. A different type of PID controller tuning mechanisms has been developed for several years as it's discussed in Section 1.6. However in this thesis FLC method is used for tuning the PID controller parameters. Two major design procedures are employed in order to achieve objectives of the study based on the system transfer functions. Those are the current (inner loop) and speed (outer loop) controller design.

Current PI controller design

In this design part the objective is to determine the PI's gains Kp and Ki (or Ti) so as to achieve a good closed loop response. In order to design the PI current controller for both q and d axis we will follow the same procedure to obtain PI controller parameter gains Kp and Ti, since Lq=Ld in surface PMSM. Therefore, the plant open loop transfer function for both axes is obtained from Section 3.6 voltage equation expression by only taking the linear part as follows.

$$G_{idq}(s) = \frac{i_{qs}}{v_{lqs}} = \frac{i_{ds}}{v_{lds}} = \frac{\frac{1}{L_s}}{s + \frac{Rs}{L_s}} \quad (5.1)$$

Wrong equation check ref 26 page 54,53 and refer your own page 30

For the design of PI-controllers it is necessary to know the closed loop transfer function using Equation (5.1) shown in Figure 5.1.

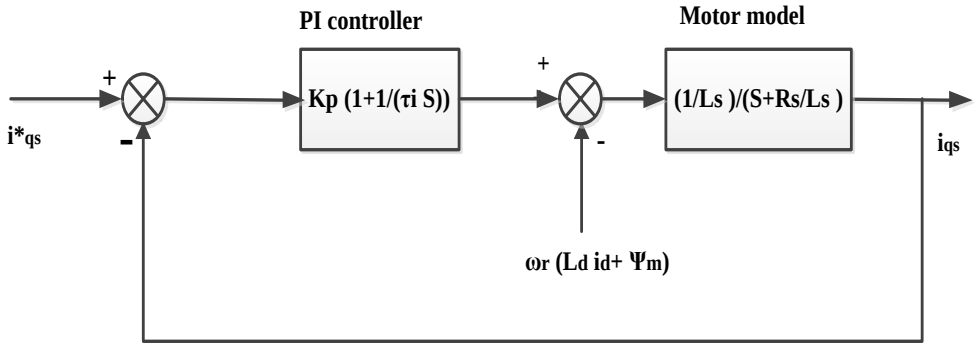

Figure 5:1 Simplified block diagram for i_qs's loop for PI current controller design

And, the transfer function of the PI d-q current controller is written as:

$$C(s) = K_p\left(1 + \frac{1}{\tau_i S}\right) \tag{5.2}$$

Using Equation (5.1) and (5.2) we will obtain the overall the system transfer function equations as:

$$G_{sys}(s) = \frac{i_{qs}}{i_{qs}^*} = \frac{K_p(\tau_i S + 1)}{\tau_i L_s S^2 + \tau_i (R_s + K_p) S + K_p} \tag{5.3}$$

By comparing this closed loop transfer function with 2nd order closed loop system performance transfer function given by in Equation (5.4).

$$T_s(s) = \frac{\omega_n^2}{S^2 + 2\xi\omega_n S + \omega_n^2} \tag{5.4}$$

Then PI controller gains, the proportional gain $K_p$and the integral time constant τ_i are determined using pole-assignment method [35]. Based on this design approach the proportional control gain and the integral time constant are determined by.

$$K_p = 2\xi\omega_n L_s - R_s \tag{5.5}$$

$$\tau_i = \frac{2\xi\omega_n L_s - R_s}{\omega^2{}_n L_s} \tag{5.6}$$

And,

$$K_i = \frac{K_p}{\tau_i}$$

Where $K_p$is proportional control gain, τ_i is integral time constant and K_i is integral control gain

In order to design the PI current controller in d axis it is followed the same procedure as q axis. Using the d-axis stator voltage equation the block diagram of SPMSM in d-axis is shown in Figure 5.2.

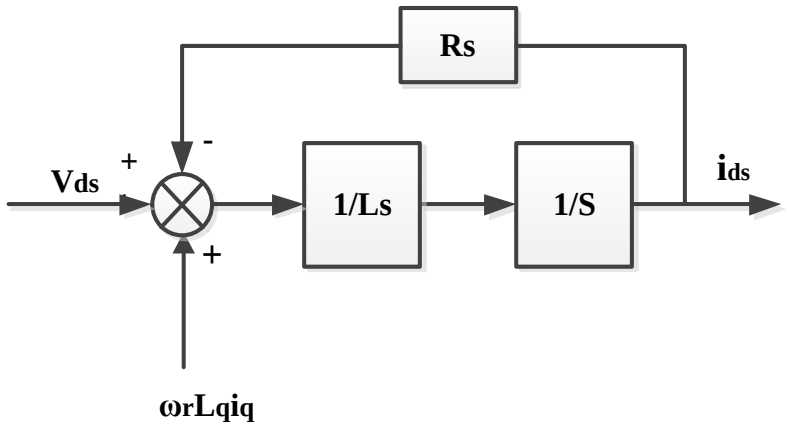

Figure 5:2 Block diagram of SPMSM in d-axis PI current controller

The transfer function between flux component, i_{ds} and input voltage, V_{ds} in d-axis stator current is given by Equation (5.1).

The design specifications of the proposed system is to have faster response speed with max overshoot to be less than 5% and rise time of 0.005 second. So to achieve this specification damping coefficient is chosen ξ =0.707 and natural frequency of the closed loop system ω_n is to be larger value to have faster speed response. Since, the open loop pole for the q axis current dynamic system is at -$\frac{Rs}{L_s}$, we can select the parameter ω_n in relative value of the magnitude of the open loop pole. So the natural frequency is determined by [35];

$$\omega_n = \frac{1}{1-\gamma}\frac{R_s}{L_s} \tag{5.7}$$

Finally the PI controller parameter gains are obtained as follows by substituting Equation (5.7) into (5.5) and (5.6).

$$K_p = \frac{0.414+\gamma}{1-\gamma}\frac{R_s}{} \tag{5.8}$$

$$\tau_i = (0.414+\gamma)(1-\gamma)\frac{L_s}{R_s} \tag{5.9}$$

Since ξ =0.707

Where γ is chosen between1 and 0.

In majority of application it is selected in the range between 0.8 and 0.95. In this thesis to have fast speed response and shorter settling time this parameter is chosen 0.8 and the natural frequency of current loop is ω_{ni}= 2128.57rad/sec. Hence, the inner loop (current) has to be very fast than the outer loop (speed) by five to ten times to have good performance. So the outer loop (speed) controller natural frequency is selected $\omega_{ns} = \frac{\omega_{ni}}{5}$ =425.74≈400rad/sec and the calculated value of each parameter gains are tuned using PID tuner.

5.1.1 Self-tuning Fuzzy PID Speed Controller Design for SPMSM

The plant transfer function for both electrical and mechanical system are first order therefore we will follow the same procedure as current controller design. Firstly, the speed controller is designed with PI speed controller then the PID controller gains are obtained by using PID tuner method with MATLAB simply.

A fuzzy PID controller takes the conventional PID controller parameter values as the basis which uses the fuzzy reasoning and variable universe of discourse to regulate the PID parameters. The characteristics of a fuzzy system such as robustness and adaptability can be successfully incorporated into the controlling method for better tuning of PID parameters.

5.1.1.2 Self-tuning Principle of Fuzzy PID Controller

The term self-tuning refers to the characteristics of the controller to tune its controlling parameters on-line automatically so as to have the most suitable values of those parameters which result in optimization of the process output. Fuzzy self-tuning PID controller works on the control rules designed on the basis of theoretical and experience analysis. Therefore, it can tune the parameters Kp, Ki, and Kd by adjusting the other controlling parameters and factors on-line. This, in result makes the precision of overall control higher and hence gives a better performance than the conventional PID controller.

5.1.2 Design and Structure of the Self-tuning Fuzzy PID Controller

In this thesis the Self-tuning fuzzy PID controller has two inputs and three output linguistic variables (K_p, K_i, and K_d) as shown in Figure 5.3. The two input variables are error "e" and rate of change-in-error "ec" take as the input to the controller makes use of the fuzzy control rules to modify PID parameters on-line. The self-tuning of the PID controller refers to finding the fuzzy relationship between the three parameters of PID, K_p, K_i, and K_d and "e(t)" and " $de(t)/dt$ ".

According to the principle of fuzzy control modifying the three parameters in order to meet different requirements for control parameters when "e(t)" and "$de(t)/dt$ " are different and making the control object produce a good dynamic and static performance. The error and rate of change of error of the speed are defined as:

Error, $e(t) = R(t) - C(t)$ Rate of change of error, rate of change in error$= de(t)/dt$, where $R(t)$ is reference speed $C(t)$ is output speed

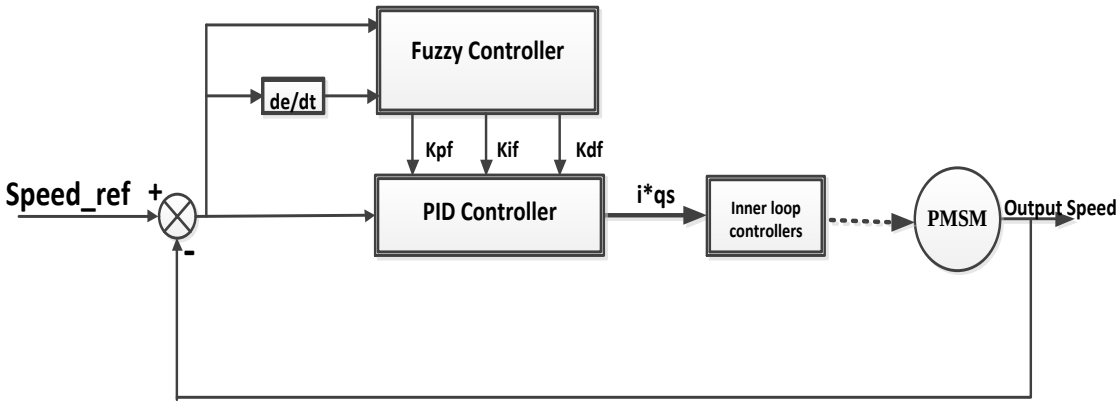

Figure 5:3 Structure of self-tuning fuzzy PID controller

The designing of self-tuning FPID speed controller have the following procedures:

1. Determining the controller inputs and outputs as the fuzzy variables.
2. Break up inputs and outputs into several fuzzy sets and label them according to the problem to be solved.
3. Assign or determine a membership function (MF) for each fuzzy set.
4. Fuzzify the inputs
5. Develop the fuzzy IF-THEN rules to solve the problem.
6. Choose Inference Mechanism engine procedure.
7. Aggregate the fuzzy outputs of each rule.
8. Choose a defuzzification method.

These designing procedures can be summarized as in three basic steps.

Fuzzification stage

The purpose of fuzzification is to map the inputs to values from 0 to 1 using a set of input membership functions under a given universe of discourse. In this stage the input linguistic variables are assigned degrees of membership in various classes.

In this thesis for each input variable seven linguistic values are selected in a triangular membership functions (MF) type. NL, NM, NS, Z, PS, PM, PL are the set of linguistic values which respectively represents "Negative Large", "Negative Medium", "Negative Small", "Zero", "Positive Small", "Positive Medium" and "Positive Large". And the output linguistic values are PVS (Positive Very Small), PMS (Positive Medium Small), PS (Positive Small), PM (Negative Medium), PL (Positive Large), PML (Positive Medium Large) and PVL (Positive Very Large). The membership functions for input (Error) and output (Kpf) linguistic variables are show in Figure 5.4 and 5.5.

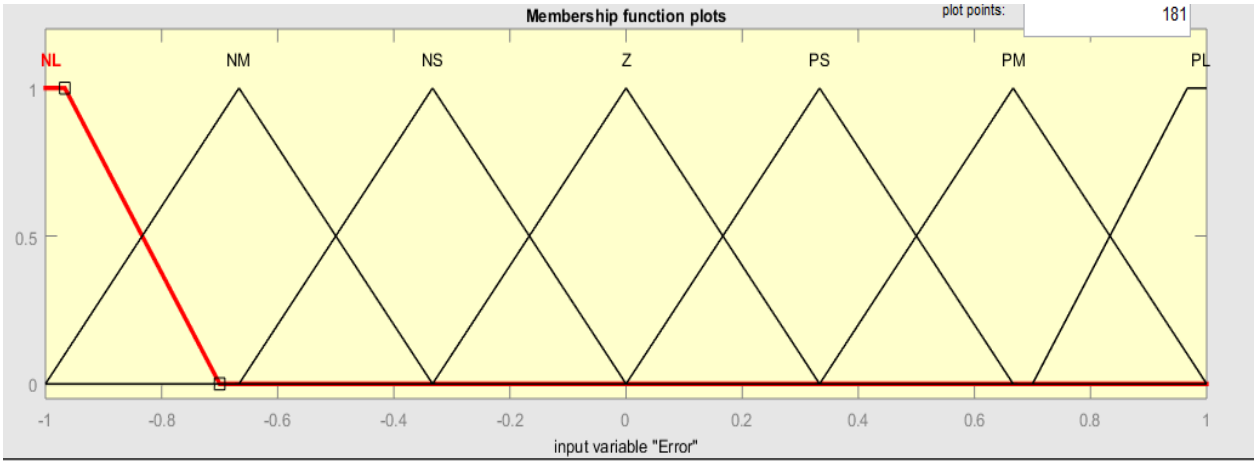

Figure 5:4 Membership function for input variable "Error"

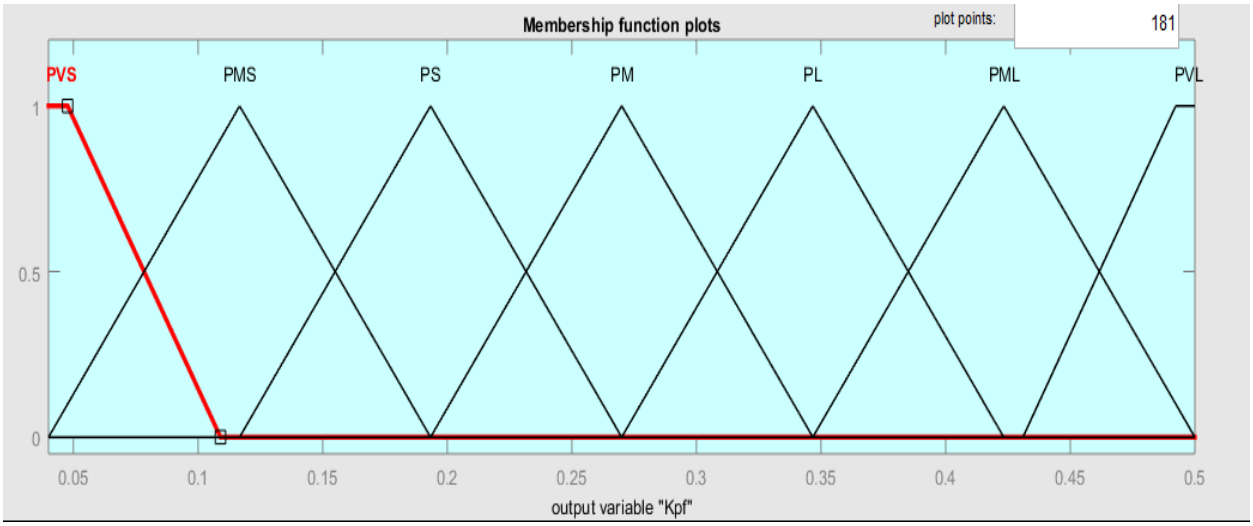

Figure 5:5 Membership function fuzzy output for proportional gain "Kpf"

Rule base (decision making) definition

Once the input and output variables and MF are defined, we have to design the rule-base composed of expert IF <antecedents> THEN < consequent > rules. These rules transform the input variables to an output that will tell us how the speed of the motor is going to be as the desired speed by manipulating the PID parameters. Depending on the number of MF for input and output variables, we have got 49 rules. The fuzzy inference system block of the system is shown in Figure 5.6.

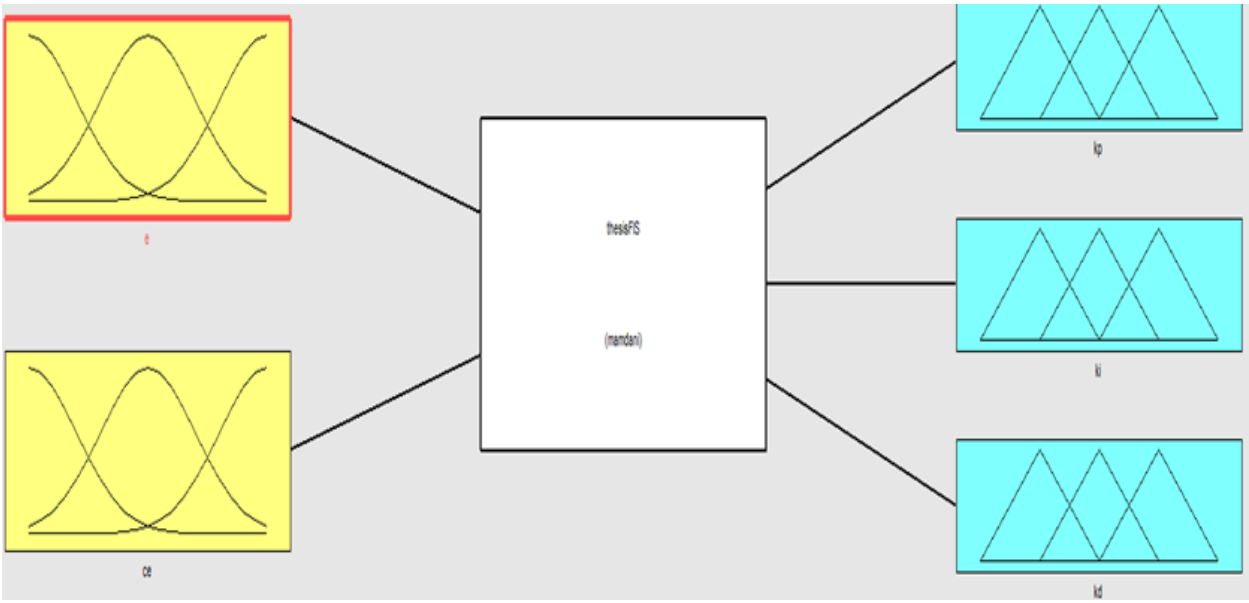

Figure 5:6 Fuzzy Inference System of the proposed system

Here in this thesis we derive the rules based on the typical step response of the process shown in Figure 5.7. At the beginning, around a1, a big control signal is needed in order to achieve a fast rise time. To produce a big control signal, we need a large proportional gain Kp, a small derivative gain Kd, and a large integral gain Ki. Consequently, the rule around a1 is:

IF e(t) is PB (Positive Big) and ce(t) is Z, THEN K_{pf} is Big, K_{if} is Big, K_{df} is Small.

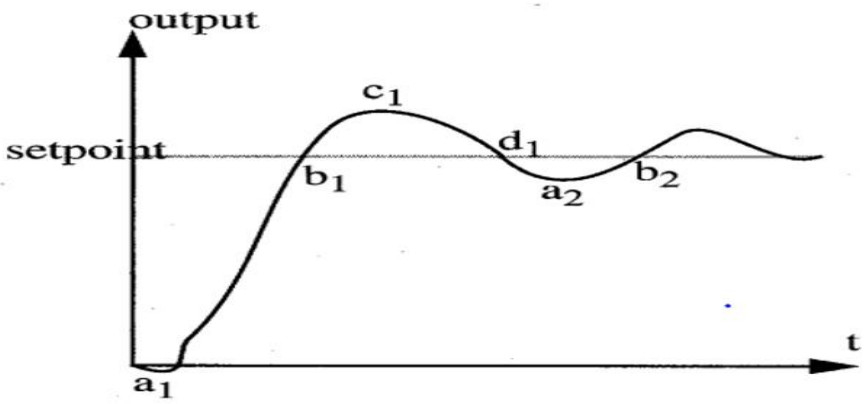

Figure 5:7 Typical step response of the system [34]

Around point b1 in Figure 5.7, the control single has to be small to avoid a large overshoot. So we need a small proportional gain, a small integral gain and a large derivative gain. Thus, the following rule is taken:

IF $e(t)$ is ~~ZO~~ and $ce(t)$ is NB (Negative Big), THEN K_{pf} is Small, K_{if} is Small, K_{df} is Big.

The control signal actions around points around c1 and d1 are similar to those around points a1 and b1 respectively.

Based on this concept three set of rules for K_{pf}, K_{if} and K_{df} has been determined and each set consists of 49 rules. These three set of rules are shown in Table 5.1- 5.3 respectively.

Table 5.1 Fuzzy rule for Kpf

No ZO ,please check others again

e \ ec	NL	NM	NS	~~ZO~~	PS	PM	PL
NL	PVL	PVL	PVL	PVL	PVL	PVL	PVL
NM	PML	PML	PML	PVL	PVL	PVL	PVL
NS	PVS	PVS	PS	PS	PM	PM	PMS
~~ZO~~	PVS	PVS	PVS	PS	PMS	PMS	PMS
PS	PML	PML	PML	PML	PL	PL	PL
PM	PL	PL	PL	PML	PML	PML	PML
PL	PVL	PVL	PL	PL	PL	PML	PML

Table 5.2 Fuzzy rule for Kif

e \ ec	NL	NM	NS	ZO	PS	PM	PL
NL	PM	PM	PM	PMS	PMS	PM	PMS
NM	PMS	PMS	PMS	PM	PM	PMS	PMS
NS	PS	PS	PVS	PVS	PS	PS	PS
ZO	PVS	PS	PS	PVS	PS	PS	PMS
PS	PMS	PMS	PMS	PMS	PMS	PMS	PMS
PM	PMS	PMS	PMS	PMS	PS	PS	PS
PL	PM	PM	PMS	PMS	PMS	PML	PML

Table 5.3 Fuzzy rule for Kdf

e \ ec	NL	NM	NS	ZO	PS	PM	PL
NL	PVS	PMS	PM	PMS	PML	PL	PVL
NM	PMS	PML	PML	PML	PL	PVL	PVL
NS	PM	PL	PL	PL	PVL	PVL	PVL
ZO	PML	PVL	PML	PML	PVL	PVL	PVL
PS	PML	PVL	PL	PVL	PVL	PVL	PVL
PM	PVL	PVL	PL	PL	PML	PML	PML
PL	PVL	PVL	PML	PML	PM	PVL	PVL

Defuzzification stage

In this stage all fuzzy actions combine together to a single fuzzy action and transform the single fuzzy action into a crisp, executable system output using centroid of weighted sets. The rule surface viewer of the system is also shown in Figure 5.8

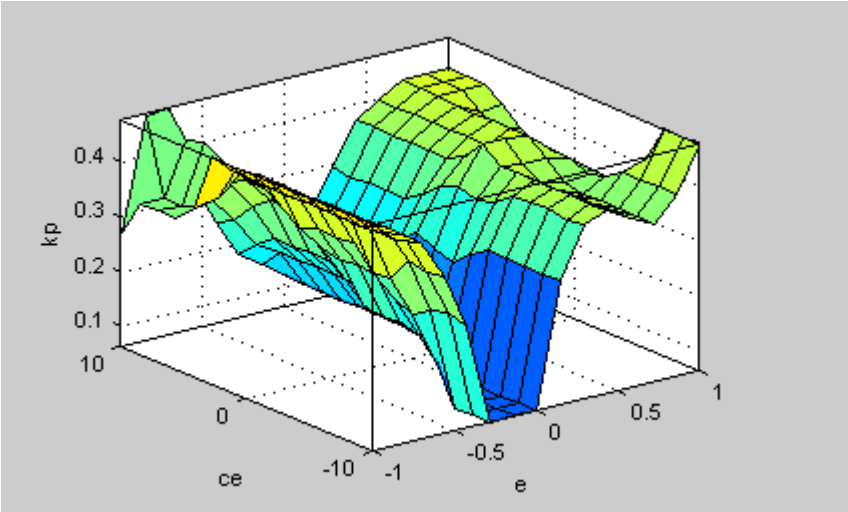

(a) Kp surface viewer

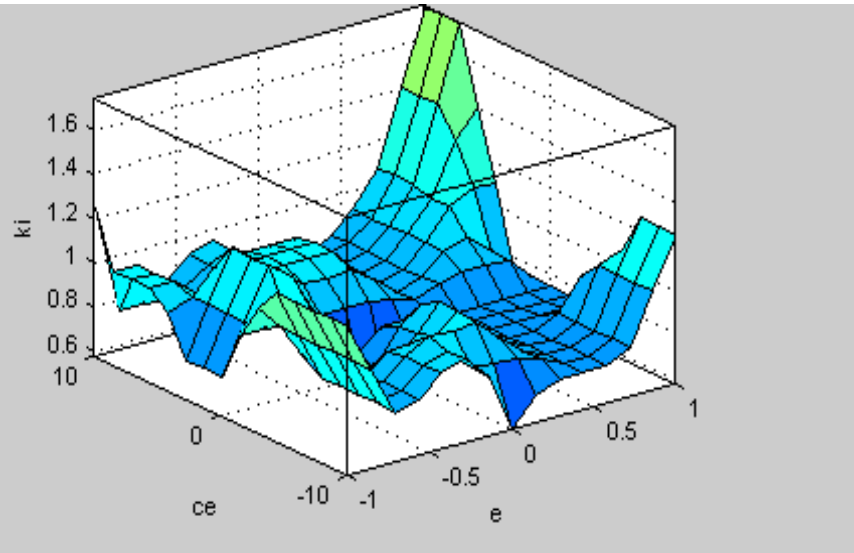

(b) Ki surface viewer

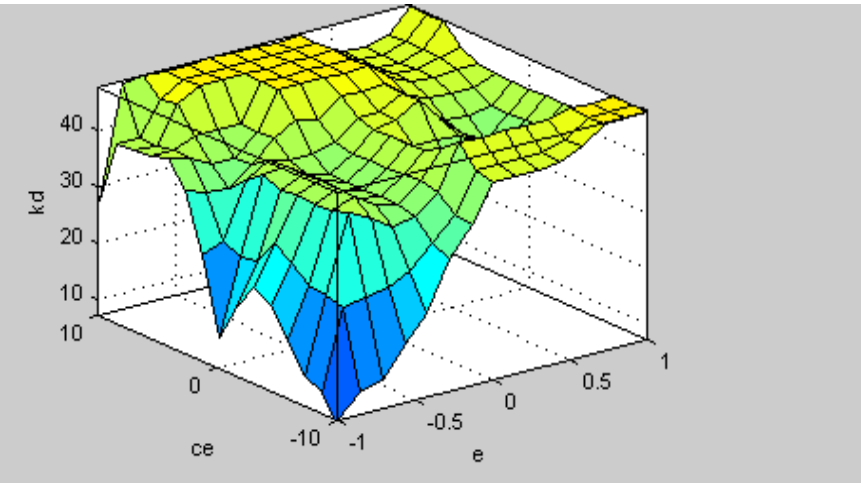

(c) Kd surface viewer

Figure 5:8 Surface viewers of the PID controller parameters

The fuzzy logic controller rule and its rule viewer are shown in Appendix B.

5.2 System Simulation

The structure and the relations of PMSM drive system and also the proposed control system are ~~fully~~ explained and analyzed in the previous sections. In this section, the overall Simulink block diagram of self-tuning fuzzy PID PMSM drive system is presented and simulated with different conditions. Then, the simulation studies the system are dynamic and transient performance using MATLAB/Simulink 2015a environment and the results, waveforms and the graphs are discussed. The proposed control system is designed by overall Simulink model and the controller parts are shown Figure 5.9 and 5.10 respectively.

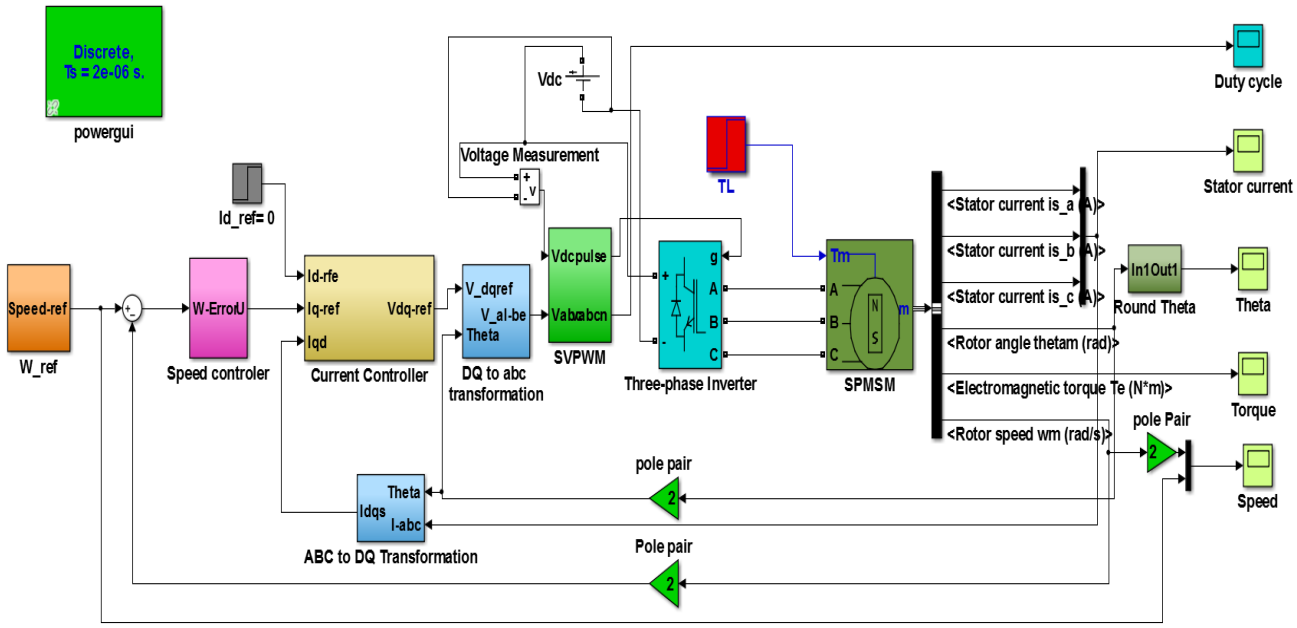

Figure 5:9 Overall Simulink model of speed control of SPMSM using FPID

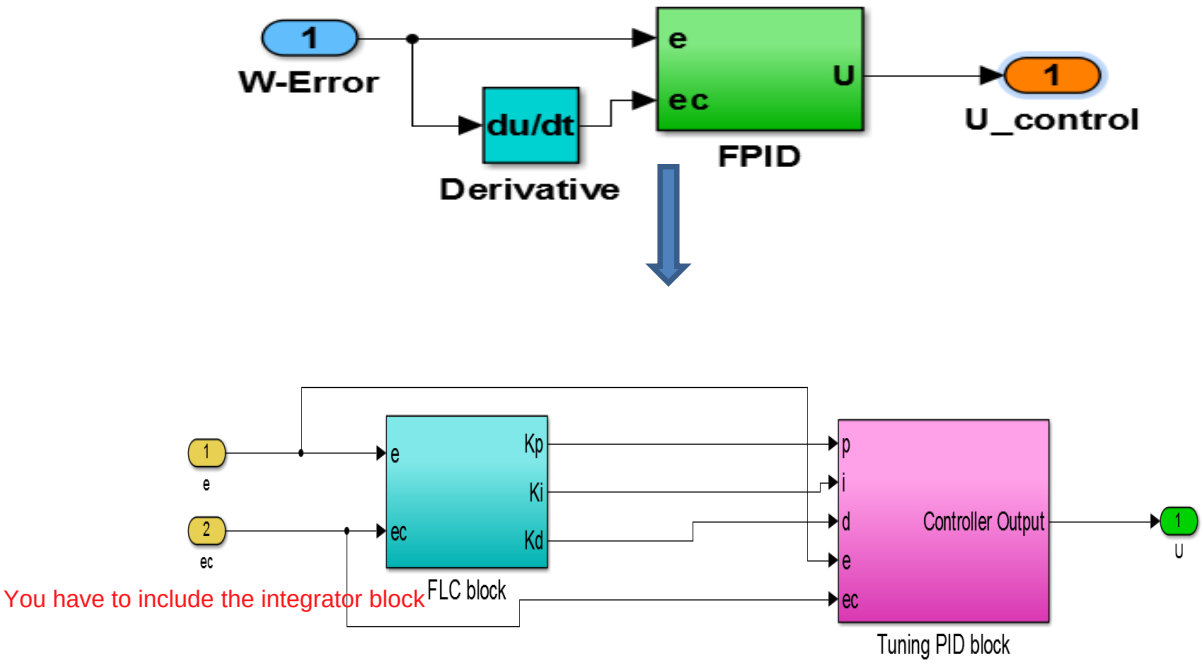

(a) Speed controller block

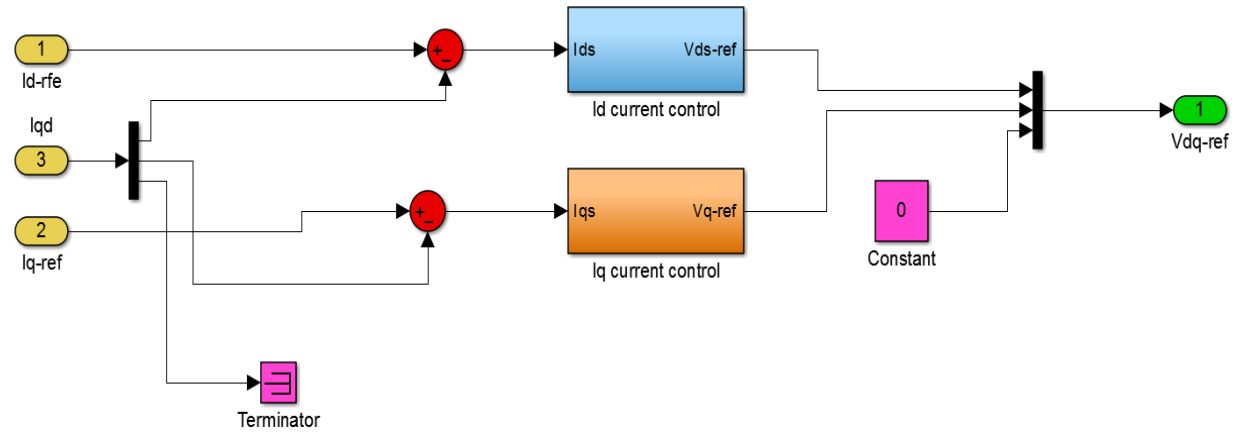

(b) Current controller block

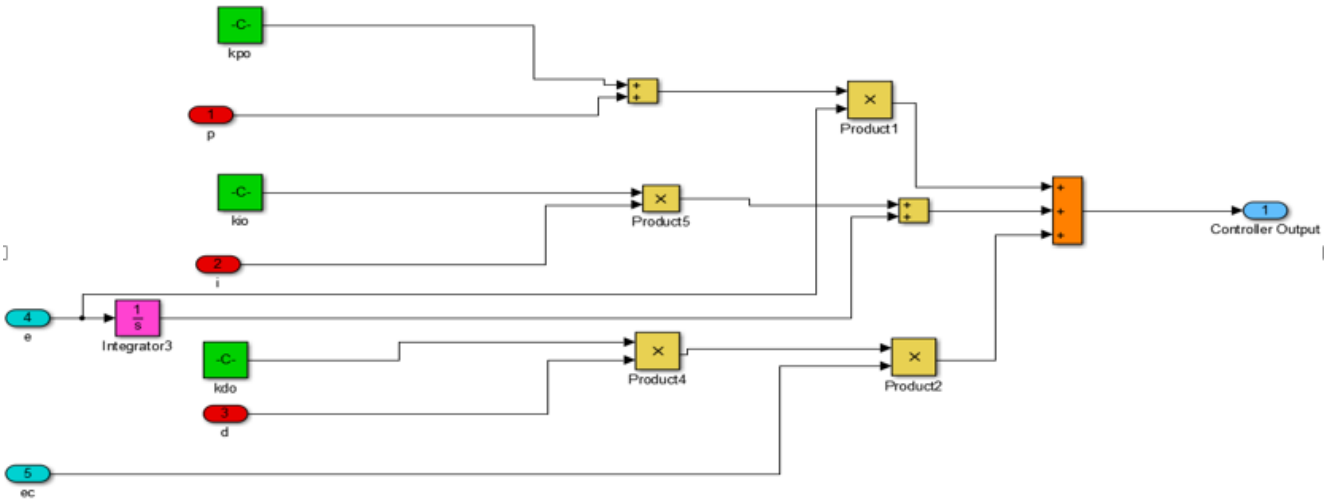

(c) PID tuninng algorthim

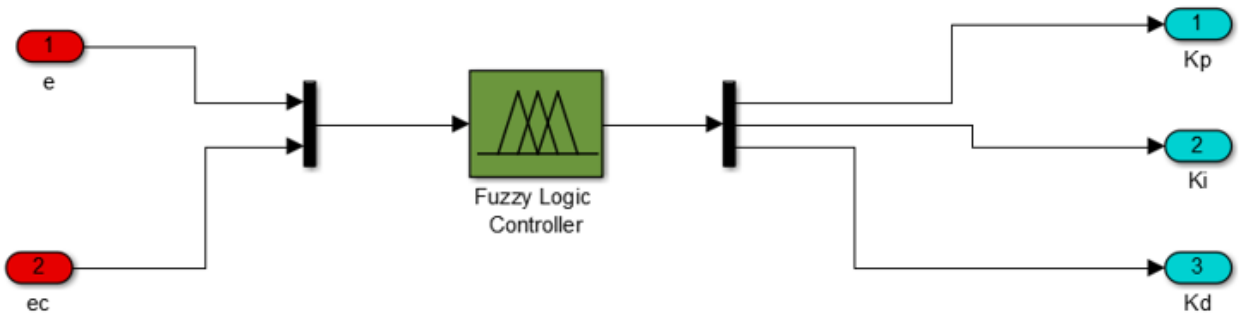

(d) Fuzzy logic controller

Figure 5:10 Speed and current controller Simulink model of the system

5.3 Simulation Results and Discussions

The simulation result of self-tuning FPID speed control of PMSM drive was carried out to evaluate its performance under different conditions. With a given motor parameters and controller gains the simulation results are obtained and the controller parameter gains have been tuned to have good simulation result.

Table 5.4 Motor parameter values [35] To my knowledge you took it from [26], otherwise you have to show me [35]

Description	**Symbol**	**Value**
Stator resistance	Rs	2.98ohm
Stator inductance	Ls	7e-3H
Rated torque	Trated	1.1Nm
Motor inertia	J	0.47e-4 Kg,m2
Viscous friction	B	1.1e-4Nm.s
Rated power	Prated	350W
Flux linkage due to permanent magnet	Ψ_m	0.125Wb
Rated speed	W_rated	630rad/sec
Rated current	I rated	2.9A

Table 5.5 Controller parameter values

Description	**Symbol**	**Value**
PWM frequency	Fs	10kHz
Sampling time	Ts	2e-6s
Speed controller parameter values		
Proportional gain	Kps	0.00342
Integral gain	Kis	5.78
Derivative gain	Kds	0.00063

Current controller parameter values for both d and q axes		
Proportional gain	Kpd=Kpq	17.88
Integral gain	Kid=Kiq	31733

The first simulation result for FPID speed control of PMSM is the three phase stator current which is generated by the three phase voltage source inverter. This three phase voltage source inverter is controlled by SVPWM blocks for appropriate stator current generation. These three phases current should be equal in magnitude and 120° phase shift with each other for appropriate rotating flux generation as shown in Figure 5.11 and its duty cycle wave form of the system also shown in Figure 5.12.

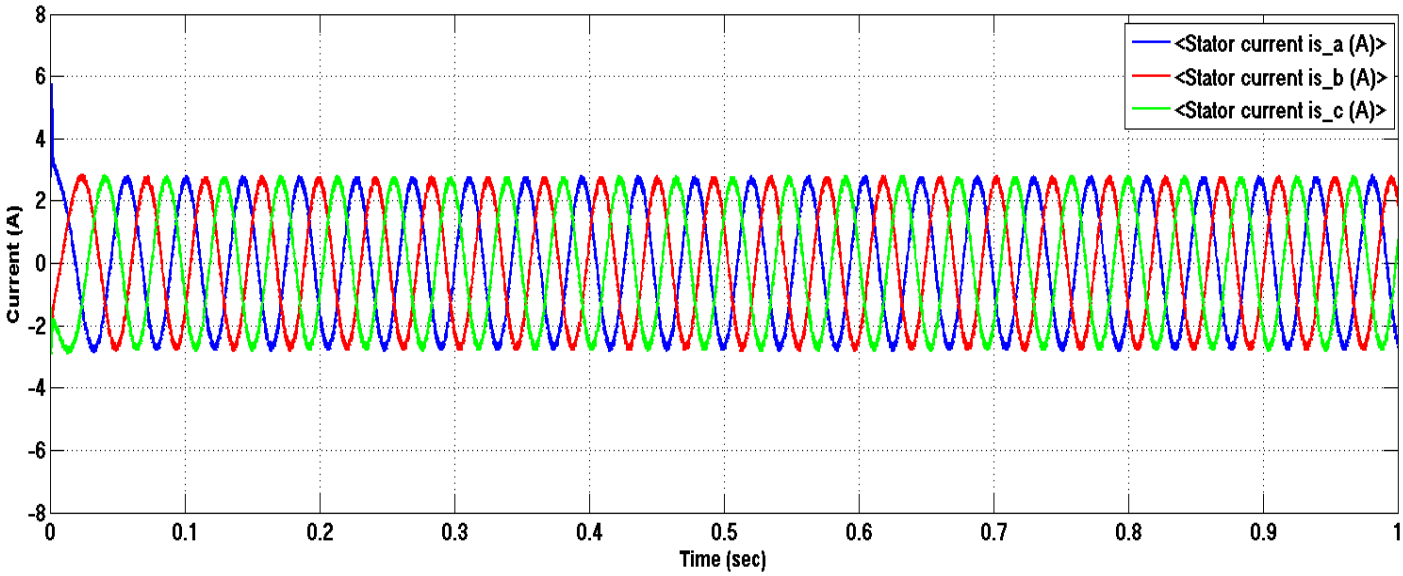

Figure 5:11 Stator current wave form with 150rad/sec

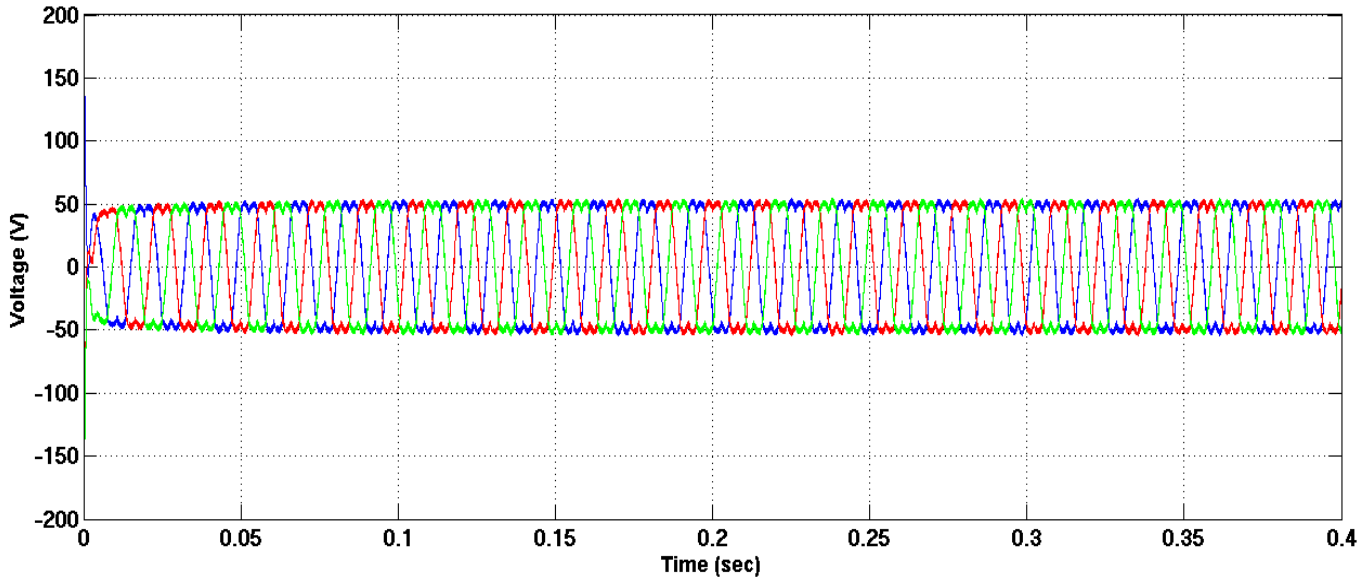

Figure 5:12 Duty cycle wave form with 300rad/sec

Figure 5.11 shows that the suitable stator phase current is generated with good accuracy as excepted. Therefore the system can feed the appropriate stator voltage to the motor. If the voltage applied to the motor is applied with appropriate magnitude and frequency, the speed of the motor is respected as set to the reference speed.

Tests without load

In this test, the speed control of SPMSM algorithm is tested at no load, for step speed input the machine is started from stand still with a constant 300 rad/sec speed at t=0second shows in Figure 5.13.In FPID controller very good response in both steady and dynamic states is noticeable with acceptable over shoot of 3.3%, settling time is less than 0.04second, rise time is 0.0053second and the maximum steady state error percentage is 0.035%. Where as in PID controller we have 15% overshoot, settling time is 0.03second, rise time is 0.0053second and the maximum steady state error is 0.217%.

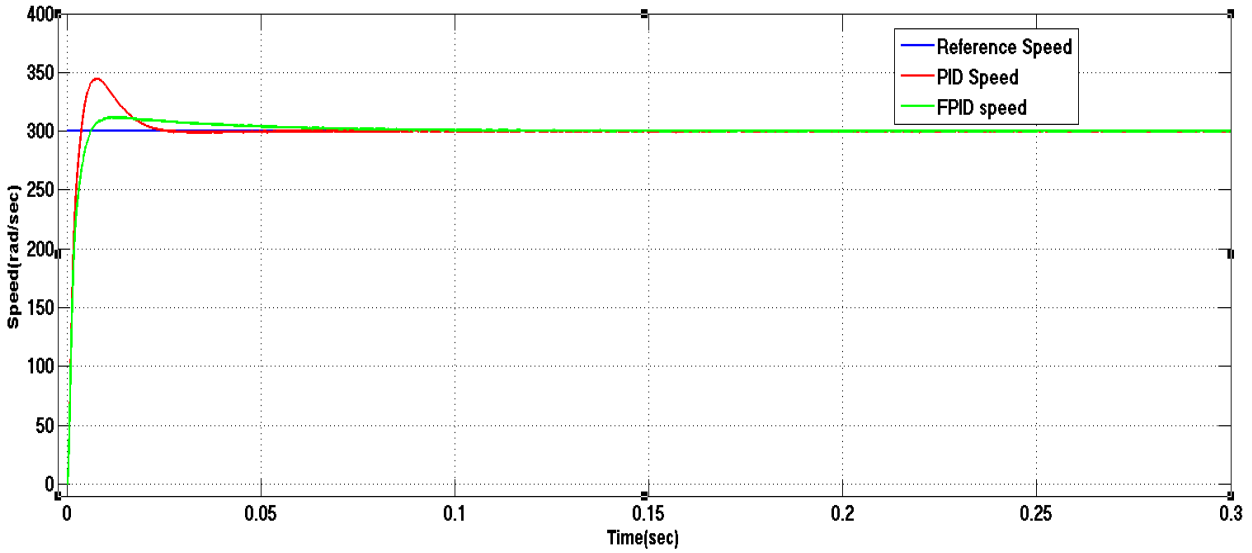

Figure 5:13 No-load test with constant step speed input graph

For incrementing step speed input commands until it reaches 600 rad/sec through several steps of different amplitude respectively shown in Figure 5.14 (a) the same result is found.

In both cases the Id current follows the reference given, while, on the other hand Iq differs from zero during mechanical transients. As we discussed in Section 3.6 the generated torque is directly proportional with Iq current component. So, when there are changes in speed due to inertia, peaks in the Iq values appear consequently the generated starting torque will be high until the rotor speed reaches to the steady state speed of FPID controller result shows in Figure 5.14 (a).

The graph of the torque is shown in order to verify that there is a difference between no-load torque and generated or electromagnetic torque in the first few seconds. In Figure 5.14 (b) around 1.8Nm generated torque is found due to the rotor acceleration in order to support the rotor acceleration to attain the reference speed in FPID controller case. So when the speed is varies continuously the generated or electrical torque variation is happed.

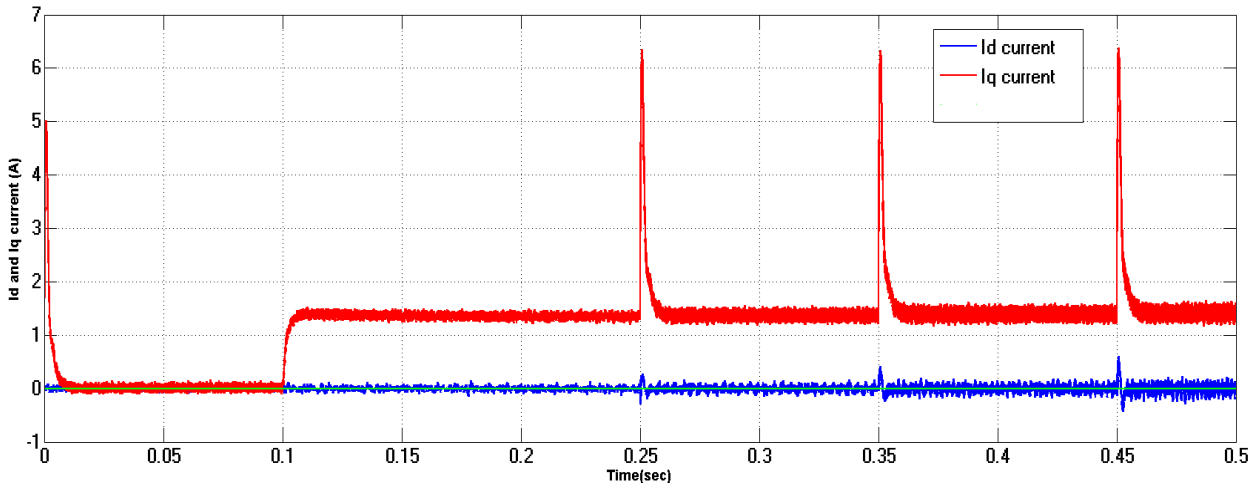

(a) Id and Iq currents

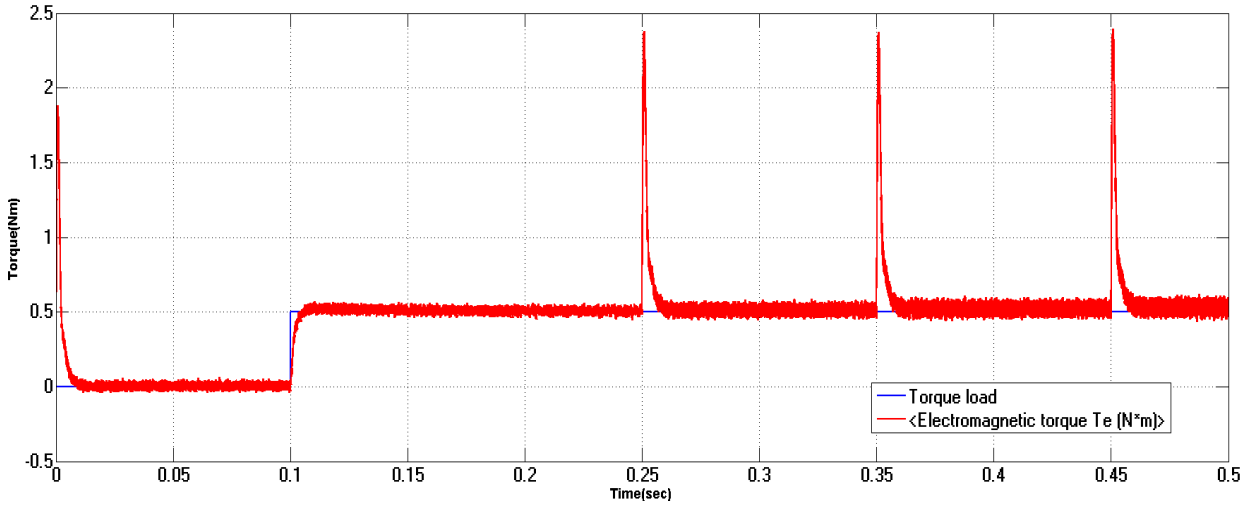

(b) Load Toruqe and Electromagnetic Torque

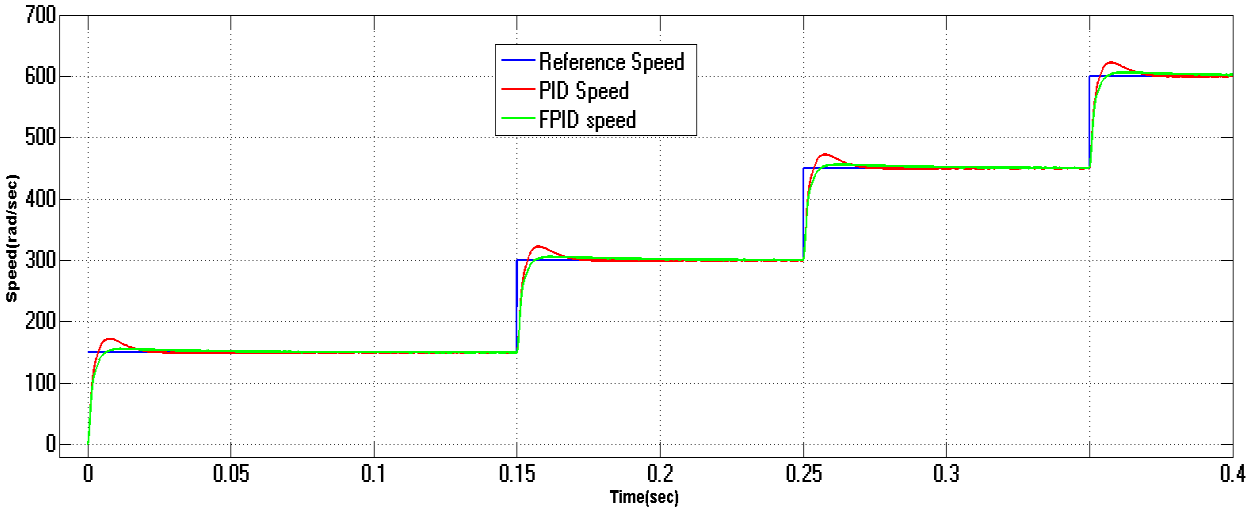

(c) Variable speed response

Figure 5:14 No-load test with increasing step input speed

Tests with load

1. When 1Nm load torque applied at t=0.2 second with constant speed

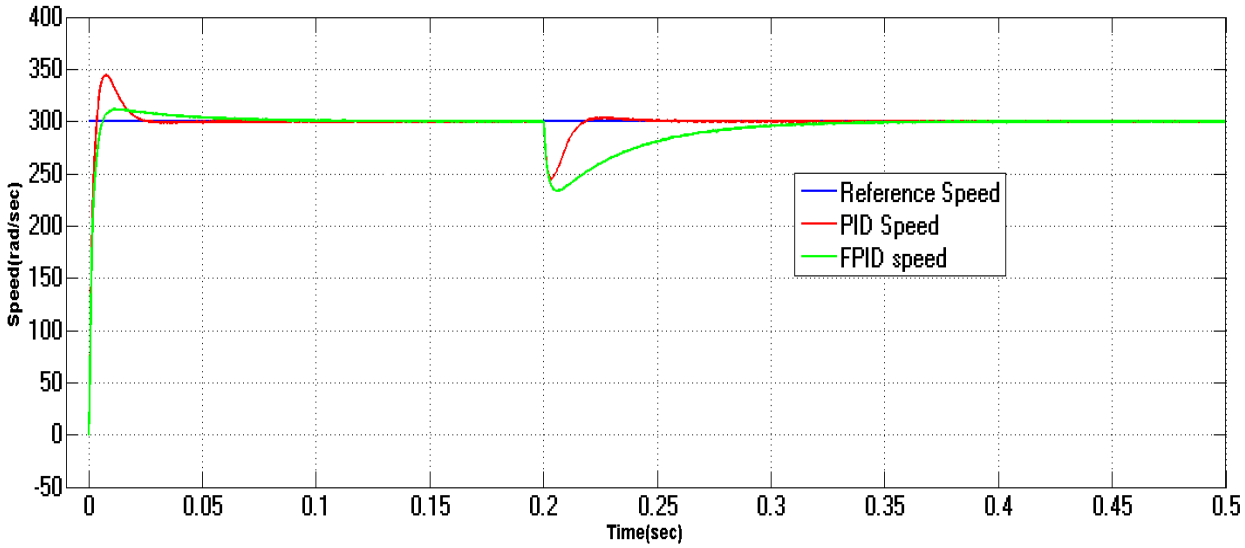

Figure 5:15 Speed response at 300rad/sec with 1Nm load torque

In this test the proposed system is tested with 1Nm applied load torque at t= 0.2 second as shown in Figure 5.15. In this test the percentage steady state error is somehow increases than no-load test with both PID and FPID controller 0.57% and 0.043%.

2. When sudden load torque is applied with constant speed

In Figure 5.16, the result shows that when 0.5Nm load torque is suddenly applied at t=0.5second the FPID controller is operating with the speed 267 rad/sec. While the time of load removal, the overshoot is 8.35%. When 1.1Nm load torque is applied again at t=1.5 is applied, then the actual speed drops to 243rad/sec for few seconds. This happens due to the generated torque (Te) is less than the load torque (Tl). To compensate this torque mismatch, the controller increases the generated torque consequently the motor speed increases until it attain the reference speed.

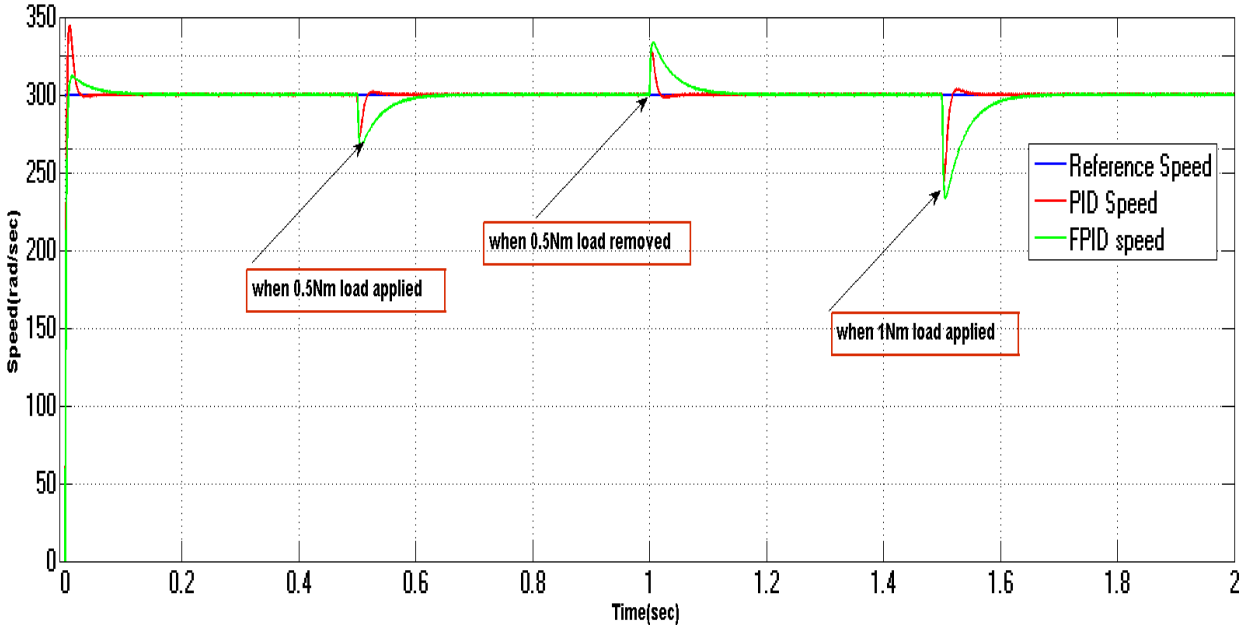

Figure 5:16 Speed response curve with sudden load torque change

3. Variable speed test with constant 1Nm load torque

In this test the motor is running in different speed region including low, medium and high speed behavior with a specified time as shown in Figure 5.17. When the time between t =0s to t =0.5s and t=1.25s to t=1.45s the motor operates in low speed region. While in the time between t =0.5s to 0.75s, and t=1second to 1.2.5second it is operating in medium region. Finally in the time between 0.75second to 1second the motor is operating in high speed region. As it is shown in figure actual speed both controllers tracking the reference speed very well.

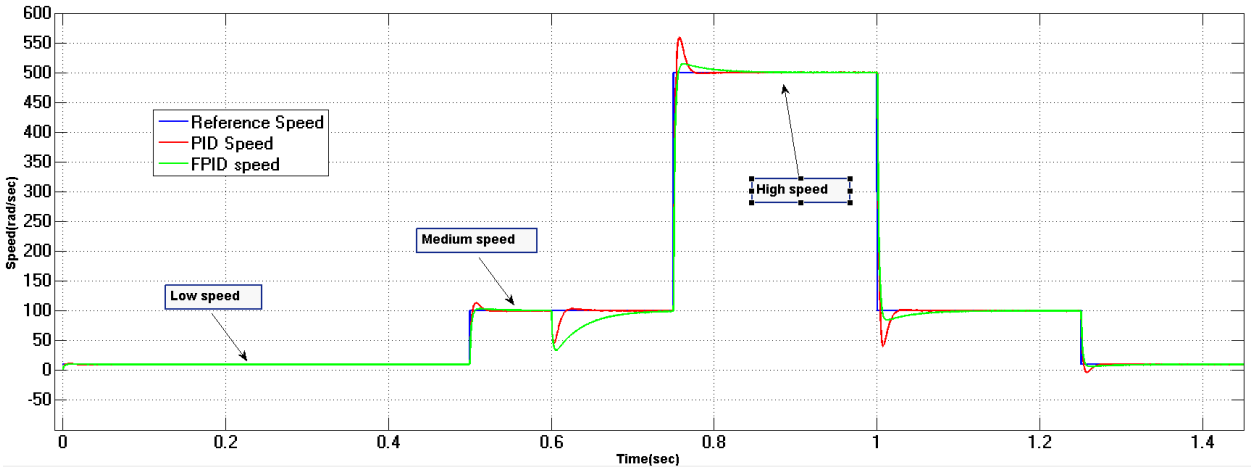

Figure 5:17 Variable speed response with constant torque with 1Nm

These two tests confirm what we have seen in the previous ones. The speed control is able to follow the speed reference, compensating for the constant load torque disturbance and in variable speed input in Figure 5.16 and 5.17 respectively.

4. Step response of drive with speed reversal test

Figure 5.18 shows that simulation result for speed reversal in step speed input. The motor reference speed is changed from 300rad/sec to -300 rad/sec at 0.55 second and again speed is set to 300 rad/sec at 1.5 second. The result shows that the actual speed follows the reference speed with good accuracy.

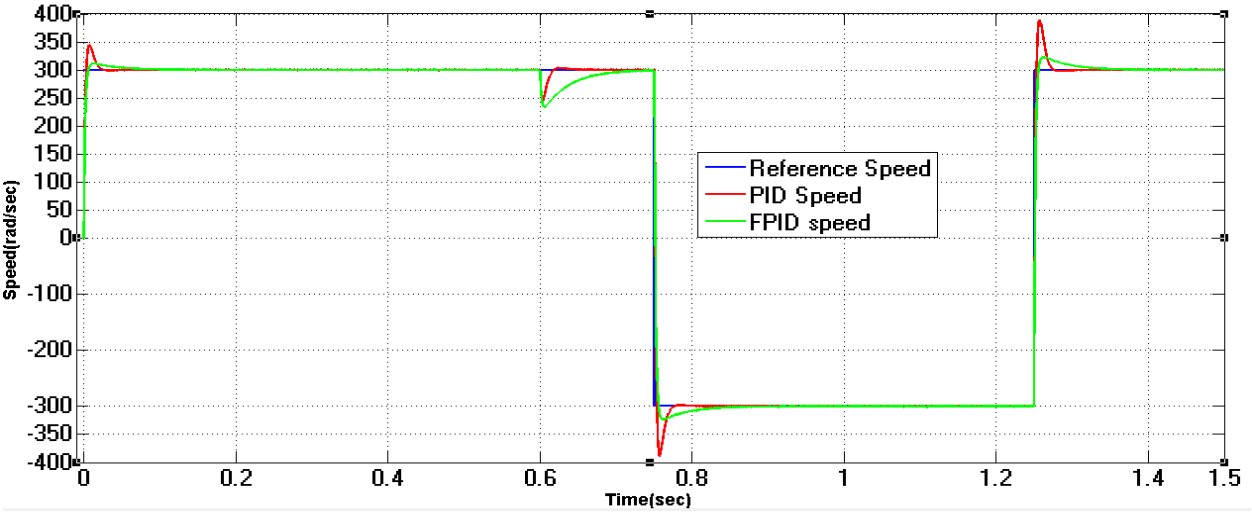

Figure 5:18 Speed response reversal with 1Nm load torque

Parameter uncertainties test

In real world environment due to the variation of temperature the given motor parameters will vary accordingly. By considering this the next tests are simulated in different conditions.

When the input speed varies starting from at t= 0s 150rad/sec speed is applied, at t= 0.25s 300rad/sec speed is applied, at t=0.35s 450rad/sec is applied and lastly at 0.45s 600rad/sec is applied with constant load torque 1Nm applied at t=0.2second as shown in figures below. With this given speed reference parameter uncertainties test is performed as follows.

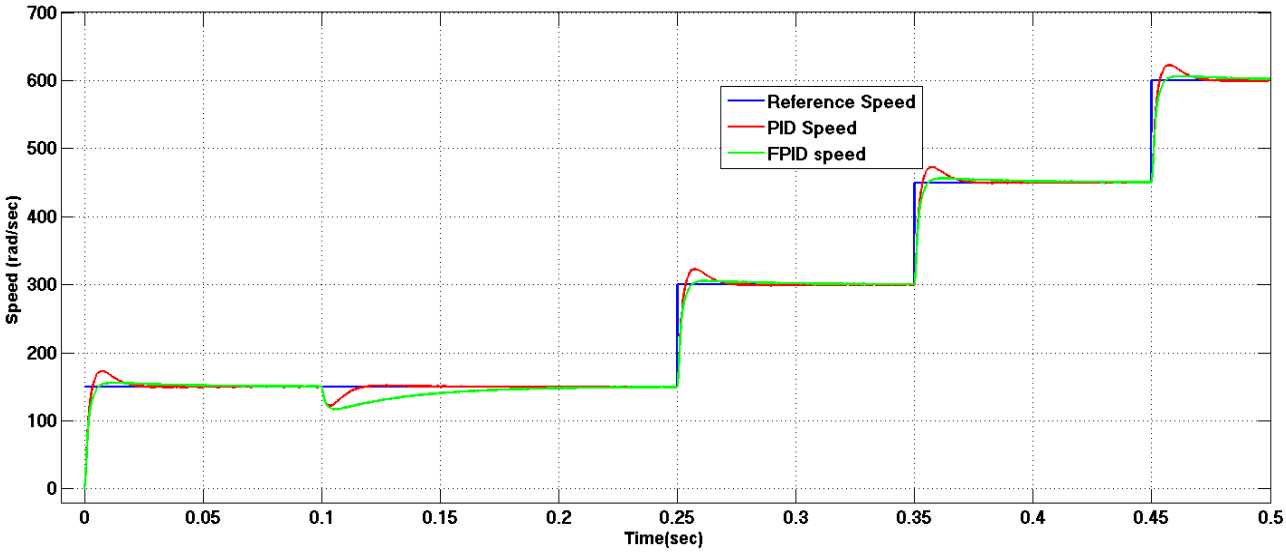

Figure 5:19 Speed responses when only Rs is increases by 75%with 1Nm load torque

The first test is done when the stator resistance Rs increases by 75% and the other parameters are in their nominal values. The result shows that 15.13% and 3.86% overshoot and the steady state error percentage is 0.22% and 0.037% for PID and FPID controller respectively as it is shown in Figure5.19.

The second test is done when the stator resistance Rs increased by 75% from its nominal value and the inductance decreases with 75% while the other parameters are in their nominal values. The simulation test result is also good enough as show in Figure 5.20 with 4% overshot, less than 0.05second settling time and steady state error percentage is 0.067% for FPID controller.

For PID controller the overshoot is 16% with 0.33% of steady state error and the system is more likely oscillatory than FPID controller result.

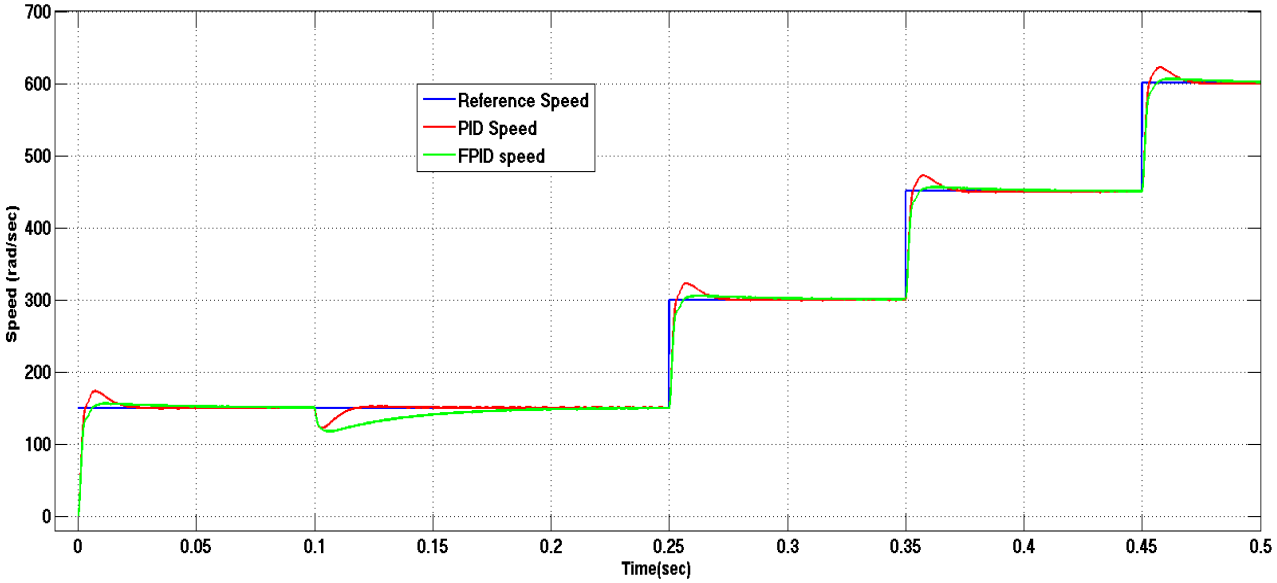

Figure 5:20 Speed response with 1Nm torque when Rs is increases and Ls is decreases by 75%

Test third, when only the motor inertia J is increases by 75% from its nominal value while the other parameters are in their nominal value the simulation test result is shows in Figure 5.21 (a). The result found in PID controller is 21.6% overshot with a 0.4% steady state error and 6% overshoot, 0.04second settling time and 0.2% steady state error percentage in FPID controller.

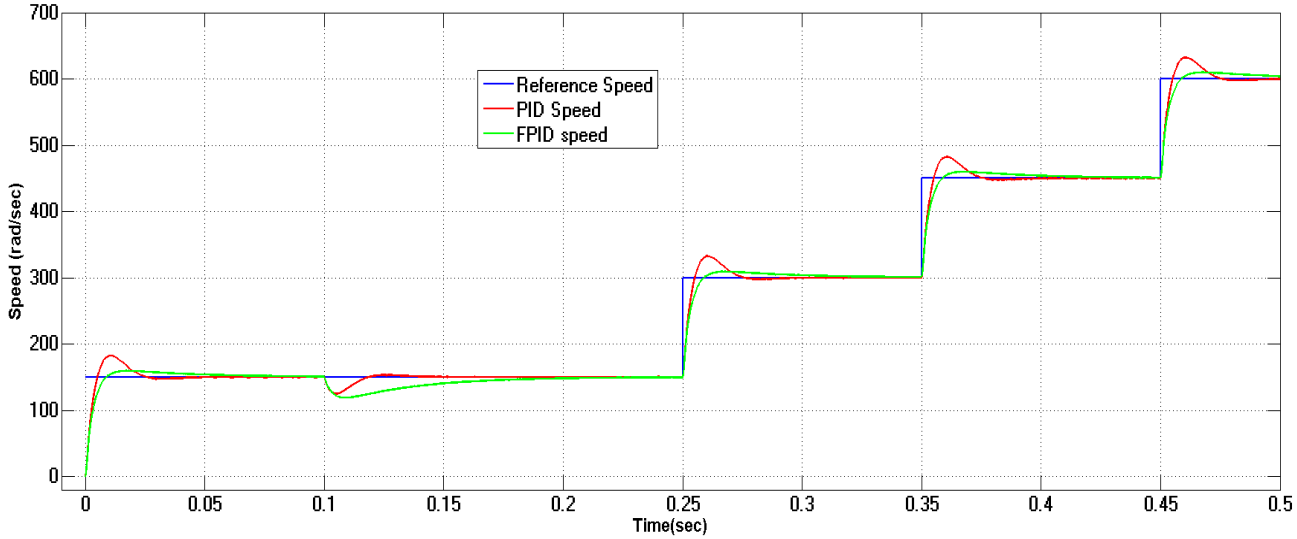

(a) J is increases by 75%

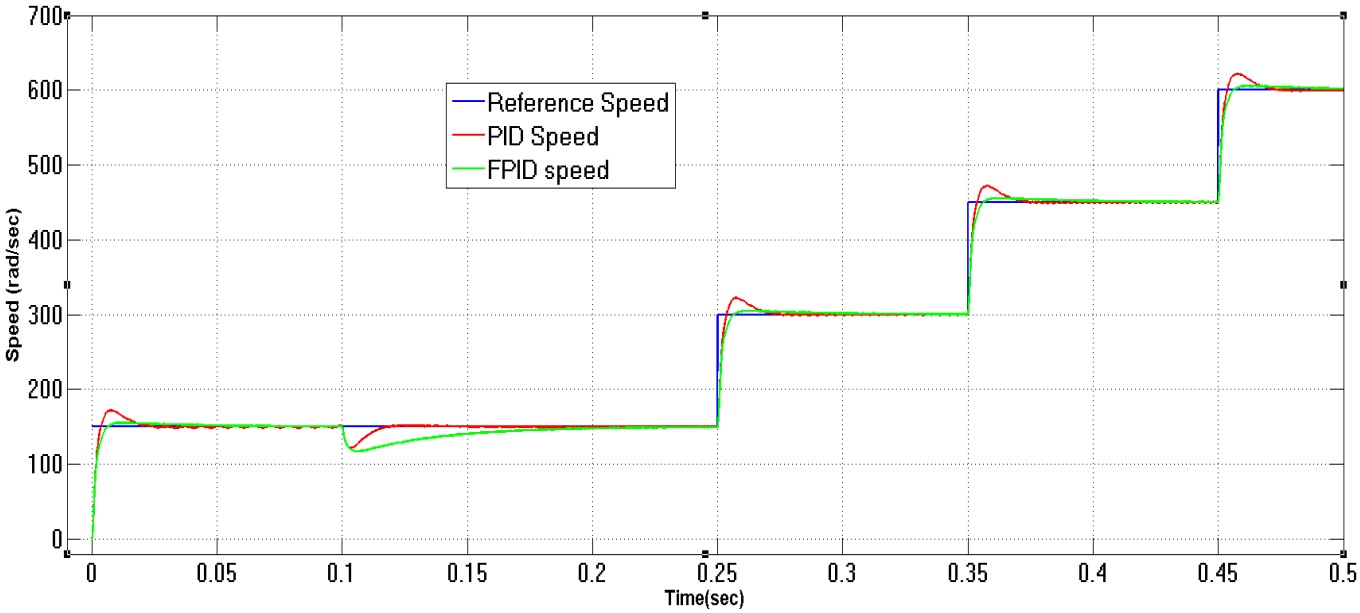

(b) B increased by 75%

Figure 5:21 Speed response with load torque of 1Nm when parameters are varies by 75%

Test four, when only the viscous friction B is increases by 75% from its nominal value while the other parameters are in their nominal value the simulation test result is shown in Figure 5.21 (b). The result found in PID controller is 14.7% overshot with 0.7% steady state error and 3.3% overshoot, 0.04second and 0.13% steady state error percentage from FPID controller. As it is clearly shows in the figure the PID controller output is more oscillatory.

Test five, when the motor inertia J and viscous friction B are increases by 100% from its nominal value while the other parameters are in their nominal value the simulation test result is shown in Figure 5.22. The result found in PID controller is 21.3% overshot, 0.055 second settling time and 0.4% steady state error. And 5.87% overshoot, 0.06second and 0.087% steady state error percentage from FPID controller.

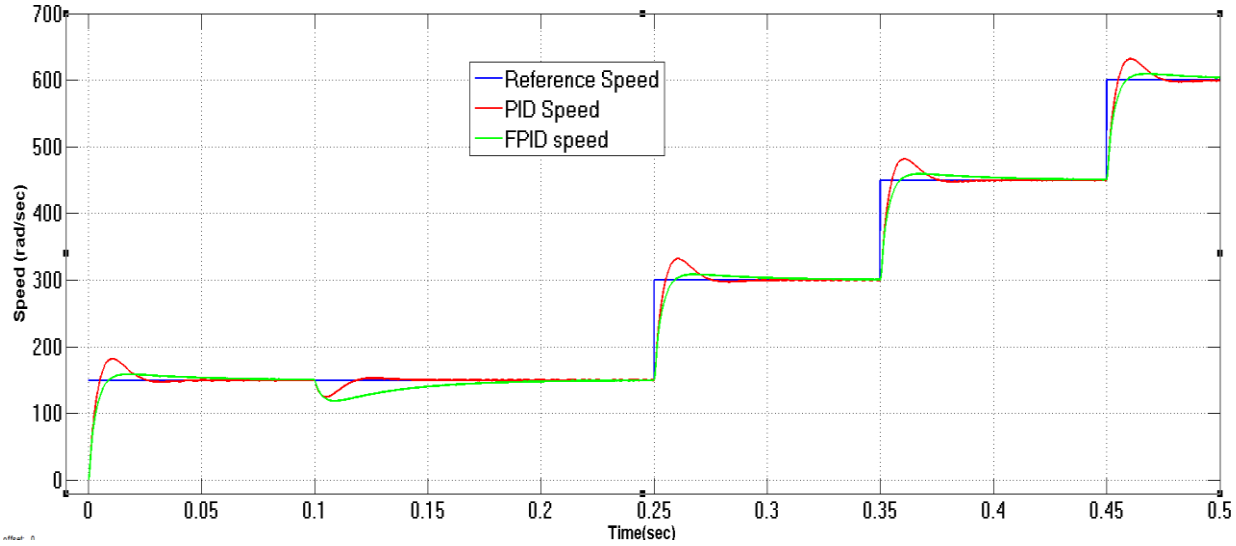

Figure 5:22 Speed response when J and B increases by 100%

Test six, when Rs is decreases by 75% and Ls is increases by 75% but the others are in their nominal values the simulation test result is shown in Figure 5.23. The result found in PID controller is 16.7% overshot, 0.05 second settling time and 0.57% steady state error. And 4.1% overshoot, 0.05 second and 0.1% steady state error percentage from FPID controller. But in this test the PID controller result is more oscillatory than the others test.

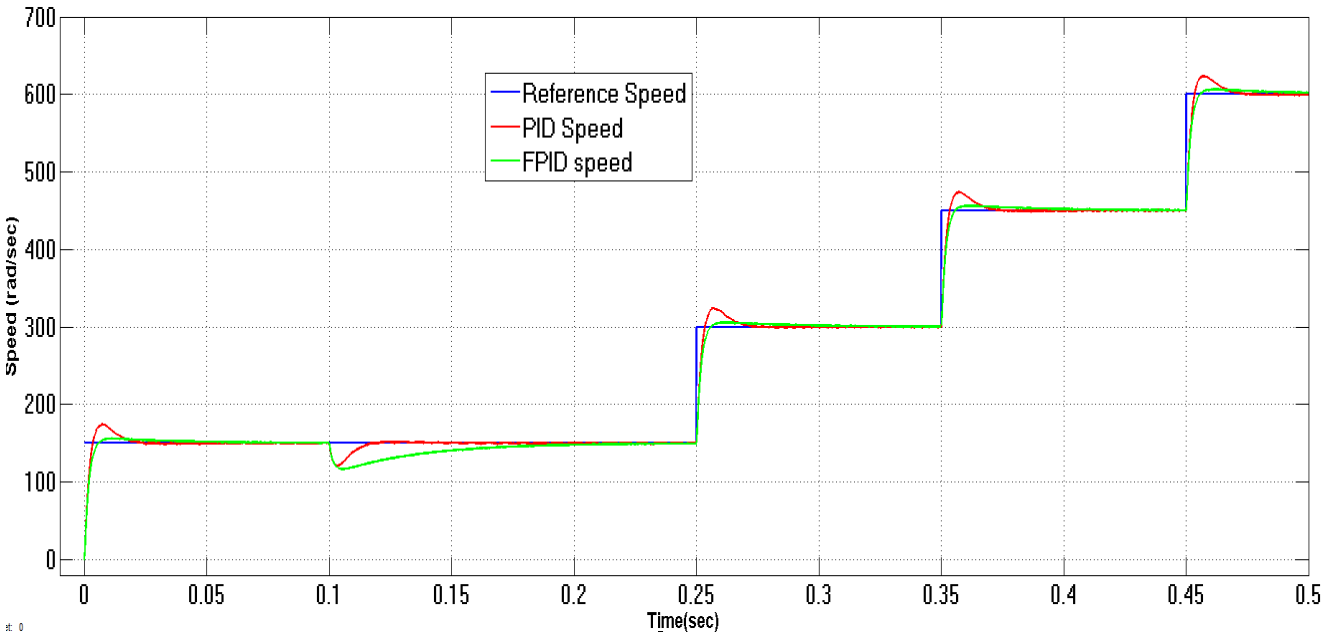

Figure 5:23 Speed response when Rs decrease and Ls increase by 75%

Test with different input signals

The first test is done with constant speed for the time between t=0 second to t=0.5second with 20rad/second, for time t=0.5second to t=1second is ramp speed input varies from -20rad/sec to 20rad/sec and at t= 1.5second the speed is 20rad/sec as shown in Figure 5.24.

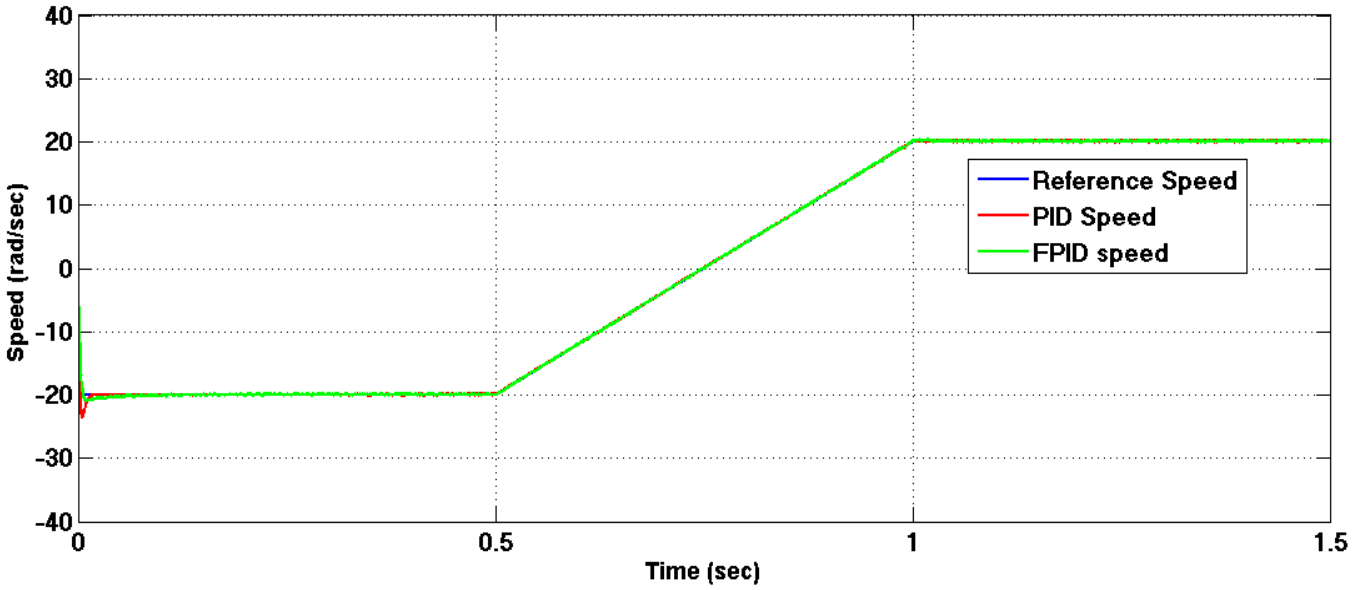

Figure 5:24 Speed response with ramp input without load

The second test is done when the input is sinusoidal speed with 100rad/second amplitude and the frequency or bandwidth is 10Hz and 5Hz shown in Figure 5.25.

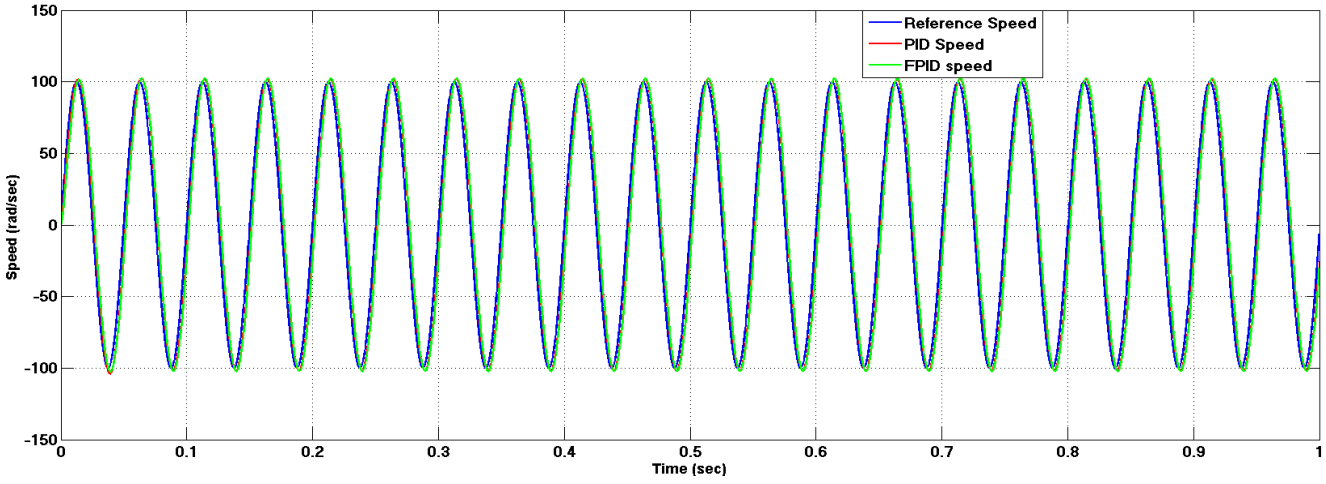

(a) When bandwidth is 10Hz

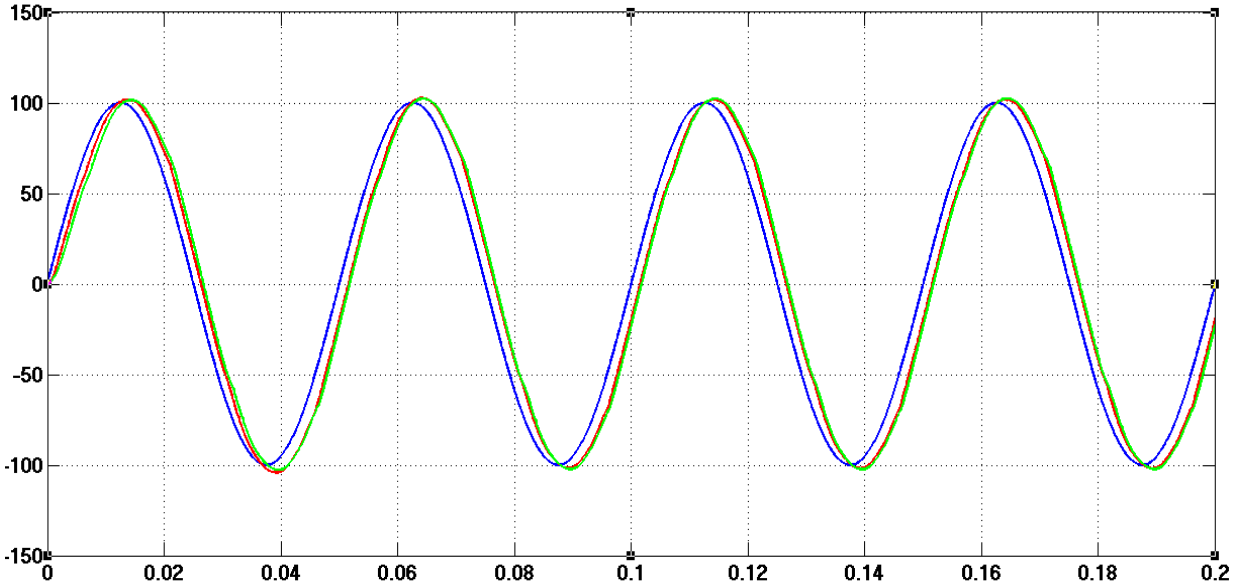

Cut view between 0 and 0.2 sec with 10Hz bandwidth

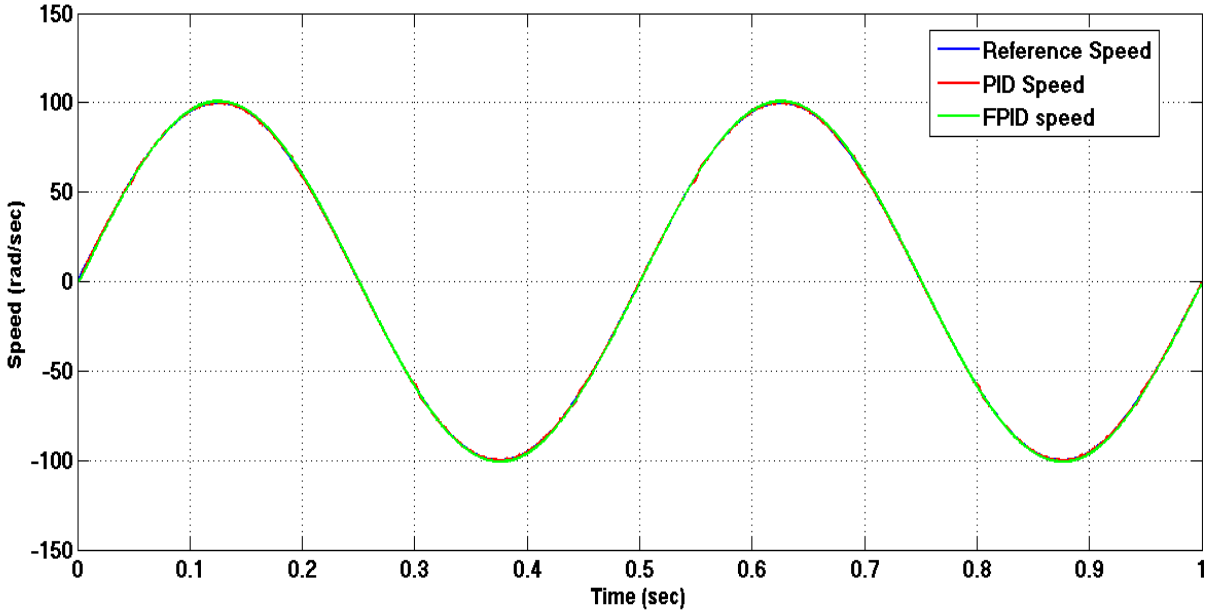

(a) When bandwidth is 5Hz

Figure 5:25 Speed response for different bandwidth sinusoidal input

As it is shown in Figure 5.25 when the bandwidth is decreasing to 5Hz the actual speed is perfectly track the reference speed.

Performance comparison of the FPID controller with conventional Controllers

The stability and performance is evaluated by observing the system responses in the above simulation results and discussions its parameters like overshoot, rise time, settling time, and comparisons are illustrated in the Table 5.6 below. The comparison between the output graphs of controllers without load and load is shown in Figure 5.26 and 5.27.

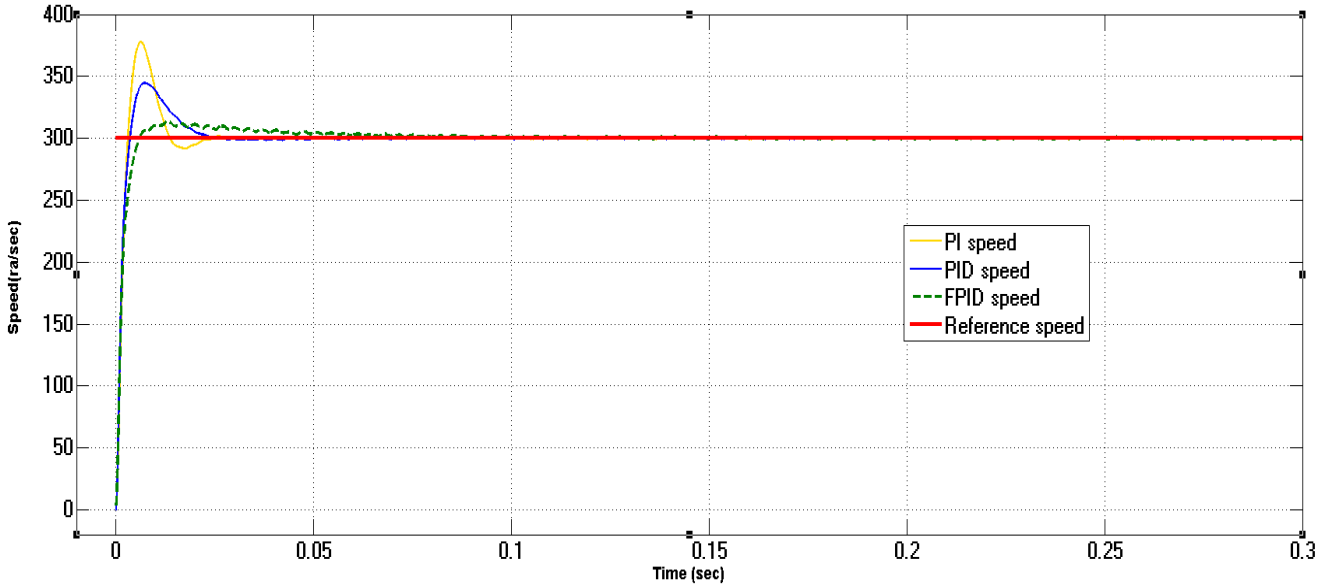

Figure 5:26 Speed response for the controllers 300rad/sec with no load

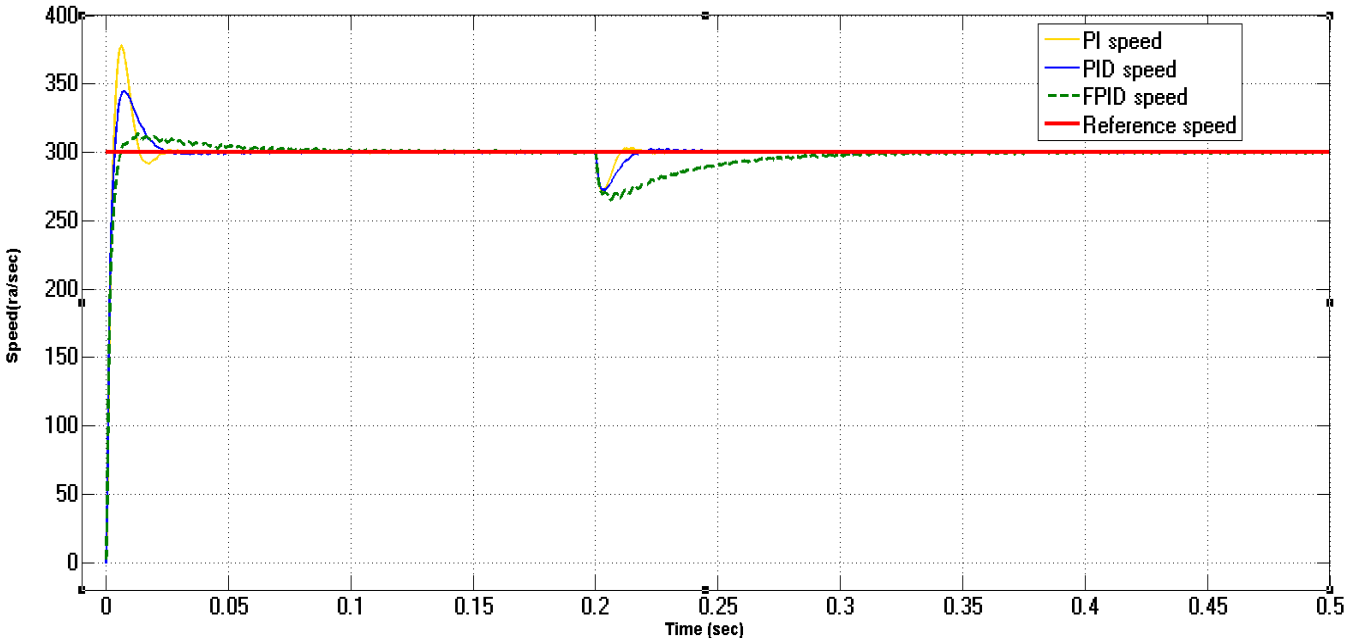

Figure 5:27 Speed response for the controllers 300rad/sec with 1Nm load toque

Table 5.6 Performance comparison table

Tests	Performance parameters	PI controller	PID controller	FPID controller
Without load torque	Over shoot	24.3%	15%	3.3%
	Rise time	0.005sec	0.0053sec	0.0053sec
	Settling time	0.05sec	0.03sec	0.04sec
	Ess error	0.28%	0.217%	0.035%
With 1Nm load torque at t=0.2 second	Over shoot	25.2%	15.3%	3.8%
	Rise time	0.005sec	0.0053sec	0.0053sec
	Settling time	0.07sec	0.03sec	0.043sec
	Ess error	0.356%	0.57%	0.043%

In speed of response (Rise time and Settling time) of FPID is always inferior .whether in no load or load case. You have to show this clearly on this table.

Chapter Six

Conclusion and Recommendations

6.1 Conclusion

In this thesis, design and simulation of self-tuning fuzzy logic PID speed control of PMSM has been done. The result of traditional PI and PID controller mechanisms as speed control of PMSM are not satisfactory to the higher degree of accuracy conditions and when load disturbance and parameter uncertainties happens to the system. However, the FLC mechanism not only has the prominent advantage in complex system control and also does not need the exact mathematical model of the system to be controlled.

A self-tuning FLC that tunes the gains of PID controller was developed according to the PMSM drive system characteristic, which can adjust the PID controller parameters on-line according to the speed error and the speed error change rate. As it is discussed on chapter three, the simulation result shows the proposed controller mechanism has a very good performance in terms of overshoot minimization and percentage steady state error than the conventional controller methods. From no–load test the simulation results shows that FPID controller has more significant overshoot reduction (by 11.7% and 21% compared to PID and PI controllers respectively), and good transient response with rise time of 0.0053 second, settling time 0.035second and the maximum steady state error percentage of 0.035% has been achieved. While in the case of load test the steady state error percentage is increases to 0.043%. The performance of self-tuning fuzzy logic PID controller of PMSM was analyzed in terms of speed tracking capability, torque response quickness; high and low speed behavior, step response of drive with speed reversal, and sensitivity to motor parameter uncertainty. Generally, the system also gives good performance at no load and loaded condition. Hence, it can work with different load torque conditions and with parameters variation.

with respect to overshoot and steady state error.

You have to state the inferiority of FPID to PID with respect to speed of response.

6.2 Recommendations

This thesis paper is working only in base speed region. So as recommendation the thesis can also be extended to operate the motor in the speed region beyond the rated speed; in field weakening region. A flux-weakening technique is applied when extension of the motor speed beyond base speed is desired. And if all materials are available this thesis can be implemented using DSP board with sensor. However implementing with sensor-less or using rotor position is more preferable in terms of cost minimization.

References

[1] R. Krishnan, Permanent Magnet Synchronous and Brushless DC Motor Drives, Virginia: CRC Press, 2010

[2] R. Krishnan, Electric Motor Drives Modeling, Analysis, and Control, Virginia: Virginia Tech Blacksburg, 2001.

[3] T. Sabastial, G.R. Slemon and M.A. Rahman, "Modeling of Permanent Magnet Synchronous," *IEEE,* vol. 22, September 1986.

[4] Abdullah I. Al-Odienat and Ayman A. Al-Lawama, "The Advantages of PID Fuzzy Controllers," *American Journal of Applied Sciences.*

[5] Rajesh Kumar, R. A. Gupta and Bhim Singh, "Intelligent Tuned PID Controllers for PMSM Drive-A Critical Analysis," *Malaviya National Institute of Technology.*

[6] Siva Gangadhara Rao Venna, Sneha Vattikonda & Sravani Mandarapu, "Mathematical Modeling and simulation of Permanent Magnet synchronous Motor," *International Journal of Advanced Research in Electrical, Electronics and Instrumentation Engineering,* vol. 2, no. 8, August 2013.

[7] Puspendu Maji, Prof. G Kpanda & Prof. P Ksaha, "Field Oriented Control of Permanent Magnet Synchronous Motor Using PID Controller," *International Journal of Advanced Research in Electrical , Electronics and Instrumentation Engineering,* vol. 4, no. 2, February 2015.

[8] Davendra Yadav, Sunil Bansal & Munendra Kumar, "Design, Development & Simulation of Fuzzy Logic Controller to Control the Speed of Permanent Magnet Synchronous Motor Drive System," *International Journal of Scientific Research Engineering & Technology,* vol. 1, no. 5, August 2012.

[9] Harshada V. Deo, R. U. Shekokar, "Simulation of PMSM Speed Control System with Vector Control Method based on MATLAB," *International Journal of Multidisciplinary Research and Development* , vol. 2, no. 6, pp. 354-359 , June 2015.

[10] Jin-Woo Jung, Han Ho Choi & Tae-Heoung Kim, "Fuzzy PD Speed Controller for Permanent Magnet Synchronous Motors," 2011.

[11] N. Tesla, A New System of Alternate Current Motors and Transformers, AIEE Transactions, 1888.

[12] A. Ivanov-Smolensky, Electrical Machine, vol. 2, Moscow: Moscow,MIR, 1988.

[13] A. Opritescu, "Control of a Saturated Permanent Magnet Synchronus Motor," PED 1034 , AALBORG UNIVERSITY, DENMARK, 2010.

[14] Dr. Prema kumar & B. Vanajakshi, "Speed Control of PMSM Drive Using Conventional and Self Tuning Fuzzy PI Controller," *International Journal of Emerging Trends in Electrical and Electronics*, vol. 10, no. 2, Mar-2014.

[15] Haitham Abu-Rub, Atif Iqbal & Jaroslaw Guzinski, High Performance Control of AC Drives With Matlab/Simulink Models, 1st ed., Chichester,UK: John Wiley & Sons Ltd., 2012.

[16] J. F. Gieras, Permanent Magnet Motor Technology Design and Application, 3rd ed., CRC Press Taylor & Francis Group, 2012.

[17] D.W.Novotny & T.A Lipo, Vector Control and Dynamics of AC Drives, 1st ed., Oxford Science Publication, 1996.

[18] Abdulaziz Bello & Ibrahim Muhammad Kilishi, "Comparative Review of PMSM and BLDCM Based on Direct Torque Control Method," vol. 3, no. 3, March 2014.

[19] "Motor Control Portfolio Information in Arizona," *"http://www.freescale.com/motorcontrol.*

[20] C. Busca, "Open loop low speed control for PMSM in High Dynamic Applications," Aalborg University, Aalborg, Denmark, 2010.

[21] V. P. K. A. P.Samyuktha, "Vector Control Drive of Permanent Magnet Synchronous Motor Using Resolver Sensor," Global Institute of Engineering & Technology, Hyderabad.

[22] M. Plantic, "Field Orientated Control of 3-Phase AC-Motors," Texas Instruments, 1998.

[23] M. Plantic, "Implementation of a Speed Field Oriented Control of 3-phase PMSM Motor using TMS320F240," Texas Instruments Inc., 1999.

[24] H. A.Toliyat & S.Campbell, DSP-Based Electromechanical Motion Control, Florence: CRC Press Inc., 2003.

[25] H. A. Toliyat & S.Campbell, DSP-Based Electromechanical Motion Control, Boca Raton: CRC Press, 2004.

[26] J. Holtz, W. Lotzkat, & A.M. Khambadkone, "On Continuous Control of PWM Inverters in the Over-modulation Range Including the Six-Step Mode," *IEEE Trans-actions on Power Electronics*, vol. 8, no. 4, October 1993.

[27] K. Zhou & D. Wang, "Relationship between Space-Vector Modulation and Three- Phase Carrier-Based PWM: A Comprehensive Analysis," *IEEE Transactions on Industrial Electronics*, vol. 49, no. 1, February 2002.

[28] B. Bose, Modern Power electronics and AC drive, New Jersey, USA: Prentice-Hall PTR, Inc., 2002.

[29] E. Hendawi, F. Khater & A. Shaltout, "Analysis, Simulation and Implementation of Space Vector Pulse Width Modulation Inverter," in *International Conference on Application of Electrical Engineering*, Egypt, 2010.

[30] B. Wu., High-Power Converters and AC Drives., New Jersey: John Wiley and Sons Inc.,, 2006.

[31] R. Sehab & B. Barbedette, PID CONTROLLER DESIGN APPROACHES – THEORY, TUNING AND APPLICATION TO FRONTIER AREAS, M. Vagia, Ed., Rijeka,Croatia: In Tech Janeza Trdine 9, .

remove the capitalization

[32] Zulfatman & M. F. Rahmat, "Application of Self-tuning Fuzzy PID Controller on Industrial Hydraulic Actuator using System Identification Approach," *International Journal On Smart Sensing And Intelligent Systems*, vol. 2, no. 2, June 2009.

[33] Wang, LI-Xi, A Course in Fuzzy Systems and Controls, Hong Kong: Prentice –Hall International.

formerly Wang was [34] and Lee was 35, clearly this affects ur reference usage in your writing, please check if u have changed it accordingly in the body of ur writing.

[34] C. C. Lee, "Fuzzy Logic in Control System: Fuzzy Logic Controller Part-I," *IEEE Transactions, MAN, AND CYBERNETICS*, vol. 20, no. 2, 1990.

[35] Liuping Wang, Shan Chai & Dae Yoo, PID and Predictive Control of Electrical Drives and Power Converters Using MATLAB/Simulink, 1st ed., Singapore: John Wiley & Sons Ltd., 2015.

Appendixes

Appendix A

Simulation block of SVPWM Max-Min offset design

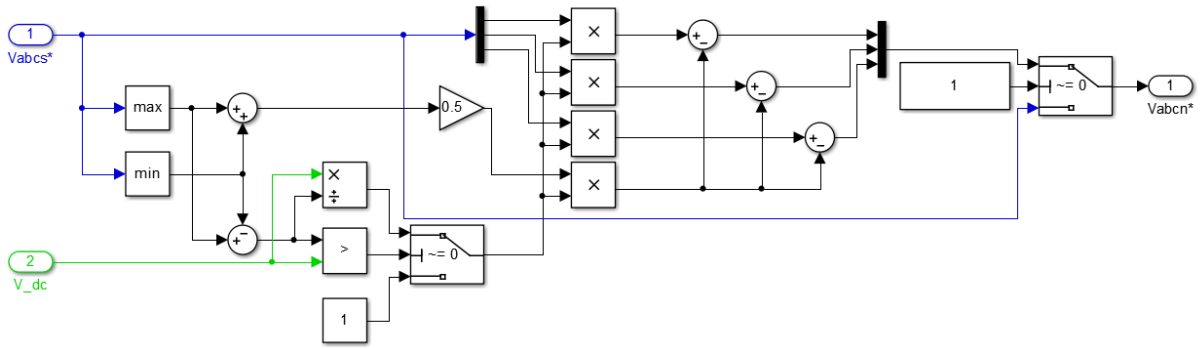

Appendix B

Fuzzy logic controller 49 rules

Rule Editor: thesisFIS

File Edit View Options

1. If (e is NL) and (ce is NL) then (kp is PVL)(ki is PM)(kd is PVS) (1)
2. If (e is NL) and (ce is NM) then (kp is PVL)(ki is PM)(kd is PMS) (1)
3. If (e is NL) and (ce is NS) then (kp is PVL)(ki is PM)(kd is PM) (1)
4. If (e is NL) and (ce is Z) then (kp is PVL)(ki is PMS)(kd is PMS) (1)
5. If (e is NL) and (ce is PS) then (kp is PVL)(ki is PMS)(kd is PML) (1)
6. If (e is NL) and (ce is PM) then (kp is PVL)(ki is PM)(kd is PL) (1)
7. If (e is NL) and (ce is PM) then (kp is PM)(ki is PMS)(kd is PVL) (1)
8. If (e is NM) and (ce is NL) then (kp is PML)(ki is PMS)(kd is PMS) (1)
9. If (e is NM) and (ce is NM) then (kp is PML)(ki is PMS)(kd is PML) (1)
10. If (e is NM) and (ce is NS) then (kp is PML)(ki is PMS)(kd is PML) (1)
11. If (e is NM) and (ce is Z) then (kp is PML)(ki is PM)(kd is PML) (1)
12. If (e is NM) and (ce is PS) then (kp is PML)(ki is PM)(kd is PL) (1)
13. If (e is NM) and (ce is PM) then (kp is PVL)(ki is PMS)(kd is PVL) (1)
14. If (e is NM) and (ce is PL) then (kp is PVL)(ki is PMS)(kd is PVL) (1)
15. If (e is NS) and (ce is NL) then (kp is PVS)(ki is PS)(kd is PM) (1)
16. If (e is NS) and (ce is NM) then (kp is PVS)(ki is PS)(kd is PL) (1)
17. If (e is NS) and (ce is NS) then (kp is PS)(ki is PVS)(kd is PL) (1)
18. If (e is NS) and (ce is Z) then (kp is PS)(ki is PVS)(kd is PL) (1)
19. If (e is NS) and (ce is PS) then (kp is PM)(ki is PS)(kd is PVL) (1)
20. If (e is NS) and (ce is PM) then (kp is PM)(ki is PS)(kd is PVL) (1)
21. If (e is NS) and (ce is PL) then (kp is PS)(ki is PS)(kd is PVL) (1)
22. If (e is Z) and (ce is NL) then (kp is PVS)(ki is PVS)(kd is PML) (1)
23. If (e is Z) and (ce is NM) then (kp is PVS)(ki is PS)(kd is PVL) (1)
24. If (e is Z) and (ce is NS) then (kp is PVS)(ki is PS)(kd is PML) (1)

Rule Editor: thesisFIS

File Edit View Options

25. If (e is Z) and (ce is Z) then (kp is PMS)(ki is PVS)(kd is PML) (1)
26. If (e is Z) and (ce is PS) then (kp is PMS)(ki is PS)(kd is PVL) (1)
27. If (e is Z) and (ce is PM) then (kp is PMS)(ki is PS)(kd is PVL) (1)
28. If (e is Z) and (ce is PL) then (kp is PMS)(ki is PMS)(kd is PVL) (1)
29. If (e is PS) and (ce is NL) then (kp is PML)(ki is PMS)(kd is PML) (1)
30. If (e is PS) and (ce is NM) then (kp is PML)(ki is PMS)(kd is PVL) (1)
31. If (e is PS) and (ce is NS) then (kp is PML)(ki is PMS)(kd is PL) (1)
32. If (e is PS) and (ce is Z) then (kp is PML)(ki is PMS)(kd is PVL) (1)
33. If (e is PS) and (ce is PS) then (kp is PL)(ki is PMS)(kd is PVL) (1)
34. If (e is PS) and (ce is PM) then (kp is PL)(ki is PMS)(kd is PVL) (1)
35. If (e is PS) and (ce is PL) then (kp is PL)(ki is PMS)(kd is PVL) (1)
36. If (e is PM) and (ce is NL) then (kp is PL)(ki is PMS)(kd is PVL) (1)
37. If (e is PM) and (ce is NM) then (kp is PL)(ki is PMS)(kd is PVL) (1)
38. If (e is PM) and (ce is NS) then (kp is PL)(ki is PMS)(kd is PL) (1)
39. If (e is PM) and (ce is Z) then (kp is PML)(ki is PMS)(kd is PL) (1)
40. If (e is PM) and (ce is PS) then (kp is PML)(ki is PS)(kd is PML) (1)
41. If (e is PM) and (ce is PM) then (kp is PML)(ki is PS)(kd is PML) (1)
42. If (e is PM) and (ce is PL) then (kp is PML)(ki is PS)(kd is PML) (1)
43. If (e is PL) and (ce is NL) then (kp is PVL)(ki is PM)(kd is PVL) (1)
44. If (e is PL) and (ce is NM) then (kp is PVL)(ki is PM)(kd is PVL) (1)
45. If (e is PL) and (ce is NS) then (kp is PL)(ki is PMS)(kd is PML) (1)
46. If (e is PL) and (ce is Z) then (kp is PL)(ki is PMS)(kd is PML) (1)
47. If (e is PL) and (ce is PS) then (kp is PL)(ki is PMS)(kd is PML) (1)
48. If (e is PL) and (ce is PM) then (kp is PML)(ki is PML)(kd is PVL) (1)
49. If (e is PL) and (ce is PL) then (kp is PML)(ki is PML)(kd is PVL) (1)

Partial rule views of the FIS